DSPACE

https://dspace.org/

Characteristics of particulate matter over the South African industrialized Highveld

Alade, Omotayo Lydia

2011-02-25
http://hdl.handle.net/10539/9101

Downloaded from a DSpace repository. https://dspace.org/

CHARACTERISTICS OF PARTICULATE MATTER OVER THE SOUTH AFRICAN INDUSTRIALIZED HIGHVELD

School of Geography, Archaeology and Environmental Studies
University of the Witwatersrand

Alade Omotayo Lydia

A research report submitted to the Faculty of Science, University of the Witwatersrand, Johannesburg, in fulfillment of the requirements for the degree of Master of Science.

June, 2010

DECLARATION

I declare that this dissertation is my own, unaided work, except where otherwise acknowledged. It is being submitted for the Degree of Master of Science in the University of the Witwatersrand, Johannesburg. It has not been submitted before for any degree or examination in any other University.

Signed this — day of June 2010

_____

Alade Omotayo Lydia

ABSTRACT

Atmospheric aerosols through their role in heterogeneous chemistry significantly influence the earth's radiation balance and the radiative budget of the Earth's atmosphere. The aim of this study is to investigate the characteristics of particulate matter over the industrialised Highveld of South Africa. Elandsfontein, a supersite surrounded by coal mines, coal-fired power stations and a petrochemical plant, is situated on the industrialized Highveld. It provides the monitoring station for the study because it is representative of general conditions of high emissions on the industrialised Highveld region. Continuous measurements of PM10, black carbon, nitrates, sulphur dioxide, particulate sulphate, light scattering properties of aerosol by nephelometer, and meteorological parameters were collected at Eskom's Elandsfontein air quality monitoring site from January to December 2005. The temporal behaviors of the atmospheric aerosols are investigated on diurnal and seasonal time scales. Effects of meteorological parameters such as temperature, humidity, wind direction, and wind speed on the concentration and properties of the aerosols are determined. Also identified is the fraction of PM10 on the Highveld composed of sulphates, nitrates and black carbon. The causes of particularly high particulate concentrations are discussed. The sources of aerosols are identified and the seasonal effects on the concentration of aerosols are investigated using pollution roses and wind roses. Average concentrations of atmospheric aerosols on the industrialized Highveld are highest during late evenings and at night (18:00-22:00) and lowest during the afternoon (12:00-17:00). Maximum concentrations of aerosols in the early morning and at night indicate the trapping effects of stable atmospheric conditions and surface inversions, suggesting that most particulate matter is derived from sources at the surface or at least from sources below the subsidence inversion layer. Higher humidity in the morning may also enhance particulate matter mass concentration. Concentrations are at a minimum during the day due to atmospheric instability and mixing. Concentrations of nitrate are higher at night especially during winter and are predominantly affected by the same stability phenomenon. Higher concentrations of nitrate during winter nights may be a result of fossil fuel combustion at low level e.g. use of coal for space heating and cooking in townships. During the day NO_2 is slowly converted to NO_3 by reaction with O_3. At night however, the principal reaction of NO_3 is with NO_2 to set up equilibrium with N_2O_5. The subsequent heterogeneous dissolution of HNO_3 and N_2O_5 into water droplets gives rise to aerosol nitrate. The night time chemistry of NO_3 differs from the daytime behaviour in that it provides a route for conversion of NO_x to HNO_3 which could be as high as 50% of the daytime route. Sulphate aerosol and sulphur dioxide concentrations peak during the day and are lower at night. Higher concentrations during the day are related to the influence of tall stack emissions from where the sulphur dioxide is derived. Particulate sulphate concentrations are higher in well aged air masses and are controlled by the local meteorology as well as the recirculation pattern of atmospheric aerosol over southern Africa. Particulate concentrations are highest in association with north-westerly winds and lowest in association with easterly winds, since major industries and power plants are located north and south of Elandsfontein. Particulate sulphates sources include oxidation of sulphur dioxide from coal combustion in coal-fired power plants and other industries, and long range air mass transport of sulphate aerosols. The contribution of black carbon and sulphate to PM10 mass is highest in spring while the nitrate contribution to PM10 mass is highest in winter. Some episodes of high particulate matter concentration appear to be related to industrial emissions and fossil fuel combustion. Other episodes are not related to industrial emissions but are mainly due to suspended dust.

This dissertation is dedicated to my husband and children

Sunday Paul Alade

and

Precious Oluwademilade Alade

and

Emmanuel Oluwadamilola Alade

To the acknowledgement of the mystery of God, and of the Father, and of Christ; in whom are hid all the treasures of wisdom and knowledge

Colossians 2: 2b-3

For in Him we live and move and have our being, as also certain of your own poets have said, for we are also His offspring

Acts 17:28

PREFACE

Aerosols comprise a heterogeneous mixture of solid particles and liquid droplets stable over a period of time. Aerosols are derived from a multitude of sources and have significant effects on global climate, air quality and human health. Presently, aerosols' radiative effect represents the largest uncertainty in quantifying the forcing of climate as a result of anthropogenic changes in the composition of the atmosphere.

The industrialized Highveld region of South Africa was selected as the air quality monitoring site for the measurement of various aerosols. It has many sources of pollutants including agricultural activities, coal-fired power stations, timber and related industries, metal smelters, petrochemical plants and coal mines. There are also brick, stonework, fertilizer, explosives, charcoal and chemical producers. Found in this area as well are smaller industrial operations. This study focuses on the Highveld due to the high emission density in that region owing to the high concentration of industrial activity.

The monitoring site to be utilized for this study, Elandsfontein, is a supersite situated on the industrialized Highveld 45km south-south-east of Witbank and is located on top of a small hill which is elevated from the surrounding plain by 150m. Attached to the monitoring station are meteorological measuring devices for establishing the influence of weather on the observed concentration of the aerosols.

The aim of this study is to investigate the characteristics of particulate matter over the industrialised Highveld of South Africa. Temporal behaviour of aerosols will be investigated at the Elandsfontein monitoring site on the time scales of seasonal variation and diurnal variability.

Specifically, the objectives of this research are to:

- Identify the seasonal variations in aerosol concentrations and factors causing minimum and maximum aerosol concentrations.
- Establish the diurnal variation of aerosol concentrations on the Highveld.

- Investigate the sources of aerosols and seasonal effects on the concentration of aerosols.
- Determine the fraction of PM10 composed of sulphates, nitrates and black carbon on the Highveld.

This dissertation is divided into five chapters. **In Chapter One** background information on aerosols in southern Africa, their sources and major form of transport is given. The significance of aerosols regarding health, air quality and global climatic effects is also highlighted. Aerosol size distribution, chemical composition, and optical properties are explained. In **Chapter Two** the data to be utilized is presented and the site of data collection described. There is also a description of analysis methodologies. Instruments which range from a beta gauge to a particulate sulphate monitor used for data collection are presented. In **Chapter Three** the temporal variation of pollutants analyzed over seasonal and diurnal time scales is presented. **In Chapter Four** aerosol sources were identified using pollution and wind roses. Chemical composition of PM10 and also time series of pollution episodes are shown. In **Chapter Five** the summary and conclusions of the study are presented.

ACKNOWLEDGEMENTS

- Firstly I want to ascribe greatness to the Lord my rock whose work is perfect and all His ways are just. All glory to the almighty God for giving me the opportunity to study in South Africa.

- My deepest appreciation goes to my supervisor Dr Kristy Ross for nurturing me and for her untiring guidance, help and advice.

- I would also like to thank my co-supervisor Prof Stuart Piketh and Climatology Research Group for provision of funds for this project. Thanks for your invaluable contribution and constructive criticism of my project despite your hectic schedule.

- Thanks to my friends and colleagues at the Climatology Research Group especially Kirsty Ferguson, Lee-ann Sinden, Thomas Bigala and for their assistance and support throughout the course of the work.

- I also wish to thank the Adetunjis especially my dear friend Ireti. Thank you for being there as the most wonderful friend, you were there encouraging me all the way.

- I am grateful to Dr Kayode Adedapo for the way God used you at a crucial stage of the project. Thank you for that timely word of advice.

- Eskom Sustainability and Innovation Department is also thanked for the provision of air quality data from the Elandsfontein monitoring site used for the project.

- My sincere gratitude goes to Thabisani Ndlovu for the proof-reading and grammatical review given to this dissertation.

- A very special thank you to my parents and siblings for your love, encouragement and most importantly your prayers.

- To my daughter and son, Demilade and Damilola you are the most wonderful gift I could ever have at this time, thank you for bearing with mummy especially with my ever demanding schedule.

- My deepest appreciation goes to my husband Sunday Alade who encouraged me to study for my MSc. Thanks, for believing in me and for standing by me. Indeed two are better than one and I couldn't have done it without you.

LIST OF ABBREVIATIONS

SO_2 – Sulphur dioxide
SO_4^{2-} – Sulphate ion
NO_3^- – Nitrate ion
NO_x – Nitrogen oxides
NO – Nitrogen monoxide
NO_2 – Nitrogen dioxide
N_2O_5 – Di-nitrogen pentoxide
HNO_3 – Nitric acid
O_2 – Oxygen
O_3 – Ozone
OH – Hydroxyl radical
BSC – Backscat coefficient of light by nephelometer
PM – Particulate matter
PM10 – particles with a diameter less than or equal to 10 micrometers
US EPA – United State Environmental Protection Agency
WHO – World Health Organization
CCN – Cloud condensation nuclei
IPCC – International Panel on Climate Change
MAAP – Multi angle absorption photometer

CONTENTS

DECLARATION i

ABSTRACT ii

PREFACE v

ACKNOWLEDGEMENTS vii

LIST OF ABBREVIATIONS viii

CONTENTS ix

LIST OF FIGURES xii

LIST OF TABLES xv

CHAPTER ONE: OVERVIEW 1

1.1 Introduction 1

1.2 Literature review 3

1.2.1 Meteorological and climatological characteristics over the Highveld ... 3

1.2.2 Transport of aerosols over southern Africa 6

1.2.3 Aerosol size distribution 10

1.2.4 Impacts of aerosols on health 13

1.2.5 Effects of aerosols on air quality 15

1.2.6 Aerosol chemical composition 15

1.2.7 Nature of PM10, black carbon, sulphate and nitrate 18

1.2.8 Overview of meteorological parameters 26

1.3 Research objectives 29

CHAPTER TWO: METHODOLOGY 30

2.1 Elandsfontein and the Highveld 30

2.2 Data capture 33

2.3 Instrumention 34

2.3.1 Beta gauge 35

2.3.2 Multi-angle absorption photometer 37

2.3.3 Nephelometer 41

2.3.4 Rupprecht and Patashnick ambient particulate nitrate monitor 44

2.3.5 Rupprecht and Patashnick ambient particulate sulphate monitor 46

2.4 Data analysis 49

2.4.1 Seasonal variation 49

2.4.2 Diurnal variation 49

2.4.3 Pollution roses and wind roses 50

2.4.4 Aerosol chemical composition 51

2.4.5 Causes of high aerosol concentrations 51

CHAPTER THREE: TEMPORAL VARIATIONS 53

3.1 Monthly concentrations of data captured at the Elandsfontein site 53

3.2 Seasonal pattern between PM10, black carbon, sulphate and nitrate 55

3.3 Seasonal variations in atmospheric aerosol concentrations 57

3.4 Diurnal variations in atmospheric aerosol concentrations 65

CHAPTER FOUR: AEROSOL SOURCES AND CHEMICAL COMPOSITION 73

4.1 Overview of meteorology 73

4.1.1 Wind roses 73

4.2 Pollution roses 75

4.3 Chemical composition 81

4.4 Causes of high aerosol concentrations 83

CHAPTER FIVE: SUMMARY AND CONCLUSIONS 88

REFERENCES 92

LIST OF FIGURES

Figure 1.1: Monthly mean winds, contours of the 850 and 500 hPa surfaces (gpm) and 850-500 hPa thickness (gpm).....4
Figure 1.2: Important features of the surface atmospheric circulation over southern Africa.....6
Figure 1.3: The stable stratification of the atmosphere over South Africa on no-rain days….....7
Figure 1.4: Forward trajectories to show recirculation at different scales over southern Africa.....8
Figure 1.5: Illustration of number, surface, and volume distributions for a typical urban model aerosol……12
Figure 1.6: Size distribution of a typical urban aerosol.....13
Figure 1.7: Daytime Interconversions of oxidized nitrogen compounds in the troposphere…….26
Figure 1.8: Nighttime Interconversions of oxidised nitrogen compounds in the troposphere…...26
Figure 2.1: Map of South Africa indicating the Highveld region in thick broken lines……31
Figure 2.2: Map of Eskom's power stations and air quality monitoring stations on the South African Highveld.....32
Figure 2.3: Principle of operation of particulate continuous monitoring.....36
Figure 2.4: Schematic representation of radiation processes in the two layer system consisting of an aerosol-loaded filter layer and the particle-free filter matrix (right); multiple reflections of radiation between the two layers (left).....38
Figure 2.5: Optical sensor of the MAAP. Left: position of the photodetectors at detection angles $\theta 0 = 0^\circ$, $\theta 1 = 130^\circ$, and $\theta 2 = 165^\circ$ with respect to the incident light beam (λMAAP = 670 nm). Right: layout of the MAAP sensor unit, arrows indicate the airflow through the sensor unit across the filter tape…….....40
Figure 2.6: Schematic illustration of an integrating nephelometer……42
Figure 2.7: Schematic of the Rupprecht and Patashnick 8400N particulate nitrate monitor.....46
Figure 2.8: Schematic of the Rupprecht and Patashnick 8400S particulate sulphate monitor.....48
Figure 3.1: Monthly variation of pollutant showing similarity in PM10, sulphates, nitrates and black carbon concentrations.....56

Figure 3.2: Average monthly concentration for Elandsfontein showing variations in PM10.....58
Figure 3.3: Average monthly concentration of monthly variations in black carbon at Elandsfontein.....59
Figure 3.4: Average monthly concentration of monthly variations in backscattering coefficient at Elandsfontein.....60
Figure 3.5: Average monthly concentrations of nitrate concentrations at Elandsfontein.....62
Figure 3.6: Average monthly concentrations showing monthly variations in sulphate concentrations at Elandsfontein.....63
Figure 3.7: Average monthly concentration for Elandsfontein showing monthly variation in temperature.....64
Figure 3.8: Average monthly concentration for Elandsfontein showing variations in sulphur dioxide.....65
Figure 3.9: Diurnal variation of PM10 concentration at Elandsfontein for the period 1 January to 31 December 2005.....66
Figure 3.10: Diurnal variation of pollutant concentration at Elandsfontein for the period 1 January to 31 December 2005 for black carbon.....68
Figure 3.11: Diurnal variation at Elandsfontein for the period 1 January to 31 December 2005 showing variation in nitrates concentration.....69
Figure 3.12: Diurnal variation of pollutant concentration in sulphate at Elandsfontein for the period 1 January to 31 December 2005.....71
Figure 3.13: Diurnal variation of sulphur dioxide concentration at Elandsfontein for the period 1 January to 31 December 2005.....72
Figure 4.1: Seasonal wind roses at Elandsfontein for spring (September-November), summer (December-February), autumn (March-May) and winter (June-August) for the period 1 January to 31 December 2005.....74
Figure 4.2: Pollution roses for black carbon concentrations recorded at Elandsfontein for spring (September-November), summer (December-February), autumn (March-May) and winter (June-August) for the period 1 January to 31 December 2005.....76

Figure 4.3: Pollution roses for PM10 concentrations recorded at Elandsfontein for spring (September-November), summer (December-February), autumn (March-May) and winter (June-August) for the period 1 January to 31 December 2005.....77
Figure 4.4: Pollution roses for nitrate concentrations recorded at Elandsfontein for spring (September-November), summer (December-February), autumn (March-May) and winter (June-August) for the period 1 January to 31 December 2005.....79
Figure 4.5: Pollution roses for sulphate concentrations recorded at Elandsfontein for spring (September-November), summer (December-February), autumn (March-May) and winter (June-August) for the period 1 January to 31 December 2005.....80
Figure 4.6: Pie chart showing sulphates, nitrates and black carbon as percentage of total PM10 in a. Summer; b. autumn; c. winter; and d. spring……...…..82
Figure 4.7: Time series during the pollution episode of 21-23 January 2005. a. Black carbon, sulphate, nitrate and PM10 concentrations; b. sulphur dioxide concentrations; and c. temperature, humidity, wind speed and wind direction…….84
Figure 4.8: Time series of the pollution episode from 29-31 August 2005. a. Black carbon, sulphate, nitrate and PM10 concentrations; b. sulphur dioxide concentrations; and c. temperature, humidity, wind speed and wind direction……..…86

LIST OF TABLES

Table 1.1: Data captured at the Elandsfontein monitoring site in 2005

Table 3.1: Monthly concentrations of data captured at the Elandsfontein site in 2005

CHAPTER ONE

OVERVIEW

A detailed discussion of the state of knowledge of particulate matter over the South African industrialized Highveld is given in this chapter. The meteorological characteristics over the Highveld are discussed, as well as aerosol sources and their transportation. The research objectives are also outlined.

1.1 Introduction

Particulate matter is unique among atmospheric constituents in that its definition is not based on its chemical composition but rather, its physical state. Through their role in heterogeneous chemistry and influencing the earth's radiation balance, atmospheric aerosols significantly influence the entire planet. Aerosols are liquid or solid particles suspended in the air. They have significance at local, regional and global scales and have received prominent attention in the past few years (Penner *et al*., 1994; Alfarra, 2004; Seinfeld and Pandis, 2006). Aerosols are known to significantly influence the radiative budget of the Earth's atmosphere both directly by scattering and absorbing radiation and indirectly by affecting cloud properties. The effect of aerosols on global climate, atmospheric chemistry and health impacts (later expanded on) is not well understood because aerosols are highly variable in time and space. Therefore there is a need to understand the characteristics of atmospheric aerosols (Russell *et al*., 1999; IPCC 2007).

Atmospheric aerosols are generally considered to be particles that range in size from a few nanometers (nm) to tens of micrometers (μm) in diameter, and they occur as either primary or secondary pollutants. Primary aerosols are transferred into the atmosphere in the same chemical form as the source materials while secondary aerosols are formed in the atmosphere through condensation of vapours or chemical reactions in the gas or aqueous phases (Held *et al*., 1996). Aerosols exhibit a short atmospheric lifetime from minutes to several days, but at times they may

be transported over thousands of kilometres from their source regions notwithstanding their ephemeral atmospheric life (Held *et al*., 1996; IPCC 2007; Seinfeld and Pandis, 2006).

In categorising particulate matter, the following features must be considered: the concentration, size, state (liquid or solid), chemical composition and morphology. Aerosol particles in the atmosphere come from natural sources and anthropogenic activities. Natural sources of particulate matter include soil and rock debris, forest fires, biological material such as pollen, spores and bacteria, sea spray, desert dust and volcanic activities (Cohan *et al*., 2002; Alfarra, 2004).

Anthropogenic aerosols are mainly in the form of sub-micron particles, which have longer atmospheric lifetimes and more efficient optical extinction efficiencies for photosynthetically active radiation (Seinfeld and Pandis, 1998). Emissions of particulate matter caused by anthropogenic activities arise primarily from four source categories: fuel combustion, industrial processes (mining, construction), non-industrial fugitive sources (roadway dust from paved and unpaved roads, biomass burning, wind erosion of cropland, agricultural activities) and transportation sources (Maenhaut *et al*., 1996; Seinfeld and Pandis, 2006). Examples of particulate matter are ash, soot, smoke, smog, mists, hazes, fumes, fog and dusts.

Anthropogenic emissions of atmospheric aerosols have increased dramatically over the past century and have been implicated in human health effects (Seinfeld and Pandis, 2006). Particulate matter can alter the body's defence system against foreign materials, damage lung tissues, aggravate existing respiratory and cardio vascular diseases, and can lead to cancer or premature death (Seinfeld and Pandis, 2006). Aerosols also damage materials and form atmospheric haze that degrades visibility (Held *et al*., 1996).

In this research study, the characteristics of particulate matter over the industrialised Highveld will be investigated. Measurements of atmospheric aerosols collected at one of Eskom's air quality monitoring sites, Elandsfontein, will be utilised. Measurements recorded from 1 January to 31 December 2005 will be used to identify average daily and monthly variations in aerosol concentrations, and the effects of the meteorological data on the concentration of the pollutants.

This chapter introduces aerosols and their significance at local, regional and global scales. It also states how they influence the earth's radiation balance. The literature review gives background information on aerosols in southern Africa, their sources and major atmospheric transport. The importance of aerosols in terms of health effects, air quality and global climatic effects are also highlighted. The size distribution and chemical composition of atmospheric aerosols are presented for the understanding of its removal processes and sources. Finally, temporal behaviour of aerosols on the time scales of seasonal and diurnal variability is stated as the research objectives.

1.2 Literature review

1.2.1 Meteorological and climatological characteristics over the Highveld

The southern African region has been recognised as a major source of aerosols in the southern hemisphere and it is known to be significant in the production and transportation of aerosols with urban and industrial areas as major sources (Siversten *et al*., 1995; Piketh *et al*., 1999). Aeolian dust and industrial sulphur are the major constituents of the inorganic fraction of the aerosols in the haze layer in areas downwind of the major urban and industrial areas of the Highveld plateau of South Africa. Emissions from biomass burning contribute a relatively insignificant fraction to the total aerosol loading of the major transport plume that transports materials out of the sub-continental sector to the Indian Ocean (Piketh *et al*., 1999).

The industrial Highveld region accounts for approximately 90% of South Africa's scheduled emissions of particulate matter, SO_2 and NO_x (Held *et al*., 1996). Emissions from the industrialised Highveld are transported directly towards the Indian Ocean over Inhaca Island approximately 40% of the time (Freiman and Piketh, 2003). The atmospheric circulation over the Highveld is controlled by semi-permanent anticyclones which result in large-scale subsidence in the atmosphere, which in turn causes elevated temperature inversions, effectively limiting vertical dispersion of pollutants (Held *et al*., 1996).

Southern Africa is situated in the sub-tropical high pressure belt which causes the general circulation over the subcontinent to be anticyclonic except near the surface. Anticyclones are

prevalent throughout the year and undergo seasonal intensification. An exceptional situation occurs during winter when the mean anticyclone intensifies and moves northward. Upper level westerlies expand and the upper tropical easterlies are displaced equator-ward (Figure 1.1). The Intertropical Convergence Zone moves further south during summer (Garstang *et al*., 1996b; Tyson and Preston-Whyte, 2000). The near surface circulation at 850 hPa during the summer months (January) consists of a weak heat with occurrence of cyclonic circulations when troughs develop over the central interior of the country. In contrast to the January condition, at 850 hPa the low-level July mean pressure field is strongly anticyclonic (Held *et al*., 1996; Tyson and Preston-Whyte, 2000). However, the mean circulation of the atmosphere largely controls the climate of the subcontinent but has little effect on individual weather systems. The weather system is controlled by the synoptic and smaller scale disturbances such as subtropical, tropical and temperate features of the general circulation.

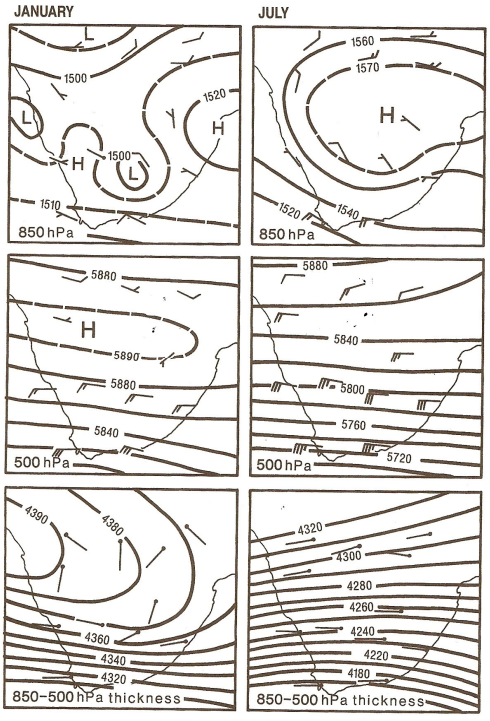

Figure 1.1. Monthly mean winds, contours of the 850 and 500 hPa surfaces (gpm) and 850-500 hPa thickness (gpm) (Tyson and Preston-Whyte, 2000).

The continental high, the semi-permanent South Indian anticyclone and the South Atlantic anticyclone are elements of the discontinuous high pressure belt that surrounds the southern hemisphere. These features control the subtropical disturbances (Figure 1.2). Subtropical anticyclones are associated with divergence in the near surface wind field, fine clear conditions with little or no rain, occurrence of inversions and strong subsidence (Tyson and Preston-Whyte, 2000). The tropical disturbances are controlled through the easterlies, which is the occurrence of easterly waves and lows. They are usually associated with the Inter-Tropical Convergence Zone and the warm humid easterly winds between the Zone and the subtropical high pressure belt. Tropical easterlies with their annual cycle have by far the greatest effect with much control on the summer rainfall over the interior and affect most of southern Africa during the summer period (Garstang *et al*., 1996b).

Temperate disturbances are affected through travelling waves or troughs in the westerlies that take the form of westerly waves and lows. Temperate disturbances occur with a local nature sometimes by the west-coast troughs and the shallow coastal lows (Tyson *et al*., 1996b; Tyson and Preston-Whyte, 2000). The mean circulation of the atmosphere over the subcontinent is also affected by the low-level westerlies which extend to about 500 hPa during summer and in winter move northward and are shallower. Northward expansion and intensification of the circumpolar westerlies during winter are evident at the 200 hPa level (Garstang and Tyson, 1997).

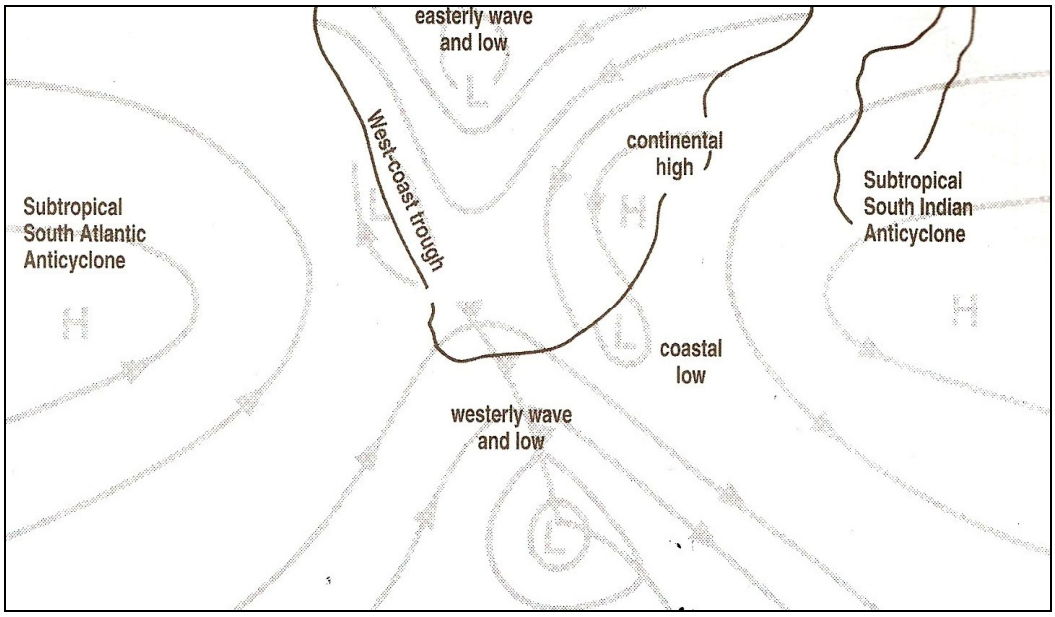

Figure 1.2. Important features of the surface atmospheric circulation over southern Africa (Tyson and Preston-Whyte, 2000).

1.2.2 Transport of aerosols over southern Africa

The atmospheric circulation pattern determines the transport of aerosols over southern Africa. In the first instance, easterly wave circumstances favour transport to the west over the tropical Atlantic Ocean in the Angolan while the combination of anticyclonic circulation and westerly disturbances results in atmospheric transport from southern Equatorial Africa to the east over the Indian Ocean through the Natal plume (Garstang *et al*., 1996b). Only 5 per cent of air circulating over the subcontinent is transported by semi-permanent continental anticyclones to the Atlantic Ocean. Under these conditions the anticyclones tend to occur most frequently in autumn, spring and winter months, and are almost isolated from South Atlantic High. Also they are by no means absent in summer (Tyson and Preston-Whyte, 2000). Furthermore, transient mid-latitude ridging anticyclones give maximum transport of aerosols and trace gases originating in the mid-latitudes and flowing towards the southern Atlantic Ocean (Garstang *et al*., 1996b). These conditions frequently occur more in the summer periods, on no rain days, and are related to the large, semi-

permanent anticyclones situated over the Atlantic and Indian Oceans. This anticyclonic flow can also produce considerable recirculation which may be confined to the continent or may extend over and return from the Indian Ocean (Tyson *et al*., 1996a).

Large-scale continental anticyclones in the upper atmosphere are significant to the characteristics of the southern Africa atmosphere. These systems are attributed to the well-known meridional Hadley circulation causing subsidence over the tropics. These anticyclones result in the adiabatic warming and drying of the air and the formation of extensive and persistent inversions and stable layers (Figure 1.3) on days with no rain (Garstang *et al*., 1996b). The lowest of the stable layers is associated with the top of the mixing and is found at 700 hPa while the second layer is in association with the main subsidence inversion and occurs at 550 hPa. The third layer is formed intermittently between the main subsidence feature and the troposphere at 350 hPa (Cosijn and Tyson, 1996).

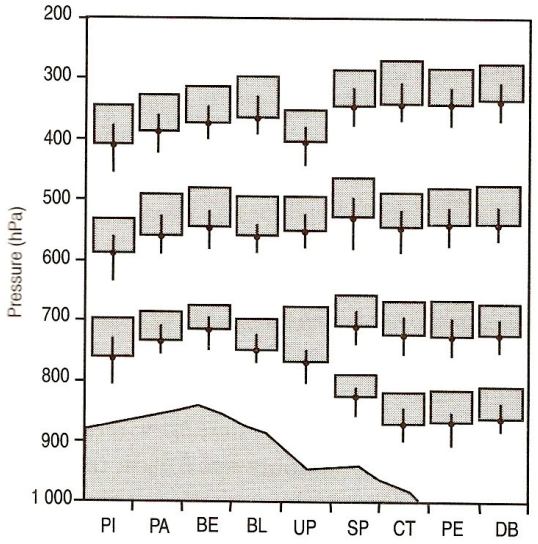

Figure 1.3. The stable stratification of the atmosphere over South Africa on no-rain days. Absolutely stable layers are indicated. Of these the 500 hPa layer is the most persistent (Tyson and Preston-Whyte, 2000).

Consequently, with most of the different types of synoptic conditions that occur in the lowest layers of the atmosphere in southern Africa, the transport of air, aerosols and other atmospheric

constituents is largely towards the east coast and the Indian Ocean (Tyson and Preston-Whyte, 2000). Anticyclones linked with transient ridging highs moving with the passage of westerly waves and cold fronts cause recirculation of air, aerosols and trace gases over the subcontinent. Recirculation occurs in a range of spatial and time scales over southern Africa, ranging from the local to the sub continental (Figure 1.4). During the process of recirculation over southern Africa, air trapped between various stable layers may be decoupled from those circulating in the upper and lower layers. For instance, anticyclonic transport over periods of 12 and 9 days is evident in trajectories crossing the vertical aerosol section over Gauteng at both the 850 and 500 hPa levels respectively. In contrast, air is recirculated twice over the region over a 20 day period before exit to the east in the westerly transport plume from southern Africa at 700 hPa level (Tyson *et al.*, 1996a).

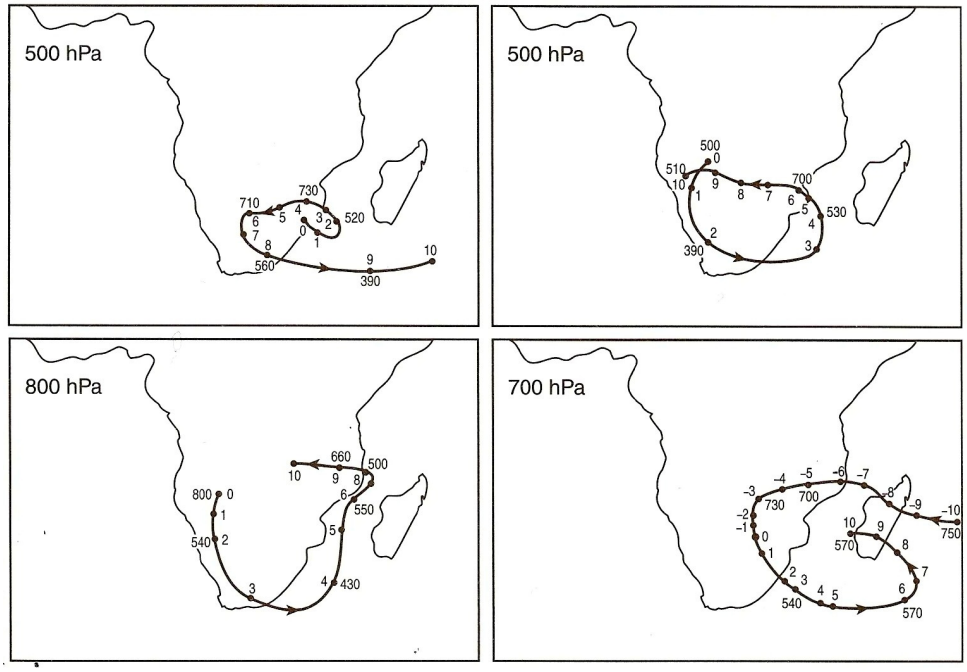

Figure 1.4. Forward trajectories to show recirculation at different scales over southern Africa. Geopotential height, hPa, is specified at designated days along the trajectories. Positive days indicate time after leaving the source point, negative days indicate the time before reaching the point (Tyson and Preston-Whyte, 2000).

Atmospheric stability is a key factor in atmospheric pollution dispersion. Hence, these circulations and atmospheric conditions are major determinants of the low-level field especially during the night and in winter as they control to a large extent the transport and dispersion of low-level emissions of pollutants (Held *et al*., 1996). Radiative surface inversion begins shortly before sunset when the surface cools through radiational loss of heat and by 21:00 it may be several hundreds of meters deep. It occurs under clear, calm and dry conditions at night. Sudden deepening of a surface inversion rarely occurs but its occurrence could be as a result of advection or following the onset of abrupt but slight turbulent mixing (Preston-Whyte and Tyson, 1993).

Annual frequencies of 01:30 nocturnal surface inversions are greatest over the interior of Namibia and Botswana as a result of low relative humidity particularly during winter. In contrast to the nocturnal situation, midday (13:30) surface inversions rarely occur over southern Africa but the winter nocturnal surface inversion has a depth of 400-600 m and strength of 5-7 ^{o}C over southern Africa as a whole (Tyson and Preston-Whyte, 2000). The more stable the atmosphere the more likely stronger inversions will develop. Therefore pollution released into stable inversion air is seldom able to rise through it and disperses slowly in clearly defined plumes. Surface inversions have been observed on a frequency of 80-90 % during winter over the Highveld (Held *et al*, 1996). Mean early morning winter surface inversions over the Highveld region vary from 3-11 °C in strength with extreme cases reaching up to 15 °C. It varies in depth from 100-400 m above ground level (AGL). Over the Mpumalanga Highveld region, inversions of greater than 10 °C commonly occur during 25-30 % of all winter nights for approximately 16 hours (Held *et al*, 1996).

Elevated inversions commonly occur in high pressure areas (Preston-Whyte and Tyson, 1993). Sinking air adiabatically warms to temperatures in excess of those in the mixed boundary layer. Therefore the interface between upper, gently subsiding air and the mixed boundary-layer air is marked by an absolutely stable layer or an elevated subsidence inversion (Tyson and Preston-Whyte, 2000). The basal height of the lowest absolutely stable layer is 733 hPa which is approximately 2700 m ASL (D'Abreton *et al*, 1998). In summer the mean mixing heights are higher over the interior plateau than in winter. Average summer values for the Mpumalanga Highveld range from 200 to 300 m while average winter values are in the range of 150 to 200 m. This is due to the position of the continental high over the interior in winter and the high frequency of calm air which does not allow the mechanical generation of turbulence. The

average winter base height of the first elevated inversion above the ground varies from less than 1000 m to an average height of about 1500 m (Tyson and Preston-Whyte, 2000).

Elevated inversions are caused by subsidence or by frontal movement of air masses. They have been found to occur throughout the year with frequencies of about 60 percent. On the mesoscale, the first elevated inversion above the surface inversion over the Mpumalanga Highveld was observed on 36 percent of all days with soundings (Held *et al*, 1996). The strength of the temperature discontinuity is rarely greater than 2 °C. This is adequate to trap all pollution below the inverse base and to ensure a highly adverse air pollution climate (Tyson and Preston-Whyte, 2000) Elevated inversions suppress the diffusion and vertical dispersion of pollutants by reducing the height to which such pollutants are able to mix, and consequently result in a concentration of pollutants below their bases (Scorgie, 1999). Such inversions contribute to long-range transport and re-circulation of pollution (Harrison, 1993; Garstang *et al*, 1996b).

1.2.3 Aerosol size distribution

The size distribution of atmospheric aerosols is important for the understanding of the transport of aerosols, removal processes and sources. Particle size is an important parameter for characterising the behaviour of aerosols. Aerosols range in size from a few nanometers (nm) to tens of micrometers (μm) in diameter. Particles less than 2.5 μm in diameter are referred to as fine and particles greater than 2.5 μm in diameter as coarse (Seinfeld and Pandis, 2006). Fine particles are composed of micron and sub-micron particles from anthropogenic and natural sources such as biomass and fossil fuel burning, and motor vehicles. These fine particles consist of sulphates, nitrates, ammonium, organic and elemental carbon and metal compounds. The coarse particles comprise crustal materials, including silicon, calcium, magnesium, aluminium, and iron. These elements are not present as elements; most probably they are present as oxides. The biogenic organic particles which consist of pollen grains, spores, plant and insect parts are formed through natural processes and by erosion.

Aerosol particle size distribution can also be divided into three modes: Aitken, accumulation and coarse mode (Figure 1.5). These modes are significant because they originate and transform separately, are removed from the atmosphere by different mechanisms, have different lifetimes,

have different chemical compositions and optical properties, and differ significantly in deposition patterns in the respiratory tract (Alfarra, 2004; Seinfeld and Pandis, 1998; 2006).

The Aitken mode has diameters extending from 10nm (0.01µm) to 100nm (0.1µm). Particles in this mode are formed from ambient temperature gas-to-particle conversion as well as condensation of hot vapour during combustion processes. Particles in the Aitken mode because of their small size have the greatest number of particles and coagulate quickly into accumulation mode. Their lifetime is short as they are removed principally by coagulation with larger particles in the atmosphere.

The accumulation mode has diameters between 0.1 and 1.0 µm. Source of particles in this mode is mainly the coagulation of particles with diameters smaller than 0.1 µm and the condensation of vapours onto existing particles causing them to grow into this size range. Accumulation mode particles are emitted directly through incomplete combustion of wood, oil and coal (fuels) and occur naturally in the environment as organic material and soluble inorganics like nitrates and sulphates. These particles are removed least efficiently, resulting in longer atmospheric lifetimes and accumulation in the atmosphere.

The coarse mode is defined by diameters larger than 1.0 µm. Coarse mode aerosols are formed by mechanical processes and are emitted directly into the atmosphere from both natural and anthropogenic sources. Coarse particles have sufficiently large sedimentation velocities and settle out of the atmosphere in a relatively short time. On windy days, fallout may be balanced by re-entrainment.

Atmospheric aerosols' size distributions are often described as the sum of *n* lognormal distributions.

$$n_N^{\circ}(\log D_p) = \sum_{i=1}^{n} \frac{N_i}{(2\pi)^{1/2} \log \sigma_i} \exp\left(- \frac{(\log D_p - \log \bar{D}_{pi})^2}{2 \log^2 \sigma_i} \right) \qquad (1.1)$$

Where

N_i is the number concentration of aerosol particles in the ith mode

D_{pi} is the median diameter

σ_i is the standard deviation of the ith lognormal mode

D_p is the diameter

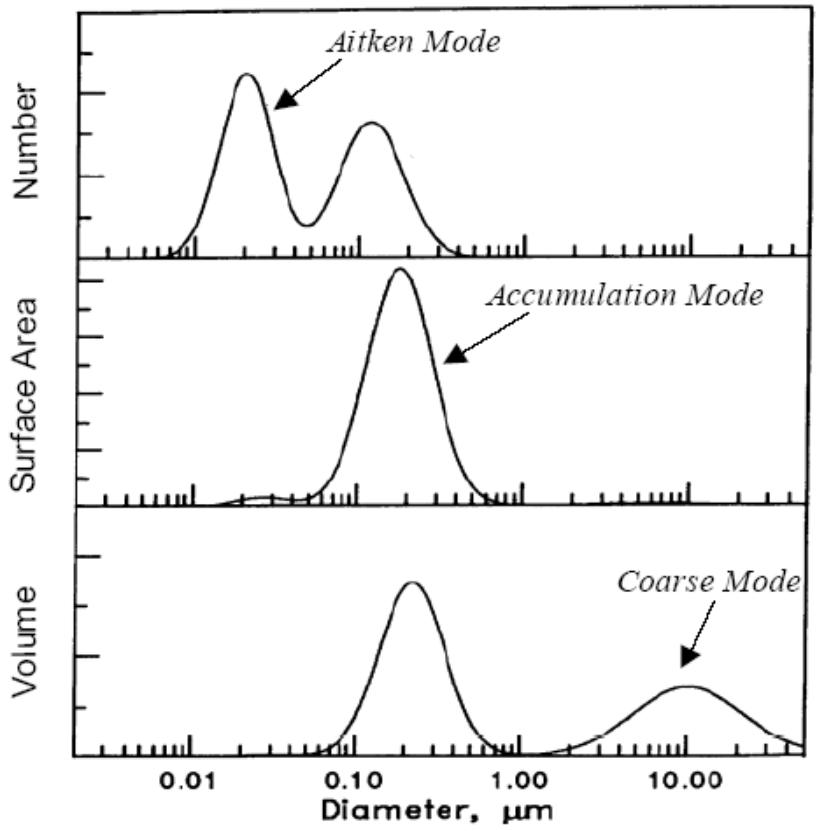

Figure 1.5. Illustration of number, surface, and volume distributions for a typical urban model aerosol (Seinfeld and Pandis, 1998).

Wall *et al*. (1988) measured the size distribution of a typical urban aerosol (Figure 1.6). They identified two modes in the 0.1 - 1.0 µm size range i.e. the condensation and droplet modes for sulphate, nitrate and ammonium, and a third mode over 1µm i.e. the coarse mode. The coarse mode contains more than half of the nitrates, and most of the sodium and chloride. The condensation mode is as a result of condensation of the secondary aerosol component from the

gaseous phase and it has a peak diameter of 0.2 µm. The droplet mode peaks around 0.7µm in diameter and its existence is attributed to heterogeneous, aqueous-phase reactions (Seinfeld and Pandis, 2006).

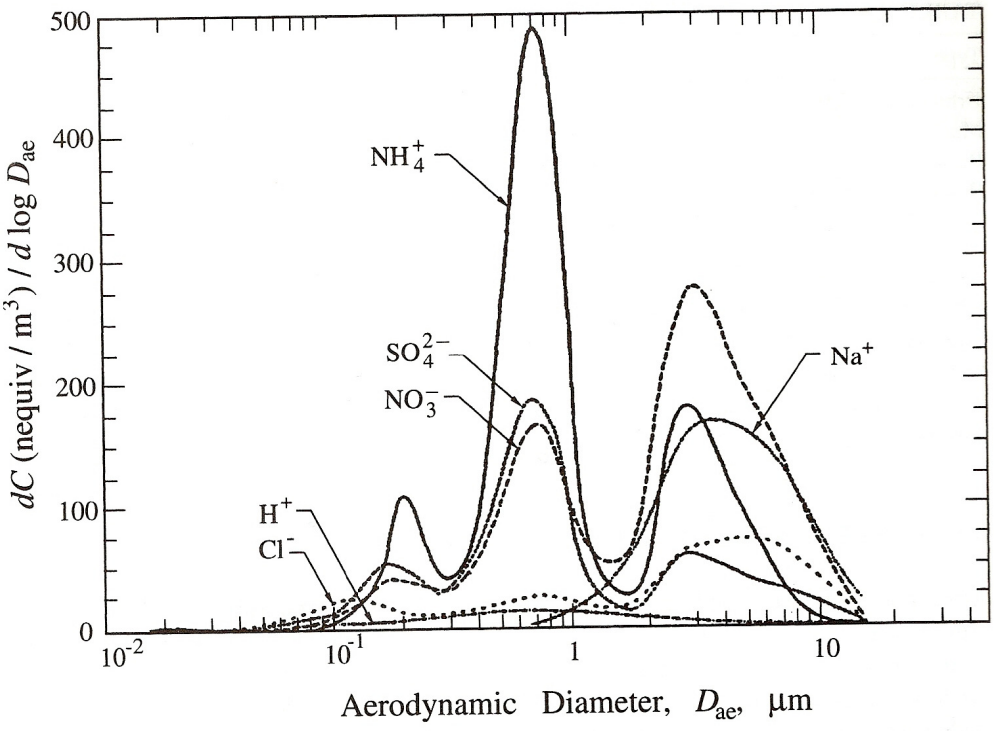

Figure 1.6. Size distribution of a typical urban aerosol (Seinfeld and Pandis, 2006).

1.2.4 Impacts of aerosols on health

Particulate matter represents the most significant criteria pollutant regarding human health risk potential in southern Africa. A large number of epidemiological studies have been conducted globally over the last two decades and associations between ambient particulate matter and excesses in daily mortality and morbidity were observed (Dockery *et al.*, 1992; Touloumi *et al.*, 1994; Lighty *et al.*, 2000). Of all the different forms of pollution, air pollution seems to cause the largest and most widespread hazards and environmental problems. The form of the air pollutant i.e. gas or particulate, produces different effects within the respiratory tracts. Humans inhale

about 7500 litres of air each day and their lungs and respiratory system are in contact with and have the potential to retain harmful substances in the air (Lippmann and Schlesinger, 1979).

The effects of air pollutants can be classified according to the type of effect they can have on human health. According to Lippmann and Schlesinger (1979), pollutants and their effects include chemical irritants, fibrotic response, asphyxiant response, allergic response, systemic reactions, and mutagenic, teratogenic and carcinogenic reactions.

The air quality standards developed in the United States of America (US) and Europe in terms of the mass of total suspended particulate matter (TSP) during the 1960s and 1970s are based on safe levels for human health, which also forms the basis for South Africa's standards. In the USA, a standard for particulate matter less than 2.5μm in diameter, PM2.5, has been introduced in addition to the standard for suspended particulate matter less than 10μm in size, PM10 (EPA, 1997). In South Africa, there is no proposed standard for PM2.5 but only PM10. PM2.5 is the smallest particles, which can penetrate into the lungs and hence produce greater adverse effects than the larger PM10 particles. The smaller particles have a bigger ratio of surface to volume, and are produced from gas-to-particle conversion or combustion processes. Carcinogens such as polycyclic aromatic hydrocarbons fall into this size range. For that reason, air quality standards are based on the smaller particles.

The US EPA revised air quality standards for fine particles (PM2.5) is 15μg/m^3 annual mean and 35μg/m^3 for the 24-hour mean. The PM10 standard for the US EPA is 150μg/m^3 for the 24-hour mean while the annual PM10 standard has been revoked due to lack of evidence linking health problems to long-term exposure to coarse particle pollution (www.epa.gov/air/criteria.html). The WHO Guideline for PM2.5 is 10μg/m^3 annual mean and 25μg/m^3 for the 24-hour mean. Also the PM10 guideline for WHO is 20μg/m^3 annual mean and 50μg/m^3 24-hour mean (www. who.int.mediacentre/factsheets). The South African proposed permissible concentration for PM10 24-hour maximum is 75μg/m^3 and the proposed concentration for the yearly maximum is 40μg/m^3 (www.deat.ecostat.co.za).

1.2.5 Effects of aerosols on air quality

An increasing load of aerosols in the troposphere (sulphates, organics, black carbon) caused by both primary particles and secondary particles contributes to climate change (Brasseur *et al*., 2003). The International Panel on Climate Change (IPCC) in their recent report conclude that changes in the atmospheric abundance of greenhouse gases and aerosols, in solar radiation and in land surface properties, alter the energy balance of the climate system (IPCC, 2007). There is good understanding that greenhouse gases warm the earth and sulphate aerosols cool it down. Contrary to sulphate aerosols, aerosol particles containing light absorbers such as elemental carbon and mineral dust cause the heating of the lower atmosphere.

Aerosols affect the Earth's radiation balance in two different ways. Directly, aerosols scatter and absorb solar and infra red radiation and force radiation through the reflection of shortwave radiation back into space, thereby increasing planetary albedo and reducing temperature in the atmosphere (Charlson *et al*., 1992; IPCC, 2007). A total direct aerosol radiative forcing combined across all aerosol types is given as -0.5 ± 0.4 W m^{-2}, with a medium-low level of scientific understanding (IPCC, 2007).

Aerosol particles can become activated to grow to fog or cloud droplets in the presence of water vapor. This fraction of aerosols is called cloud condensation nuclei (CCN) (Seinfeld and Pandis, 2006). Indirectly, aerosols in their role as CCN can influence cloud radiative properties, cloud lifetime and the equilibrium of cloud liquid-water content (Charlson *et al*., 1992; Anderson *et al*., 1996). They decrease the precipitation efficiency of warm clouds and thereby cause an indirect radiative forcing. Indirect radiative forcing by aerosols is most likely to occur in the wet season, when the emitted aerosols have the capacity to alter cloud and droplet microphysics and thus rainfall (Ross *et al*., 2003).

1.2.6 Aerosol chemical composition

A good understanding of the chemical composition of aerosol particles is important for the identification and prediction of their sources and their effect on diverse atmospheric processes. There is still a great deal of uncertainty in the complete characterisation of the chemical

composition of ambient aerosol particles, especially its organic fraction, and consequently numerous studies have been undertaken to measure chemical composition (Alfarra, 2004).

Atmospheric aerosols exist in variable concentrations and in a large range of chemical components. They are composed of sulphates, nitrates, ammonium, sodium, chloride, water and carbonaceous material, mineral dust, crustal elements and trace metals.

Warneck (1988) classified the chemical composition of particulate matter into three broad categories namely water-soluble inorganic salts, water-insoluble minerals of crustal origin and organic compounds. Inorganic primary particles are metals, insoluble minerals and ammonium while the secondary particles are sulphates and nitrates. Organic primary particles are soot (impure graphite), polar organics (alkanoic acids) and non-polar organics (PAH, alkanes). The secondary particles are mainly polar organics (multifunctional compounds). Particulate organic matter is a complex mixture of many classes of compounds, and its study is of utmost importance because of the possibility that such compounds pose a health hazard. It has been shown that certain fractions of particulate organic matter containing polycyclic aromatic hydrocarbons (PAHs) are carcinogenic in animals and mutagenic in in-vitro bioassays (Seinfeld and Pandis, 2006).

Nitrates are produced mainly from the conversion of NO, NO_2 and NH_3^- in the atmosphere (Seinfeld and Pandis, 1998; Alfarra, 2004). Sulphates are predominantly produced from the oxidation of dimethyl sulphide and sulphur dioxide which are examples of natural and anthropogenic sulphur-containing compounds. Crustal materials (that largely include soil dust and windblown materials) differ in their composition due to local geology and surface conditions.

Anthropogenic sulphate emissions derived from fossil fuel combustion and metal smelting are the largest single contributor to aerosol cooling in the earth-atmosphere (Charlson *et al*., 1992). They are produced by gas-to-particle conversions of sulphur containing gases, with diluted sulphuric acid droplets and droplets of ammonia sulphate solution as end products. Sulphates are smaller than dust and they have a longer atmospheric lifetime. Sulphate aerosols act as the main source of cloud condensation nuclei over the oceans. They increase cloud albedo and influence the climate through their light scattering properties (Charlson *et al*., 1991). The optical scattering

efficiency of sulphates is an order of magnitude larger than the optical efficiency of dust. Furthermore, sulphate aerosols are hygroscopic in nature and when deliquescence has occurred; their optical scatterings per unit mass concentration is double that of dry particles (Charlson *et al*., 1992).

Emissions of sulphur in southern Africa derived from power production and industry are estimated to be 61 percent and 35 percent respectively. Sulphur dioxide is estimated to contribute 10-20 percent of the total natural flux of sulphur. Sulphur dioxide is injected into the atmosphere through volcanoes and is highly variable in time and space. The remaining flux mainly contains sulphur containing gases derived from terrestrial and marine biota (Ross, 2003). The anthropogenic flux of sulphate contributes a large proportion of the total aerosol suspended in southern Africa, with those from power production and industries being the major constituent of the fine aerosol fraction. Anthropogenic sulphates due to various factors are responsible for a significant perturbation of the Earth's radiation balance through direct and indirect effects (Charlson *et al*., 1992).

The carbonaceous fraction of the aerosol consists of both elemental and organic carbon. Elemental carbon (EC), also referred to as black carbon, graphitic carbon, or soot, is directly emitted into the atmosphere, predominantly from combustion processes, while organic carbon is directly emitted from sources such as biomass burning or can result from atmospheric condensation of low volatility organic gases (Alfarra, 2004; Seinfeld and Pandis, 2006).

Mineral dust is injected into the Earth's atmosphere by surface winds from dry soils where there is sparse vegetation cover. The injection of mineral dust increases in areas where the soil is disrupted by agricultural activities and where new soil surfaces are exposed to wind erosion through deforestation. The global source of mineral aerosol has been estimated to range between 1000 and 5000 Tg y^{-1}, and in some regions, dust can contribute the major part of aerosol mass loading (Tegen and Fung, 1995).

Mineral dust loading in the atmosphere is highly variable in time and space, making it difficult to quantify its actual distribution and global impact. Its lifetime is dependent on particle size which varies between one hour for large particles and several years for stratospheric particles. The particles that remain airborne for a longer period are transported long distances, like those from

the Sahara and Sahel which are transported into the tropical North Atlantic (Ross, 2003). Mineral dust through direct and indirect mechanisms perturbs the shortwave radiation balance, and it has the further effect of absorbing and emitting long wave radiation. Silicaceous materials absorb strongly in the thermal infrared region of the electromagnetic spectrum (Penner, *et al.*, 1994).

1.2.7 Nature of PM10, black carbon, sulphate and nitrate

Particulate matter is the generic term used for a type of air pollution that consists of complex and varying mixtures of particles suspended in the air we breathe. Particles are present everywhere, but high concentrations or specific types of particles have been found to present a serious threat to human health. Particulate matter is a combination of fine solids such as dirt, soil dust, pollens, molds, ashes, and soot as well as aerosols that are formed in the atmosphere from gaseous combustion by-products such as volatile organic compounds, sulphur dioxide and nitrogen oxides. Particulate matter levels in the atmosphere are a function of both natural and anthropogenic sources. Particulate pollution emanates from such diverse sources as factory and utility smokestacks, vehicle exhaust, power plants, wood burning, mining, construction activity, and agriculture (Etyemezian *et al*., 2007; Wang *et al*., 2009).

PM10 refers to particulate matter with an aerodynamic diameter of 10 µm or less. The variation of PM10 concentrations is controlled by the emission rate in potential PM10 sources which range from windblown dust, industries, vehicle exhaust, dust from roads (paved and unpaved road), gas-to-particle conversion processes, and forest fires to residential wood combustion (Limbeck *et al*., 2004; Cheng *et al*., 2006). PM10 is generally subdivided into a fine fraction of particles 2.5 µm or less (PM2.5), and a coarse fraction of particles larger than 2.5 µm. Furthermore, PM10 is classified as primary (emitted directly into the atmosphere) or secondary (formed in the atmosphere through chemical and physical transformations). The principal gases involved in secondary particulate formation are sulphur dioxide (SO_2), nitrogen oxides (NO_x), volatile organic carbon (VOCs) and ammonia (NH_3). Primary particles are found in both the fine and coarse fractions, whereas secondary particles such as sulphates and nitrates are found predominantly in the fine fraction. Particles (such as sulphates and nitrates) remain dry with increasing relative humidity until their deliquescent point is reached at which time a sudden uptake of water occurs with a corresponding increase in particle size. The resultant particles are

usually within the size range that is most efficient at scattering light. Therefore, particle growth through deliquescence has a large potential impact on atmospheric visibility (CEPA, 1998).

Black Carbon

Black carbon also known as elemental carbon, is a product of incomplete combustion processes and the main light-absorbing components of aerosols (Penner *et al*., 1998; Streets *et al*., 2001). Thus, the amount of black carbon depends critically on how the fuel is burned in addition to the mass of fuel burned (Novakov *et al*., 2003). Black carbon is principally derived from industrial pollution, biofuels, traffic, outdoor fires, burning coal, biomass burning and fossil fuel emissions as the principal source (Penner *et al*., 1998; Moosmuller *et al*., 2009). The absorption of light by black carbon reduces atmospheric visibility and offsets the effects of most other aerosols like sulphate aerosol, which have light-scattering properties that counteract the global-warming effects of carbon dioxide (Streets *et al*., 2001). In addition, absorption by black carbon lowers the aerosol single scattering albedo, increasing the amount of radiation absorbed in the atmosphere (Saha and Despiau, 2009). The magnitude of aerosol energy absorption on the global scale and its contribution to global warming are uncertain. Similarly, the distribution of elemental carbon is not well known although it is thought to be ubiquitous (Seinfeld, 2008).

Absorbing aerosols heat the air, alter regional atmospheric stability and vertical motions, and affect the large-scale circulation and hydrologic cycle with significant regional climate effects (Menon *et al*., 2002).The heating of light absorbing aerosols changes the local atmospheric temperature, which influences relative humidity (Moosmuller *et al*., 2009) In contrast to the other aerosol types, black carbon has a warming influence on the earth-atmosphere system and may thereby decrease the cooling by the purely scattering components of aerosols. Black carbon has the further effect of removing heat that would be deposited near the bottom of the atmosphere and rather heat the atmosphere itself (Andreae, 2001). This transfer of energy changes the vertical temperature profile of the atmosphere, and has the potential to influence convection and mixing in the planetary boundary layer (Penner *et al*., 1994). Black carbon also affects cloud albedo by altering the hygroscopic properties of cloud condensation nuclei and the solar heating caused by black carbon can reduce cloudiness (Penner *et al*., 1994; Streets *et al*., 2001). Freshly emitted black carbon particles are generally hydrophobic but transform to hydrophilic black carbon due to surface oxidation and coating in about one day. Atmospheric

lifetimes are in the order of 8 days and both wet and dry deposition may be important sinks for atmospheric black carbon (Moosmuller *et al*., 2009).

The formation of black carbon has, according to Moosmuller *et al*., (2009) yielded a generalized complex formation mechanism that includes: formation of precursor species, particle inception and particle surface growth and agglomeration. Formation of precursor species occurred with the fuel first undergoing pyrolysis which is a process of thermal degradation and cracking of complex fuel molecules that produces low molecular weight radicals. Subsequently, polycyclic aromatic hydrocarbons (PAHs), which are intermediates between an original fuel molecule and a primary soot particle, are formed through a series of radical reactions with precursors such as acetylene radicals. If the fuel is non-aromatic, the precursors experience cyclization creating aromatic rings, and the ring structure is developed into PAHs through addition of alkyl groups, which are derived from alkane molecules by removing a hydrogen atom. Continuous reactions with small precursor molecules result in the growth of the PAH structures until the molecules become large enough to serve as particle nuclei.

However particle inception is a gaseous–solid phase transition forming solid particle nuclei. These particle nuclei undergo surface growth by absorbing surrounding gas phase molecules to form larger spherules. Due to the Brownian motion of the individual spherules inside of a flame, they collide and form particle agglomerates. The last process of particle surface growth and agglomeration continues until the temperature of the agglomerates cools down as they are exiting the flame. Upon cooling, hydrocarbon species such as PAHs and aliphatics may adsorb and condense on the agglomerate surfaces as organic surface coatings (Glassman, 1996). The resulting individual spherules in agglomerates typically measure about 20–40nm in diameter, depending on flame conditions (Seinfeld and Pandis, 1998). The final size and characteristics of agglomerate depends on the temperature evolution encountered during its growth process.

Sulphate

Particulate sulphate is a chemically stable compound at tropospheric temperatures. Gas to particle conversion of sulphur dioxide is the dominant source of sulphate. Among a variety of gaseous sulphate precursors, only two make a major contribution – dimethyl sulphide (DMS), which is of biogenic origin and SO_2 which is dominated by anthropogenic sources (Penner *et al*

2001; Dentener *et al*., 2006). Sulphur dioxide volcanic emissions are emitted from mountain tops in the free troposphere. It is less subjected to dry deposition and is therefore more efficiently converted to sulphate than most anthropogenic SO_2 (Penner *et al*., 2001). Over the past century, SO_2 emissions from anthropogenic sources have grown dramatically with large quantities entering the atmosphere each year mainly from burning of fossil fuels, particularly coal, with minor additional sources from smelting and biomass burning (Andreae and Rosenfeld, 2008).
Anthropogenic sulphate emissions largely derived from fossil fuel combustion and metal smelting exceed the natural emissions of sulphur-containing gases, and are dominant in the Northern Hemisphere, where over 90% of anthropogenic emissions takes place (Charlson *et al*., 1992). Particulate sulphate like most other aerosols is known to contribute to climate forcing. The residence times of sulphate aerosol are short in comparison to its mixing rate and particles are thus concentrated downwind of industrial regions. Tropospheric sulphate aerosols have a strong seasonal cycle in the forcing with a pronounced peak in the summer months in the Northern Hemisphere (Charlson *et al*., 1992).

The oxidization of Sulphur dioxide to sulphate, can take place through many reaction mechanisms such as gas-phase processes, photochemical and radical processes, aqueous-phase processes and heterogeneous processes (Held *et al*., 1996). However, very few reactions can take place to sufficiently influence the atmospheric sulphate burden (Piketh, 2000). Most of the atmospheric sulphate aerosol is formed by oxidation of volatile precursors to gaseous H_2SO_4 followed by nucleation and condensation processes to form particles (Andreae and Rosenfeld, 2008). Anthropogenic SO_2 emissions are chemically converted to sulphuric acid in the atmosphere in the gaseous phase. Gaseous H_2SO_4 is formed via rapid oxidation of SO_2 with OH radical to form HSO_3 molecules. HSO_3 reacts with oxygen to give SO_3 and HO_2 and this is converted to H_2SO_4 (Reiner and Arnold, 1993; McGonigle *et al*., 2004). The reaction is written as

$SO_2 + OH \rightarrow HSO_3$

$HSO_3 + O_2^- \rightarrow SO_3 + HO_2$

$SO_3 + H_2O \rightarrow H_2SO_4$

Sulphur dioxide oxidation rate by the hydroxyl radical exceeds all other processes (Piketh, 2000). Its oxidation rate is highly dependent on the concentration of the hydroxyl radical, which in turn is formed by photochemistry and thus occurs most abundantly during daylight hours

(Chylek *et al*., 1995). These products of chemical transformations are accompanied by other short and long lived pollutants which may be locally generated or arise from long-range air transport (Igbafe, 2007). Heterogeneous reaction occurs in different phases of cloud or fog water, or as aerosol droplets involving the transfer of SO_2 and oxidant species to the droplet phase with subsequent liquid phase oxidation (Warnneck, 1988; Piketh, 2000). The homogenous reaction is assumed to be the dominant reaction over southern Africa. This is as a result of the dry conditions that prevail over the subcontinent for most of the year (Piketh, 2000).

Field studies of SO_2 oxidation to SO_4^{2-} have been performed in the downwind regions of sufficiently isolated sources with regard to plumes from electric power stations. The SO_2 to SO_4^{2-} conversion rate during summer undergoes a diurnal cycle with maximum values occurring at midday and minimum values at night (Wilson, 1981). Moreover, similar analysis performed at four coal-fired power stations has shown the seasonal variation of the conversion rate to be maximum in summer and minimum in winter. These results clearly establish the importance of photochemical conversion mechanisms (Meagher *et al*., 1983). The SO_2 oxidation rate is therefore much enhanced by the presence of oxidants or its precursors carried along with well-aged polluted air masses (Warneck, 1988).

Whether black carbon and sulphate principally warm or cool the atmosphere depends on the aerosol single scattering albedo (SSA) (Novakov *et al*., 2005). The radiative properties of individual aerosol particles depend on the extent to which black carbon is mixed with primarily scattering aerosol components such as sulphates and organics (Stier *et al*., 2007). The amount of light absorbed by each particle is measured by its single scattering albedo (SSA) which is the ratio between the light extinction due to scattering alone and the total light extinction from both scattering and absorption. The aerosol SSA is a key parameter in determining the influence of the aerosols on global and regional climate (Novakov *et al*., 2003). Black carbon and sulphate aerosols, as strongly absorbing and perfectly reflective aerosols respectively, have the greatest influence on the net SSA of anthropogenic aerosols. If the SSA lies below a critical value, the combined aerosol-earth system reflects less energy back to space than the Earth's surface alone, leading to a net warming of the earth. However, if the SSA lies above a critical value, aerosols will cause cooling under almost all conditions (Seinfeld, 2008).

Nitrate

Particulate nitrate arises primarily from the oxidation of NO_x (NO and NO_2), a by-product of high-temperature combustion processes associated with vehicles and industrial activity (Seinfeld and Pandis, 1998). NO_x is also produced from natural sources such as biogenic soil emissions, lightning and biomass burning (Penner *et al*., 1998; Beirle *et al*., 2004). The ultimate destination of NO_x is the formation of nitrates as either particles or acid (Yang *et al*., 2005). Nitrate has until recently not been considered in assessments of the climatic effects of aerosols. Still, current models often ignore the role of nitrate, or assume that it is only present in the coarse fraction (Derwent *et al*., 2003; Stier *et al*., 2005). Nitrate aerosol can occur either as a component of the coarse particle fraction, where it is formed by the reaction of HNO_3 with sea-salt particles or as a reaction product with mineral dust or it can be found in the fine mode as ammonium nitrate in the sub-micron size fraction (Pakkanen, 1996; Kleeman *et al*., 1999; Zhuang *et al*., 1999). The size distribution depends heavily on location and weather conditions. The production of secondary aerosol nitrate in the sub-micron fraction is strongly dependent on the abundance of gaseous NH_3 and HNO_3, particulate H_2SO_4, temperature and humidity (Metzger *et al*., 2002b; Bauer *et al*., 2007).

Fine mode nitrate is formed by the homogenous gas-phase transformation of NO_x to HNO_3, which later reacts with ammonia gas to form ammonium nitrate, or reacts with pre-existing fine particles (Zhuang, *et al*., 1999). However, ammonium nitrate has a high volatility and will therefore dissociate easily into gas-phase nitric acid and ammonia at low humidity and high temperature. While SO_2 emissions are fairly easy to reduce because they are strongly tied to sources such as power plants, the emissions of NO_x the precursor of aerosol nitrate, have proven much more difficult to control (Andreae and Rosenfeld, 2008). This suggests that the importance of aerosol nitrate is likely to increase substantially over the current century (Bauer *et al*., 2007). Nitrate influence on cloud microphysics is different in both the coarse and fine mode. Nitrate simply reduces chlorine in sea salt particles, and the CCN properties of the chemically modified particles are not significantly different from the original SSA. In contrast, the deposition of HNO_3 on otherwise insoluble dust particles, which is favorable in atmospheres rich in dust and low in gaseous ammonia, sharply increases their CCN activity (Zhang *et al*., 2003; Laskin *et al*., 2006).

The chemical formation of nitrate emitted into the atmosphere occurs with the gas-phase processes. As illustrated by Jenkin and Clemitshaw (2000) and Brasseur *et al*., (2003), throughout the diurnal cycle, NO_2 is slowly converted into NO_3 by reaction with O_3.

$$NO_2 + O_3 \rightarrow NO_3 + O_2^- \qquad (1.2)$$

During daylight however, NO_3 is efficiently removed by photolysis leading mainly to the regeneration of both NO_2 and O_3 and also by reaction with NO leading to the regeneration of NO_2.

$$NO_3 + h\nu \rightarrow NO_2 + O_3 \qquad (1.3)$$

$$NO_3 + NO \rightarrow 2NO_2 \qquad (1.4)$$

Consequently, the night time chemistry of NO_3 differs from the daytime behaviour in the sense that it provides a route for conversion of NO_x to HNO_3 which could be as high as 50% of the daytime route via $OH+NO_2$ (Brasseur *et al*., 2003). Thus, the importance of its daytime chemical formation is severely limited and less important (Jenkin and Clemitshaw, 2000) (Figure 1.7).

Considering the night time chemistry of nitrate, the concentration of the OH radical in addition to the absence of sunlight is significantly suppressed since it is produced mainly from the photolysis of stable molecules. Thus, once NO_2 is formed from the reaction in equation 1.5 it cannot be photolysed to regenerate NO, or removed at a significant rate by reaction with OH in equation 1.6. Therefore, NO is rapidly converted to NO_2 provided the ambient concentration of O_3 is sufficiently high, in which case it is slowly converted to NO_3 by equation 1.2 (Figure 1.8).

$$NO + O_3 \rightarrow NO_2 + O_2^- \qquad (1.5)$$

$$OH + NO_2 \rightarrow HNO_3 \qquad (1.6)$$

The reaction in equation 1.4 is therefore unimportant at night because NO is only present in significant concentrations close to points of emissions where O_3 has been titrated, and NO_3 cannot be formed. At night, however the principal reaction of NO_3 is often with NO_2 to set up equilibrium with N_2O_5.

$NO_3 + NO_2 \rightarrow N_2O_5$ (1.7)

$N_2O_5 + H_2O \rightarrow 2HNO_3$ (1.8)

The subsequent heterogeneous dissolution of HNO_3 and N_2O_5 into water droplets gives rise to aerosol nitrate in equation 1.8 (Yeatman *et al*., 2001). However, since the end product N_2O_5 is thermally unstable and decomposes on a similar timescale as NO_3, reaction with equation 1.7 is readily established with NO_3 and N_2O_5 present in comparable concentrations. As a result, their behavior is strongly coupled and any process removing one of the species is also a sink for the other. Thus, at sunrise both species rapidly fall to very low concentrations due to the efficient photolysis of NO_3 (Jenkin and Clemitshaw, 2000).

There are two possible pathways for the transfer of this gaseous nitric acid to the aerosol phase. The first possibility is through neutralization by a base, such as ambient ammonia released from vehicles equipped with catalytic converters which can react with nitric acid to form NH_4NO_3. This equilibrium is influenced by the ambient conditions such as temperature and humidity as well as the presence of other inorganic compounds, especially sulphate. This is because the ammonia preferentially reacts with it and only the remaining NH_3 can react with the nitric acid. This means that reductions in sulphate concentrations could cause an increase in the particulate nitrate concentration. The second pathway is absorption of the nitric acid by water droplets producing acid aerosols. Nitric acid is one of the most water-soluble atmospheric gases and after dissolution; it dissociates to nitrate increasing its solubility and the droplet acidity (Seinfeld and Pandis, 1998; Gomez-Moreno *et al*., 2007).

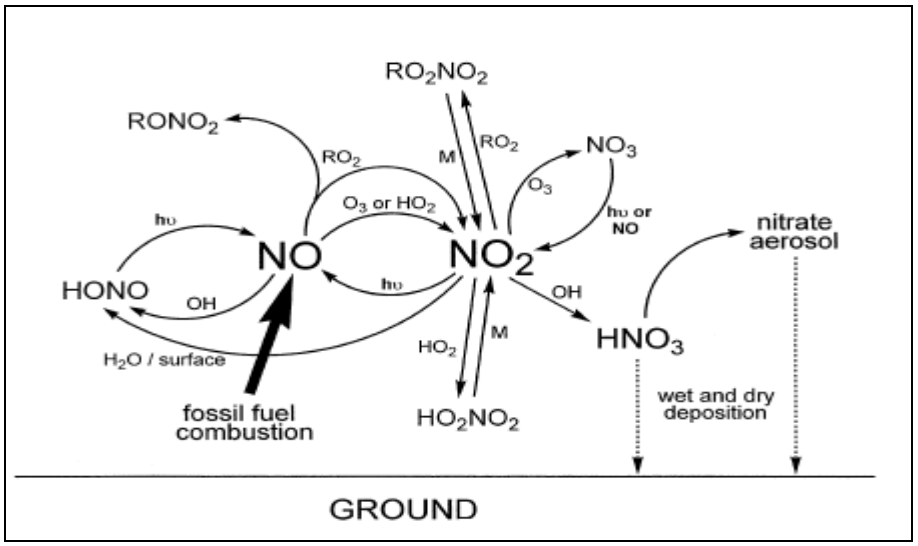

Figure 1.7. Daytime Interconversions of oxidized nitrogen compounds in the troposphere (Jenkin and Clemitshaw, 2000).

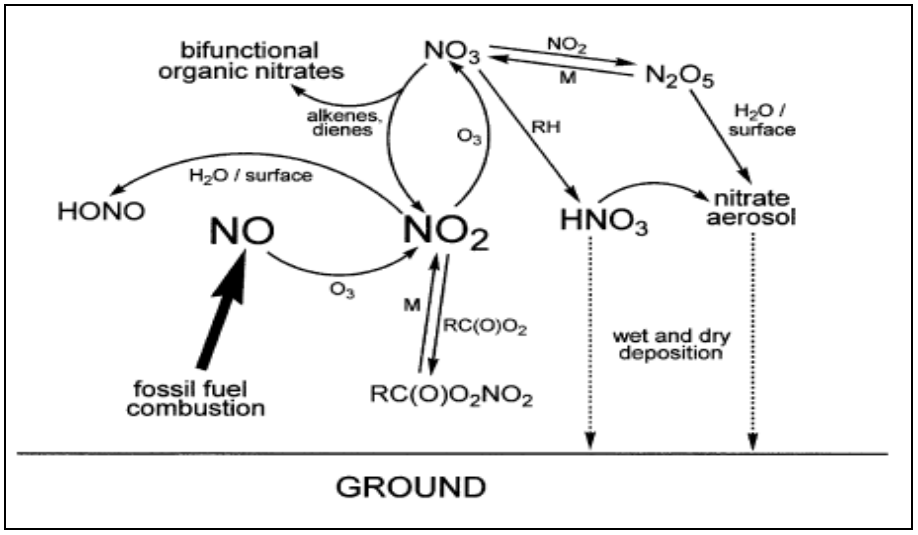

Figure 1.8. Nighttime Interconversions of oxidised nitrogen compounds in the troposphere (Jenkin and Clemitshaw, 2000).

1.2.8 Overview of meteorological parameters

The daily variation in air temperature near the earth's surface is controlled primarily by the input of energy from the sun and the outgoing energy from the earth's surface. However, whenever incoming solar radiation increases in intensity and exceeds outgoing heat energy, the air

temperature rises. Where outgoing energy exceeds incoming energy, the air temperature falls substantially to its minimum.

Relative humidity is a percentage that reflects how close the air is to saturation, where 100% relative humidity indicates fog or rain and single-digit relative humidity indicates extremely dry air. For a given amount of water vapor in the air, relative humidity will decrease as air temperature rises. As the air temperature drops, the relative humidity increases because the air is approaching saturation. Typically, the highest relative humidity occurs in the early morning during the coolest part of the day. As the air warms during the day, the relative humidity decreases, with the lowest values usually occurring during the warmest part of the afternoon. Consequently in many cases, the air's total vapor content varies only slightly during an entire day, and so it is the changing air temperature that primarily regulates the daily variation in relative humidity.

Relative humidity is a measure of the amount of water vapor contained in the air at a particular temperature compared with the total amount of water vapor the air can contain at that temperature. Extremes of temperature and relative humidity and rapid fluctuations in these two can lead to a range of problems. Acceleration of chemical deterioration processes occurs when temperature and relative humidity are too low or too high. Temperature affects the rate at which chemical reactions takes place. For example, a temperature rise from 20 to 30 ^{o}C may double the rate of some degradation reactions. This worsens if pollution also contributes to these chemical reactions. Many atmospheric aerosols-airborne particles that reflect the sun's energy away from the earth and into space are very sensitive to relative humidity changes. For instance, when a hygroscopic aerosol (an aerosol that absorbs moisture from the air) begins to dissolve, its properties change as it absorbs water and the aerosol gets larger. Most hygroscopic aerosols stay in a dry, crystalline form in the atmosphere if the local relative humidity is below some critical value, around 65 percent. If the relative humidity rises above that level, they absorb water and dissolve. As the relative humidity increases, the particles continue to grow in size by absorbing more water from the air. If the relative humidity level falls below the critical value, the aerosol begins to loose water and returns to its original state.

Wind is characterized by its direction, speed, and gustiness. On a windy day, turbulent eddies mix polluted and cleaner air and thereby accelerate dilution. When the wind is calm, dilution takes a very slow process of molecular diffusion. Accordingly, as the capacity of wind speed doubles, the concentration of air pollutants is halved. Wind speed is influenced by surface roughness and also by horizontal air pressure gradients. Over a broad area at the centre of an anticyclone, horizontal air pressure gradients are weak. Thus, pollutants do not disperse readily because winds are very light or calm. However, stronger winds and rapid dilution of air pollutant occur within a cyclone with the presence of steeper air pressure gradient. Also associated with a cyclone is the rain or snow that cleans the air by washing pollutants to the ground.

The wind acts as the driving force of atmospheric constituent. Over the Highveld, mean daytime surface winds over much of the region show a predominance of north to north-westerly winds, with easterly winds occurring as the next most frequent. As a result of increased cyclonic occurrences associated with westerly weather disturbances, the frequency of south-westerly winds increases during winter. During the night a greater incidence of north-easterly winds occurs than north-westerly winds. However, substantial increases of light and topographically induced winds occur from the east and south-easterly sectors during the night. Annual surface wind speed varies between 2 and 4 m/s with maximum speed occurring during late winter and spring (Held *et al*., 1996).

Winter period on the Highveld is mostly dominated by the existence of anticyclonic circulation, mainly sustained by the expansion of the south Indian Ocean anticyclone over the relatively colder interior of Mpumalanga. The “winter mode” 800 hPa wind circulation (about 350 m AGL) clearly indicates that the boundary layer winds are dominated by the Indian Ocean anticyclone which extends inland to the Northern Province (Tosen and Jury, 1986). As such, due to the northerly movement of the anticyclonic pressure belts in winter, the Mpumalanga Highveld is dominated by westerly and west-north-westerly winds. However, in summer, as a result of the southward migration of these pressure belts, the circulation is distinctly recognized by the presence of northerly-component winds. These winds gradually change direction towards north-north-west in late summer and afterwards are reversed to westerly with the approach of autumn (Held *et al*., 1996).

1.3 Research objectives

In this dissertation, the aim is to investigate the characteristics of particulate matter over the industrialised Highveld of South Africa. Temporal behaviour of aerosols will be investigated at the Elandsfontein monitoring site at both diurnal and seasonal time scales.

The specific objectives of this research are to:

- Identify the seasonal variations in aerosol concentrations and factors causing minimum and maximum aerosol concentrations.
- Establish the diurnal variation of aerosol concentrations on the Highveld.
- Investigate the sources of aerosols and seasonal effects on the concentration of aerosols.
- Determine the fraction of PM10 composed of sulphates, nitrates and black carbon on the Highveld.

****

The importance of aerosols in terms of air quality, size distribution and chemical composition has been discussed. Also considered are the various transport mechanisms of atmospheric aerosols ranging from recirculation and accumulation of pollutants to the sub continental scale circulation over southern Africa. Identifying temporal behaviour of aerosols on the time scales of seasonal variation and diurnal variability were highlighted as the objectives of this study.

CHAPTER TWO

METHODOLOGY

Procedures for the collection and analysis of data will be discussed in this chapter. The location of the Elandsfontein sampling site and the instruments used to obtain particulate matter data are described. Methods used to analyze the spatial and temporal distribution of aerosol loading are discussed. The compilation of pollution roses from meteorological data and the investigation of pollution episodes are described.

2.1 Elandsfontein and the Highveld

The Highveld plateau is about 1600 m above sea level. It gradually slopes downwards towards the west and south, with the eastern boundary being the escarpment of the Drakensberg. The southern area is dominated by the Vaal Basin 1400 m above sea level, which drains cold air from the surrounding plateau of the Gauteng region (Held *et al*., 1996). The Highveld region which spreads across Mpumalanga and Gauteng has a diversity of natural vegetation, cropland, and plantation forests (Figure 2.1). The land area is used for urban, industrial and mining activities with various industries (steel, mines, coal-fired power stations) operating on the Mpumalanga Highveld (Held *et al.,* 1996; Piketh *et al*., 1999). Anthropogenic aerosols are produced by major industries and the region is subjected to increased amounts of atmospheric pollutants.

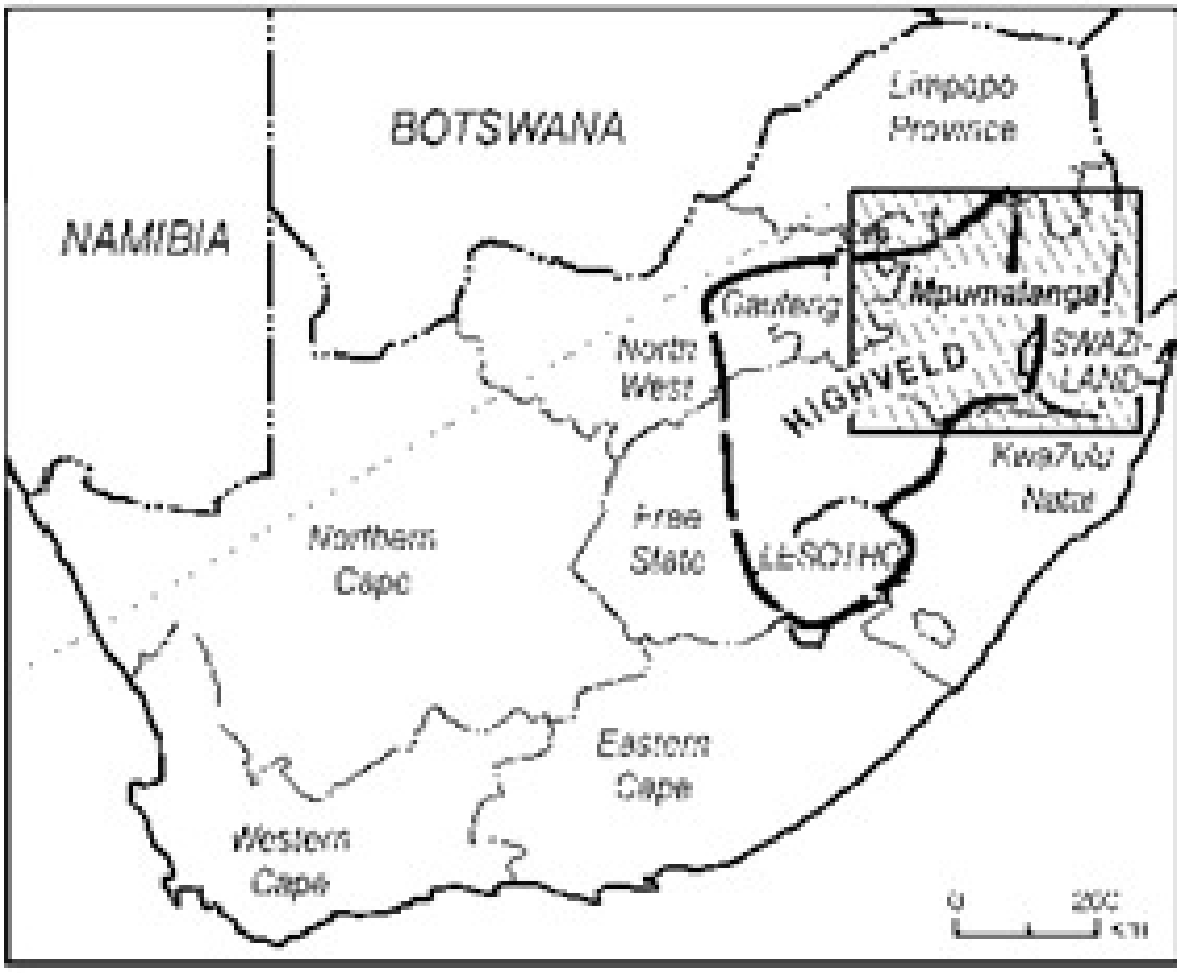

Figure 2.1. Map of South Africa indicating the Highveld region in thick broken lines.

Eskom's ambient air quality monitoring network currently consists of ten ground-based monitoring sites, generally located near power stations, in residential areas or in areas representative of a wider region. The data that will be utilised for this study was collected at the Elandsfontein air quality monitoring station, which is situated at an altitude of 1660 m (Figure 2.2). Elandsfontein is a monitoring supersite not located in the immediate vicinity of any source, but surrounded by coal mines, coal-fired power stations and a petrochemical plant. The site was chosen for this study because it is representative of general conditions on the industrialised Highveld region.

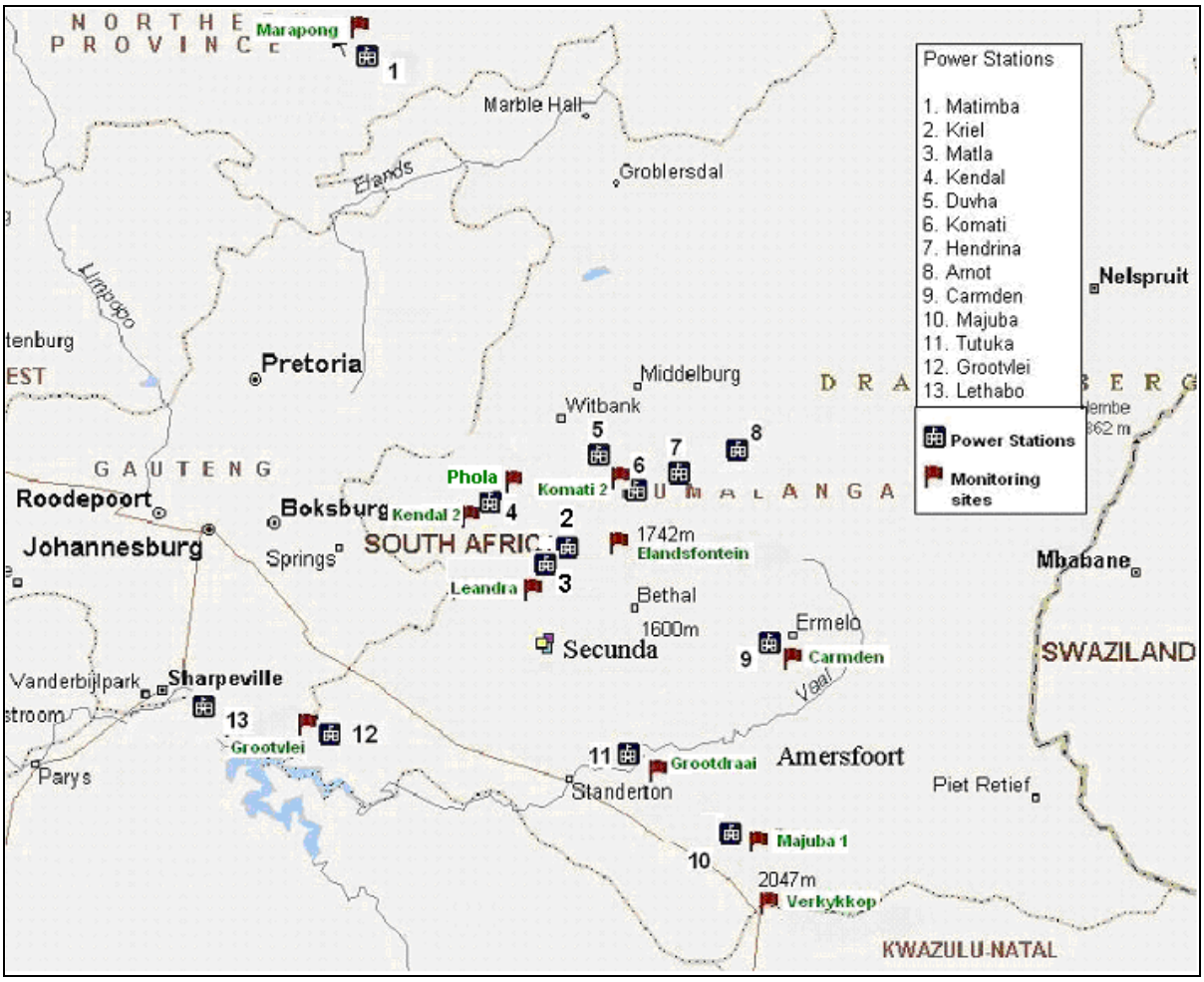

Figure 2.2. Map of Eskom's power stations and air quality monitoring stations on the South African Highveld (Eskom intranet, 2006: http://acgdev/envirmetadatabase/Metadatabse/Metadatabase_INDEX.asp).

Numerous studies have been undertaken over the Highveld where particulate matter has been characterised with respect to its regional visibility impairment, trends and seasonal variation, size distribution and optical properties (Held *et al*., 1993; Maenhaut *et al*., 1996; Tyson *et al*., 1996a; Garstang *et al*., 1996b; Scheifinger and Held *et al*., 1997), but there has been no full characterisation of the study of particulate matter utilising long-term continuous data, as has been recorded at the Elandsfontein monitoring site.

2.2 Data capture

Data availability in 2005 is shown in Table 1.1 below. The overall data capture was high and satisfactory for black carbon, PM10, backscattering coefficient of light, temperature, relative humidity, sulphur dioxide, sulphates, wind direction, and wind speed. Data recovery for the nitrate was limited to 53% owing to periodic particulate nitrate monitor malfunction.

Table 1.1. Data captured at the Elandsfontein monitoring site in 2005.

Parameters	Data capture (%)
Black carbon	99.36
Backscat coefficient of light	84.65
PM10 by beta gauge	95.59
Temperature	99.48
Relative humidity	97.23
Nitrates	53.65
Sulphur dioxide	95.85
Sulphates	84.95
Wind direction	99.48
Wind speed	99.48
Average data availability	92.70

2.3 Instrumentation

Particulate matter data were measured at the Elandsfontein air quality monitoring site using a Thermo ESM Andersen beta gauge, a Thermo Electron Corporation multi-angle absorption photometer, an Ecotech integrating nephelometer, a Rupprecht and Patashnick particulate nitrate monitor, and Rupprecht and Patashnick ambient particulate sulphate monitor. In addition, key meteorological parameters were also recorded at the site.

Sample collection

The samples were collected on site at Elandsfontein monitoring station. All the instruments used were housed in an air-conditioned hut. Sample inlets for each of the instruments come through the roof of the monitoring station with approximately 3.5 m above ground level. Each instrument draws its sample from the main borosilicate glass inlet sample manifold. An air sampling extraction fan forces flow through the glass inlet manifold and exhausts unused air. The sample collection flow rates for each instrument include: beta gauge 1000Lpm, multi-angle absorption photometer 1004 L/h, Rupprecht and Patashnick ambient particulate nitrate and sulphate monitor 900 ± 50 cc/mm and nephelometer 0.3 L/m.

Beta gauge and multi-angle absorption photometer uses a glass fibre filter tape as supplied by the instrument manufacturers. These instruments are continuous monitors, whereby the sample tape moves to a new position automatically every 24 hours at which time the instrument carries out an automatic zero check and adjustment. Span calibrations are carried out approximately every 3 months using calibration foils. The sulphate monitor is fitted with a 25 mm membrane filter between the pulse generator and pulse analyser. The nitrate monitor on the other hand is fitted with a 25 mm Teflon filter. According to the manufacturers instructions these filters were changed every month or as required otherwise. The sulphate and nitrate monitor had zero and span checks conducted every two weeks, and full dynamic calibrations were conducted every three months. Calibrations for all the instruments were conducted in accordance to the manufacturers, USEPA and SANAS requirements using a gas dilution method.

Nephelometer does not use any filters and it works based on the principle of back scattering of light. Calibration and background check is carried out every four to six weeks. The sample collection time interval for all instruments is by hourly averages. Readings from all analysers are logged every ten seconds; the logger calculates the mean and reports it on an hourly basis.

2.3.1 Beta gauge

PM10 is measured with continuous particulate monitoring instrument model FH 621R manufactured by Thermo ESM Andersen (Figure 2.3). This instrument is designed to continuously measure the mass concentration of the suspended particles in ambient air (Chueinta and Hopke, 2001). The particulate measurement utilizes the radiometric principle of beta attenuation through a two beam compensation method. This process achieved very high measurement stability to the extent that as each measurement value is determined, a simultaneous reference value is also determined in a separate measuring section. The dual beam compensation method eliminates physical temperature and pressure changes. It has a short time resolution of one second which determines particulate concentrations at very low concentration levels. The instrument simultaneously measures, observes and displays accumulated particle mass during the collection of the dust.

Ambient air is drawn into the Thermo ESM Andersen through the sampling system. The procedure starts by a clean section of the filter tape moving into the dust sampling measuring position. Ambient air containing dust particles is then sampled and deposited on the filter tape, with enough of the sample drawn through the filter tape to provide a measurable amount of particulate. The dirty filter tape is then taken back under the beta source and measured again for exactly the same amount of time as the initial baseline measurement. The difference between the two measurements i.e. beta rays measured from the clean filter tape and from the collected sample spot is proportional to the mass concentration on the tape. This difference is used to determine the particulate concentration. The influence of air temperature, unsteady humidity in ambient air especially during summer and the danger of water condensation in the sampling tube are the major limitations of the instrument. These limitations can be prevented through the utilization of the heated sampling tube (Chueinta and Hopke, 2001).

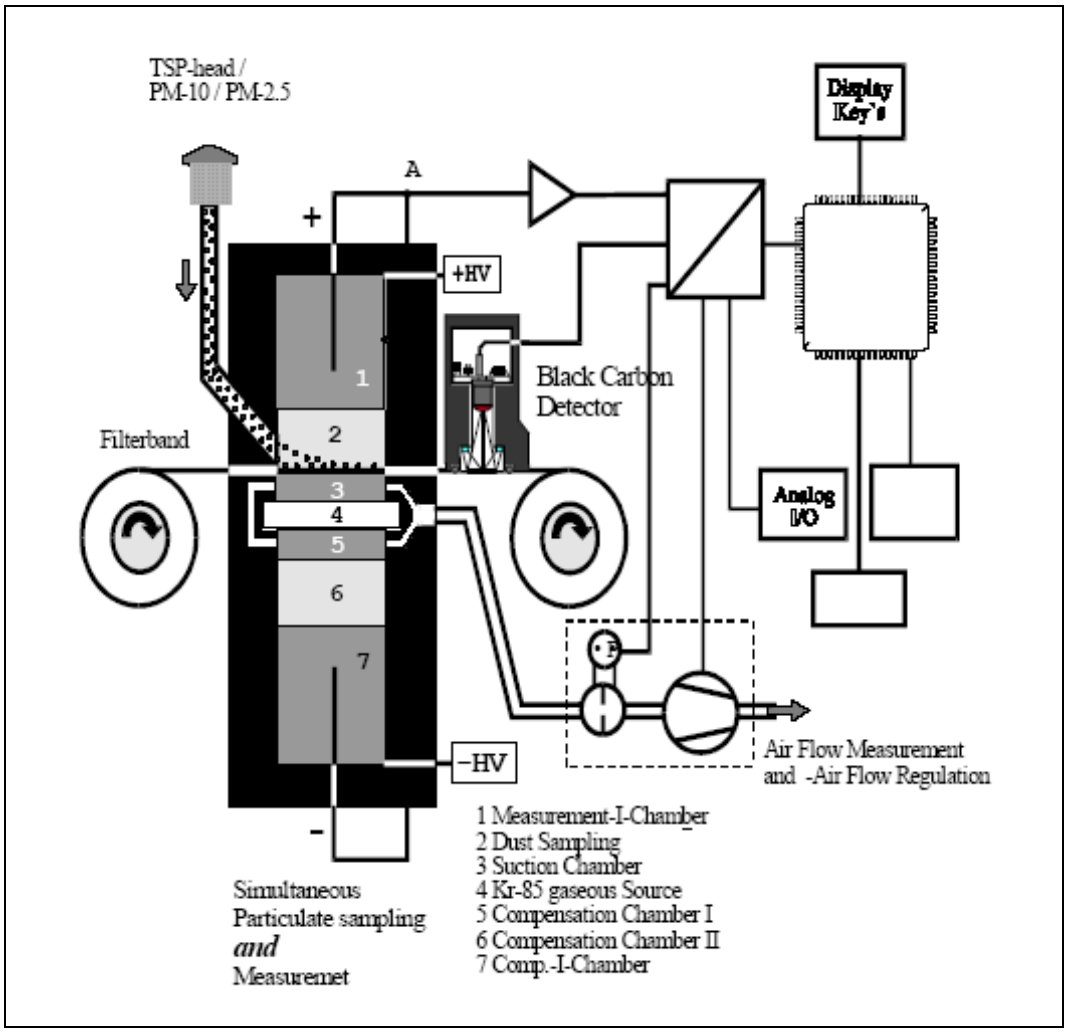

Figure 2.3. Principle of operation of particulate continuous monitoring (http://www.instrumentcompaniet.no/files/THERMO_Datablad/FH621R-english.pdf).

In the beginning, beta gauges were particularly used for aerosol monitoring near sources such as in smokestacks and in coal mines (Salkowski, 1964; Dresia and Spohr, 1971; Lilienfeld and Dulchinos, 1972). Later, they were improved to monitor ambient aerosol concentrations (Husar, 1974; Stevens *et al*., 1980; Courtney et al., 1982; Jaklevic *et al*., 1983; Gourdon, 1983; Gotoh, 1992). With developments in technology, beta gauges are now used for continuous and semi continuous aerosol mass monitoring (Chueinta and Hopke, 2001).

2.3.2 Multi-angle absorption photometer

Black carbon is the most efficient light-absorbing aerosol species in the visible spectral range. Thus, the measurement of aerosol light absorption in the visible spectral range is strongly correlated to the measurement of black carbon (Lindberg *et al*., 1993; Petzold and Schonlinner, 2004). Aerosol light absorption is measured with Multi-angle Absorption photometer (MAAP) model 5012, manufactured by Thermo Electron Corporation. An approach used for aerosol absorption measurement is the collection of aerosol particles on a fibre filter matrix and the subsequent analysis of the sampled aerosol by optical means (Petzold *et al*., 2005). This method has an advantage of sampling over a long period of time in order to improve the limit of detectable absorption coefficients well below 10^{-6} m^{-1} ($\equiv$1 M m^{-1}). Fibre filters are depth filters where the particles are collected not only at the very surface of the filter but also penetrate into the interior of the filter matrix. This filter type has an advantage of simple handling and robustness during sampling period and very high deposition efficiency for even sub 100 nm particles (Petzold and Schonlinner, 2004).

Multi-angle absorption photometer (MAAP) combines simultaneous transmittance and reflectance measurements with the analysis of the particle-loaded filter by a two stream approximation radiative transfer scheme. The black carbon content of the aerosols is continuously determined by simultaneously measuring the optical absorption and scattering of light by the particles collected on the filter tape. The explicit treatment of light-scattering effects caused by the aerosol and by the filter matrix in the radiative transfer scheme is expected to improve the determination of the aerosol absorption coefficient by MAAP (Petzold *et al*., 2002).

The instrument is based on simultaneous measurement of radiation penetrating through and scattered back from a particle-loaded fibre filter. The particle-loaded filter is treated as a two-layer system. The uppermost layer is composed of particles deposited on filter fibres. This layer is referred to as the aerosol-loaded layer of the filter while the remaining part of the filter consists of the particle-free filter matrix (Figure 2.4, below). Particle deposition is observed only within the upper 10–15% of the filter sample thickness. The transition region between particle-loaded filter layer and particle-free matrix extends over less than 5% of the particle-loaded layer depth. Hence, the microscopy analysis of filter cross-sections supports the assumption of a two layer model (Petzold and Schonlinner, 2004).

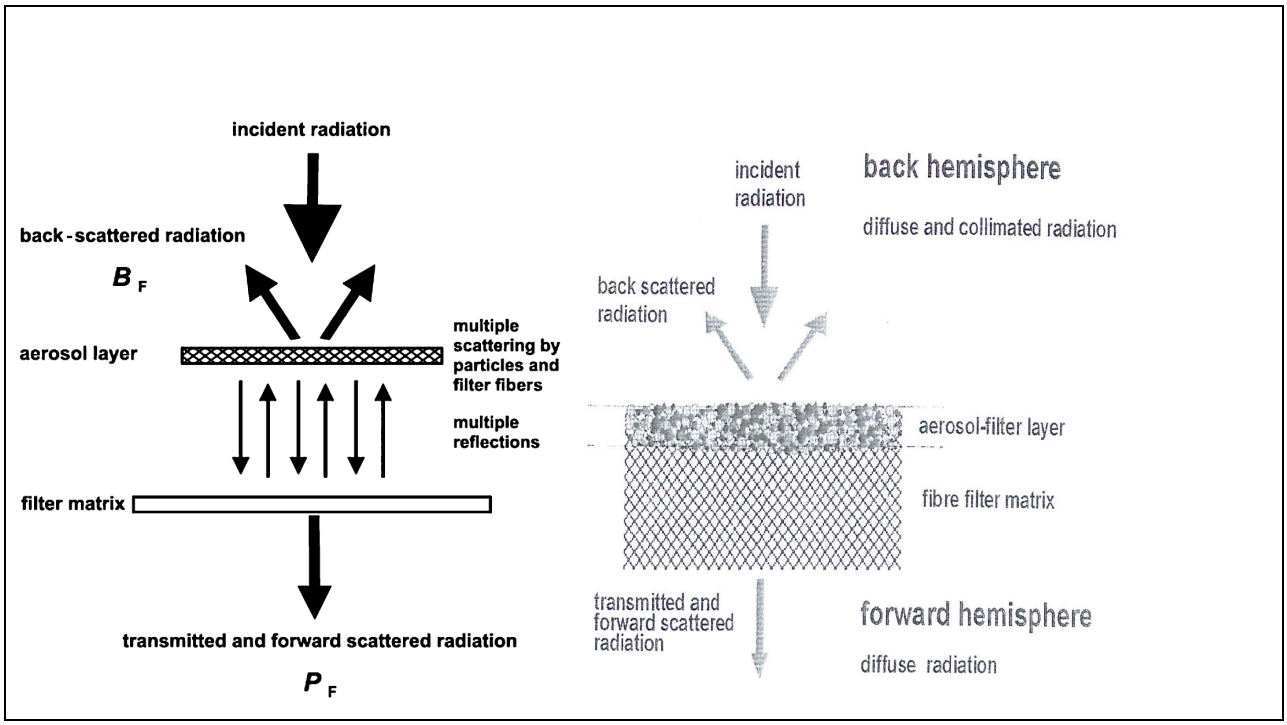

Figure 2.4. Schematic representation of radiation processes in the two layer system consisting of an aerosol-loaded filter layer and the particle-free filter matrix (right); multiple reflections of radiation between the two layers (left) (Petzold and Schonlinner, 2004).

Radiative transfer technique is used for the determination of the aerosol absorption coefficient of the deposited aerosol. These radiative processes affect two different processes. First, the radiative interaction within the aerosol-filter layer which depends on the optical properties of the layer, i.e., optical thickness, single scattering albedo, and angular distribution of scattered radiation. Second, the radiative interaction between the particle-loaded aerosol-filter layer and the particle-free filter matrix. The radiative interaction within the particle-free filter matrix is not considered because the optical properties of this layer are not affected by deposited particles and therefore remain unchanged from particle-free to particle-loaded filter samples (Petzold and Schonlinner, 2004).

Considering the radiative processes, the perpendicularly incident radiation is collimated (lined up). The radiation passing through the aerosol-filter layer is mostly diffuse due to multiple scattering processes with only a small fraction remaining collimated. The radiation invading on the particle-free filter matrix is thus partly collimated (transmitted through the aerosol-filter layer) and partly diffuse (scattered forward by the aerosol-filter layer) (Figure 2.4, left). The radiation scattered back from the aerosol-filter layer as well as from the filter matrix toward the aerosol-filter layer is considered to be diffused (Petzold *et al*., 2002).

Radiative properties of the particle-loaded filter measured are the transmitted, forward-scattered and the back-scattered radiation. These properties are described in terms of energy budget equations for the particle-loaded filter, the aerosol-filter layer alone, and the blank filter alone (equation 2.1 and 2.2) (Hanel, 1987). The optical properties of the various layers are described as the fractions of forward scattered, back scattered and transmitted radiation by the parameters F, B, and T, respectively. The total fraction of radiation passing through a layer is P=T+F. The different layers are denoted by subscripts 'L' for the particle-loaded aerosol-filter layer, 'M' for the particle-free filter matrix, and 'F' for the composite system consisting of the aerosol-filter layer and the particle-free filter matrix. The superscript '0' indicates the blank filter while no superscript denotes a particle-loaded filter sample. Additional budget properties for an illumination by diffuse radiation are needed. These are marked by the superscript '*'.

The radiative transfer approximation is positioned in two ways. First, the measurable budget properties of the particle-loaded filter, i.e., radiation passage P_F and back scattering B_F for collimated incident radiation, are calculated using a simplified adding method (Hanel, 1987). The adding method considers radiative interactions between the aerosol-filter layer and the particle-free filter matrix. It presupposes multiple scattering within each of these layers. The resulting budget equations have been outlined in detail by Hanel, (1987) as:

$$\frac{P_F}{P_F^{(0)}} = \frac{T_L + F_L}{1 - B_L^* B_M}. \qquad (2.1)$$

$$\frac{B_F}{B_F^{(0)}} = P_L^* \frac{T_L + F_L}{1 - B_L^* B_M} + \frac{B_L}{B_M}. \qquad (2.2)$$

First, the filter properties $P_F/P_F^{(0)}$ and $B_F/B_F^{(0)}$ of equation (2.1) and (2.2) are the measurable fractions of radiation passing through and scattered back from a particle-loaded filter sample with respect to the particle-free filter. Second, the budget properties of the aerosol-filter layer alone, i.e., forward scattering F_L for collimated radiation, back scattering B_L for collimated and B_L^* for diffuse radiation, and radiation passage $P_L^*=F_L^*+T_L^*$ for diffuse radiation are explained in terms of the optical properties of the deposited particles. For this purpose, a two stream approximation is used for the calculation of the aerosol-filter layer budget properties.

One possible approach for determining the diffuse fraction α is to position a second detector in the back hemisphere (Petzold and Schonlinner, 2004). The arrangement of the light source and the detectors in the MAAP optical sensor (left) and the physical realization in the instrument (right) is illustrated in Figure 2.5 below. The measurement of the angular distribution of light scattered back and penetrated through a particle-loaded fiber filter shows that the radiation that has penetrated through the filter is completely diffuse and can be parameterized by a cos θ relationship, with θ being the scattering angle relative to the incident radiation (Petzold *et al*., 2005).

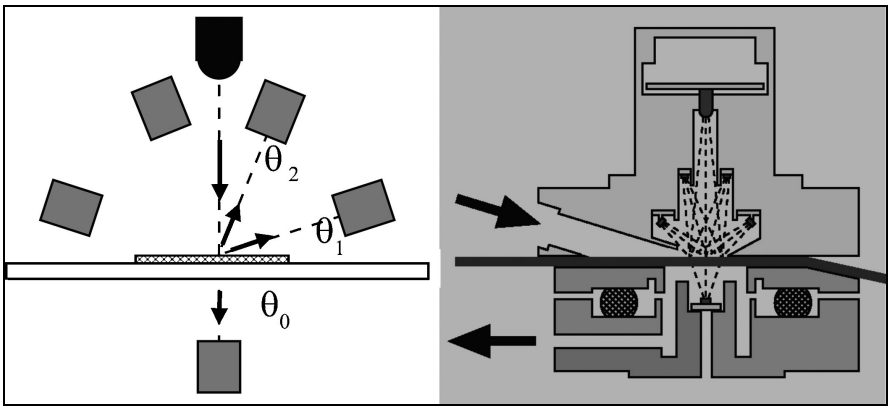

Figure 2.5. Optical sensor of the MAAP. Left: position of the photodetectors at detection angles $\theta 0 = 0\circ$, $\theta 1 = 130\circ$, and $\theta 2 = 165\circ$ with respect to the incident light beam (λMAAP = 670 nm). Right: layout of the MAAP sensor unit, arrows indicate the airflow through the sensor unit across the filter tape ((Petzold *et al*., 2005).

The back-scattered radiation contains a diffusely scattered fraction proportional to cos ($\theta - \pi$) and a fraction that is parameterized best by a Gauss law proportional to exp [$-1/2(\theta - \pi)2/\rho 2$], with ρ being a measure for the surface roughness of the aerosol layer deposited on the filter. The Gaussian-distributed fraction of the back-scattered radiation can be taken as radiation "reflected" from a rough surface (Petzold *et al*., 2005). The partitioning of back-scattered radiation between diffuse and Gaussian type depends on the sampled aerosol. The measurement of the radiation penetrating through the filter at the scattering angle $\theta = 0^{o}$ and the simultaneous measurement of the radiation scattered back from the filter at two detection angles $\theta = 130^{o}$ and 165°, permits the full determination of the irradiances in the forward and back hemisphere relative to the incident light beam (Petzold and Schonlinner, 2004). The exact position of the detection angles was chosen such that the partitioning between diffuse and Gaussian types can be determined with highest resolution (Petzold *et al*., 2005).

There are two major constraints that affect the measurement of aerosol optical properties from filter deposited aerosol samples. First, the influence of the aerosol loading of the filter sample on the measured absorption coefficient and second, an enhancement of the aerosol absorption coefficient caused by multiple scattering effects of the fibrous filter matrix and of the light-scattering aerosol components (Bond *et al*., 1999, Ballach *et al*., 2001; Petzold *et al*., 2005). It has been demonstrated in field studies, laboratory experiments, and model studies that the most frequently used filter transmission measurement method for the determination of the aerosol absorption coefficient shows a cross sensitivity to aerosol related light-scattering effects and to multiple scattering effects caused by the filter matrix (Petzold *et al*., 1997; Bond *et al*., 1999; Lindberg *et al*., 1999). In addition, the aerosol loading on the filter and its impacts on the measurement signal requires correction. Thus, a simultaneous measurement of the aerosol scattering coefficient is a requirement for data correction, and this need for data correction poses a serious limitation for filter transmittance methods (Weingartner *et al*., 2003; Petzold *et al*., 2005).

2.3.3 Nephelometer

The light scattering properties of aerosol particles are measured using an ECOTECH M9003 integrating nephelometer. The ECOTECH integrating nephelometer has a standard single

wavelength of 520nm (green). It measures the light scattering coefficient of particles using the geometry of a standard integrating nephelometer.

The instrument is essentially an aluminum scattering chamber that is lined with light absorbing flock paper to reduce scattering off the walls of the chamber. Aerosol enters into the scattering chamber through the inlet port which has a valve enabling direct air sampling, using an external blower capable of delivering a variable flow (Figure 2.6). This depends on the diameter and length of sampling line used and any restriction on the outlet of the nephelometer. At this point a backscatter shutter is added if the backscatter signal is required. The aerosol sample is illuminated at that point over an angle of 7 to 170 degrees by a halogen light source directed through an optical pipe. Subsequently, the sample is viewed by photo multiplier tube (PMT) through a series of apertures which are located at one end of the instrument while aerosol scattering is viewed against the backdrop of a very efficient light trap. The light trap, apertures and a highly light-absorbing coating on all the internal surfaces combine to give a very low scatter signal from the walls of the instrument. The scattered light by the aerosol passes through a series of apertures, the reference chopper, and a lens and then filtered through band pass colour filters (Heintzenberg and Erfurt, 2000).

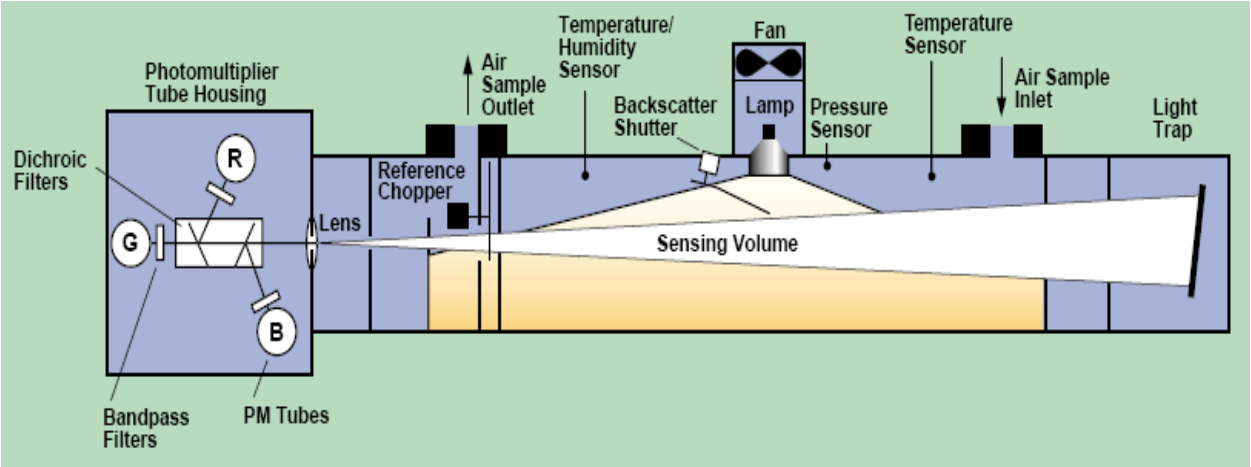

Figure 2.6. Schematic illustration of an integrating nephelometer (http://www.esrl.noaa.gov/gmd/aero/instrumentation/neph_desc.html).

The reference chopper is a circular plate used for calibration of the nephelometer, makes a full rotation 23 times per second and provides three modes of signal detection. The first mode, described above, is a measure of the aerosol light-scattering signal allowed by an opening in the rotating shutter. The second mode blocks all light from detection and give a measurement of the PMT dark current, which is subtracted from the measurement signal. The third mode inserts a translucent portion of the shutter into the direct path of the light to provide a measure of the light-source signal. Consequently, the instrument compensates for any change in the light source (Anderson *et al*., 1996; Heintzenberg and Charlson, 1996).

The backscatter shutter when occupied is positioned between the light source and the aperture and is rotated out of the way when the total scattering signal is required. The nephelometer has a restricted internal geometry which means that the angular integration is shortened between 7 and 170 degrees. This is particularly important for forward scattering. The inside of the instrument undergoes heating through the sampling line. The heater is provided to ensure that under all operating conditions the temperature inside the nephelometer scattering chamber is higher than the ambient air and also to avoid condensational growth on the nephelometer signal (Heintzenberg and Erfurt, 2000).

The output data of the instruments is photon counts. The data are scaled and corrected for time delays in the output of the photo multiplier tubes and in the period of the reference chopper. The scaled and corrected photon counts output data is then passed through a smoothing filter. The smoothing filter is a running boxcar average which depends on the averaging time set by the user. The boxcar average is 1 second for sampling time less than 5 minutes. Utilizing the frequent measurement of the background scattering signal from the wall of the instrument, the nephelometer converts the smoothed, scaled and corrected photon counts to scattering coefficients which are then passed to the logging computer. If there is any zero background measurement performed during the operation of the nephelometer, it will also be logged into the computer (Anderson *et al*., 1996; Heintzenberg and Charlson, 1996).

The instrument has its mode of operation in two modes, polled and unpolled. In unpolled mode, the nephelometer outputs data to a computer at predetermined time intervals. This provides good and accurate timing signals. However, in unpolled mode communication with the instrument is stopped and can only be resumed via the execution of a terminal command or via the serial data

port. In polled mode used for this project, the instrument receives its entire timing information from the logging computer and will output data at intervals set by the user under the software. This provides the user maximum control over the instrument enabling alterations to be made to system parameters (Anderson and Ogren, 1998; Carr and Burridge, 2004).

The nephelometer has a limitation in situations where usage of filtered air is an option. Although unfiltered air was used in this case but during ordinary sampling, the instrument can become contaminated if the air is highly polluted. It is necessary to periodically measure the background signal to ensure that the most accurate aerosol scattering coefficient is made available to users. Another limitation is that the measurement taken will not be accurate when the wall of the instrument reaches 80% of dirt except the nephelometer is thoroughly cleaned. The humidity response of the sensing volume and its distribution inside the chamber remains a major challenge in the quantification of aerosol optical properties at ambient relative humidity (Anderson *et al*., 1999; Heintzenberg and Erfurt, 2000).

2.3.4 Rupprecht and Patashnick ambient particulate nitrate monitor

The Rupprecht and Patashnick ambient particulate nitrate monitor series 8400N measures the concentration of particulate nitrate contained in PM2.5 suspended in ambient air (Stolzenburg and Hering, 2000). The instrument consists of a pulse generator, pulse analyzer, pump, and sampling system. The 8400N series nitrate monitor takes measurements in a default data cycle of ten minutes consisting of an 8 minute sample collection period followed by a 2 minute analysis period. A sample of ambient air containing particulate matter enters into the pulse generator through a PM2.5 sharp cut cyclone operated at 5 L/min (Figure 2.7). The pulse generator is a sample flow line which is enclosed by a sheath air flow. The sheath air flow is made in such a way that it keeps the sample stream and the inside of the instrument as close as possible to the ambient air temperature (Long and McClenny, 2006). Coarse particles are removed from the sample stream by PM2.5 sharp cut cyclone and afterwards the flow is split into a 4 L/min bypass and a 1 L/min sample flow. The 1 L/min sample stream passes through a honeycomb activated carbon denuder. An activated carbon denuder removes acidic gases that would otherwise interfere with the measurement of the ambient particulate nitrate concentration. The sample stream is then conditioned and humidified through a Nafion humidifier as it enters into the collection cell. The humidifier increases the sample relative humidity above the deliquescence

point of the nitrate salt, which causes the particles to grow, thus achieving higher collection efficiency rate. It also results in decreased evaporative losses of semi-volatile nitrate (Long and McClenny, 2006). The fine particles are collected by impaction on a flashing strip of metal that is mounted in the integration collection and vaporisation cell. After collection, the instrument switches to the analysis mode.

In the sample analysis mode, the sample stream that passes through the PM2.5 sharp cut cyclones continues to flow but is bypassed around the collection and vaporization cell while the sample processing takes place and the monitor purges the analysis cell with nitrogen gas (Stolzenburg and Hering, 2000). The nitrogen gas flows through the cell into a NO_x pulse analyzer. The monitor then sends a high current through the flashing strip for approximately 0.05 second to heat the collected particulate matter to approximately 350 ^oC. The particulate nitrate in the collected samples is converted to NO_x by vaporization decomposition processes. The amount of NO_x generated by this process is quantified by the NO_x pulse monitor which is a specially adjusted chemiluminescent NO_x analyzer (Stolzenburg and Hering, 2000). The evolved NO_x is transported by the nitrogen carrier gas into the pulse analyzer. The monitor finally computes the concentration automatically as the ambient particulate nitrate concentration in micrograms per cubic meter ($\mu g/m^3$) transmitting it to an external device through analog and serial interfaces (Harrison *et al*., 2004).

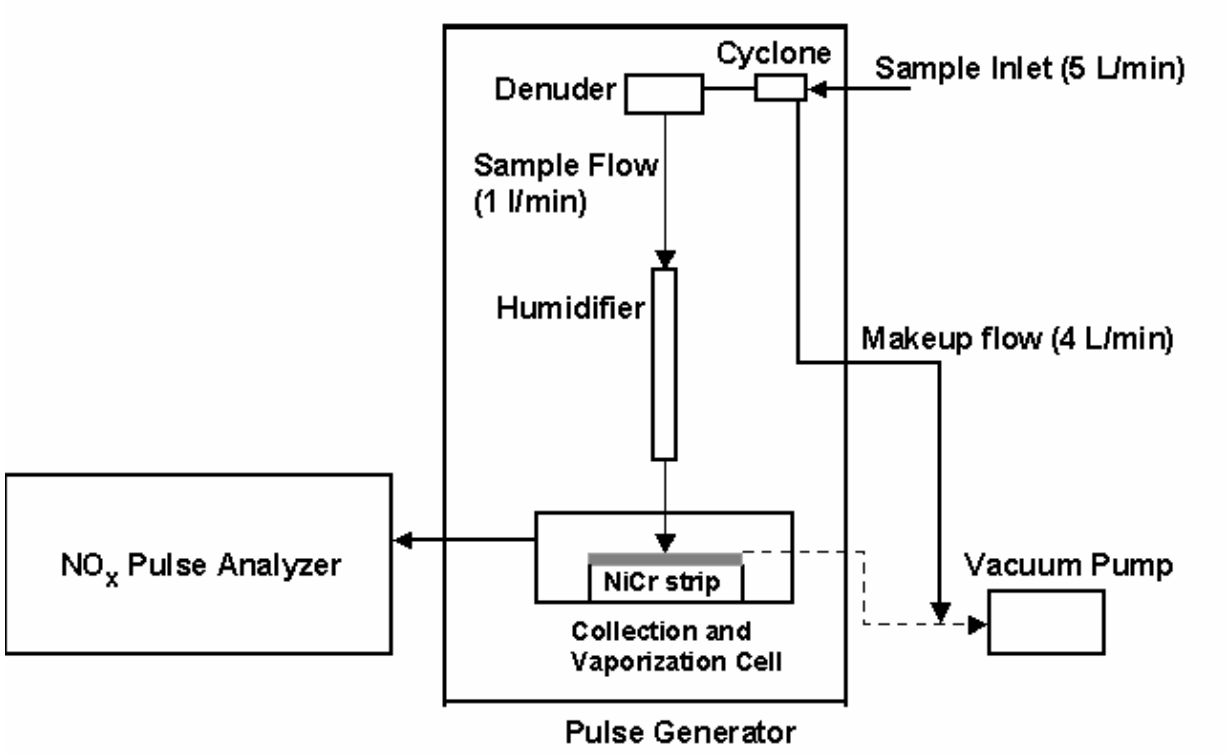

Figure 2.7. Schematic of the Rupprecht and Patashnick 8400N particulate nitrate monitor (Rupprecht and Patashnick, 2001).

The pulse analyser and C-3 pulse generator installation must be in a weather protected location where temperature is kept between 2 and 40°C. The installation of instruments in an air conditioned hut at Elandsfontein ensures that the temperature is maintained within an acceptable range. Studies showed that the Rupprecht and Patashnick instrument always underestimated the nitrate concentration value and also observed an increasing bias as the concentration increased. The incomplete collection of particles in the strip impactor (not all the particles are swollen to 0.14 μm by the humidity) and the temperature differences between the ambient and the impactor strip, especially for those samples taken during very cold days, could be some of the possible reasons for these differences (Gomez-Moreno *et al*., 2007).

2.3.5 Rupprecht and Patashnick ambient particulate sulphate monitor

Sulphate is measured using the ambient particulate sulphate monitor series 8400S manufactured by Rupprecht and Patashnick Co., Inc. The Rupprecht and Patashnick series 8400S ambient

particulate sulphate monitor measures the mass concentration of ambient particulate sulphate contained in coarse particulate matter less than or equal to 10 μm (Rupprecht and Patashnick, 2001). The design of the 8400S ambient particulate sulphate monitor utilises a method very similar to that of the series 8400N nitrate monitor described above. The 8400S consists of a weather protected inlet and transport tubing, microprocessor-based control system, user interface, sulphur detector, sample pump, gas cylinder, a pulse generator where sample conditioning, collection and flash vaporization occur, and a SO_2 pulse analyzer where sulphur oxides developed from flash vaporization and sulphate reduction are measured to determine the particulate sulphate content of ambient particulate matter with a 10 minute time resolution (Rupprecht and Patashnick, 2001).

The sample inlet comprises of a raincap, PM2.5 sharp-cut cyclone and activated carbon denuder (Figure 2.8). The ambient aerosol sample flow passes through the cyclone at a flow rate of 5 L/min to remove particles above 2.5 μm. A sub flow of 1 L/min stream of air from the initial flow passes through a honeycomb activated carbon denuder for the removal of existing H_2S or SO_2 and then through a Nafion humidifier, at which the sample air stream humidity is increased to 90%. Particles that are wet through the humidifier are collected through impaction onto a platinum flashing strip mounted in a collection and vaporization cell. The collection efficiency of this impactor is greater than 95% for particles in the range 0.1-0.8 μm (Stolzenburg and Hering, 2000; Drewnick *et al*., 2003).

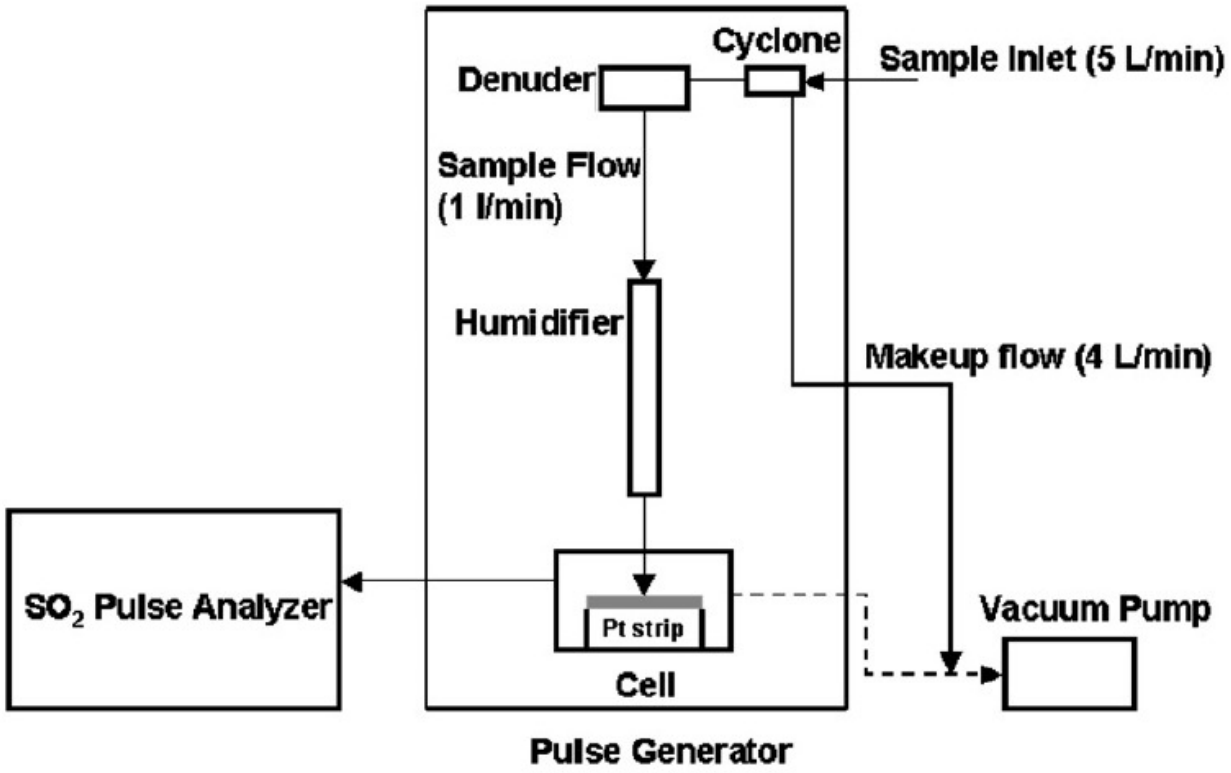

Figure 2.8. Schematic of the Rupprecht and Patashnick 8400S particulate sulphate monitor (Rupprecht and Patashnick, 2001).

The instrument has two periods of operation completed within 10 minutes which are the sampling and analysis period made up of 8 and 2 minutes respectively. In the analysis period, the air sample flow bypasses the collection cell and the sampling cell is purged with clean air from a cylinder. The clean air flows into the pulse analyzer, giving a baseline signal value. The flashing strip and the collected particles are accumulated in the pulse generator which is heated by an electric current at about 600 ^{o}C for approximately 0.01 seconds until an infrared cut off is attained. Particulate sulphate collected is flash vaporized to produce a SO_2 pulse which is interpreted by a pulse analyser. The signal from the pulse analyser is transferred to the data acquisition system where it is converted to the appropriate concentration of sulphate in $\mu g/m^3$ (Drewnick *et al*., 2003).

2.4 Data analysis

The 2005 aerosol data is analyzed to investigate diurnal and seasonal variations in aerosol concentration, pollution roses, and aerosol chemical composition. Pollution episodes were also analyzed to investigate which sources contribute to high aerosol concentrations. The mean values were obtained for the data sets by arithmetic mean, averaging over hourly interval. The non-valid or unavailable data points were removed from the data set before analysis was carried out. The data set used to investigate aerosol characteristics is not normally distributed but close to normal, hence, the usage of arithmetic mean for the values. An arithmetic mean can be viewed as a valid characteristic of an aggregate only when the distribution of the original attribute values is close to normal (Andrienko and Andrienko, 2006).

2.4.1 Seasonal variation

Average monthly concentrations for all pollutants and average monthly meteorological parameters were analyzed for one year. A year's data was divided into 12 months for each parameter. The average monthly concentrations were calculated by averaging all data over a 24-hour period and then averaging over the month. Monthly data for each parameter were averaged using arithmetic mean. The data were analyzed to determine the season where each pollutant shows the highest and lowest concentrations. Factors responsible for monthly mean variation of all pollutants and meteorological parameters are also established.

2.4.2 Diurnal variation

Hourly average temperature, relative humidity, wind speed, backscattering coefficient of light by the nephelometer, and concentrations of black carbon, PM10, nitrates, sulphates, and sulphur dioxide were analyzed to ascertain average diurnal profiles in each of the four seasons. According to Tyson and Preston-Whyte (2000), summer is considered to be December, January and February; autumn is considered to be March, April and May; winter is considered to be June, July and August whilst spring is September, October and November. The statistical analysis was performed with the data analysis tool-pack in the EXCEL spreadsheet. The 2005 aerosol data were divided into 24-hour periods and these were used to obtain a line graph for each parameter.

Mean values were obtained for the 24-hour period of each parameter by hourly averaging over the four seasons of the year.

2.4.3 Pollution roses and wind roses

Polar pollution roses are compiled for the various pollutants (black carbon, PM10, sulphates, and nitrates) and wind roses for meteorological parameters (wind speed and wind direction) data sets in order to identify the sources of aerosols. Pollution and wind roses are compiled for each of the four seasons of the twelve-month sampling period at Elandsfontein.

A pollution rose plots an angle histogram showing the percentage frequency with which concentrations of a pollutant occur from each direction. The dependence of pollutants' concentration on wind direction is useful in determining the sources of pollutants. The length of the bar represents the frequency with which the wind blows from a particular direction and the thickness and colour of the bars indicate concentration of pollutants.

Pollution roses are polar representations combining concentration (represented in the radial axis) and wind direction data in which the location of the most influential sources are indicated by the peaked form of roses. In pollution roses the 360° of the compass were divided into 16 sectors of 22.5^{o} each. The hourly means taken when the wind was from each sector were then averaged, and the values plotted in the form shown in chapter four.

A wind rose is a graphical representation of the wind direction, frequency and speed for a given date and time at a particular location. In a wind rose, the length of the bars represents the frequency with which wind blows from each of the 16 wind directions while the thickness of the bar indicates the speed at which the wind blows from a particular direction. Wind roses are calculated from wind direction and wind speed. Two basic characteristics calculated were the number of occurrences of the wind speed for a certain wind direction and the average wind speed for each wind direction.

2.4.4 Aerosol chemical composition

The composition of PM10 on the Highveld is shown using pie charts for each season or episode. Pie charts display the contribution of each value to a total. In this way, source contributions and the contribution of aerosol species not measured are indicated. The 2005 data were also divided into four seasons of spring, summer, autumn and winter as was the case with seasonal and diurnal variation. Sulphates, nitrates and black carbon were calculated as percentages of total PM10 for the data sets in each season. The unknown contribution of aerosol was calculated by deducting the total sum of sulphates, nitrates and black carbon from PM10 and likewise calculated as a percentage of total PM10. The percentage values for sulphates, nitrates, black carbon and the unknown contribution were averaged by arithmetic mean. The resulting mean values were used to plot a pie chart.

2.4.5 Causes of high aerosol concentrations

Time series of pollution episodes are shown for particulates (black carbon, PM10, sulphates, and nitrates), gases (sulphur dioxide) and meteorological data (temperature, relative humidity, wind speed, wind direction) from the 2005 data set. Episodes from 21 to 23 January 2005 and 29 to 31 August 2005 were used for the analysis. The dates chosen are an indication of the measurement of pollutants with the highest concentrations during summer and winter respectively. Pollution episode of January was chosen because PM10 concentration was supposed to be at a minimum during summer but on the contrary it has the highest concentration. The episode in August showed a significant increase in PM10 concentration as expected during winter. Therefore the analysis is undertaken to compare the pollution episodes between summer and winter and also to identify some of the causes of the high particulate concentrations recorded during the year.

****

The various methods used for the collection and analysis of data from the Elandsfontein monitoring site have been discussed. Instruments used to obtain aerosol data were described and they include the beta gauge, multi-angle absorption photometer, integrating nephelometer, particulate nitrate monitor, and ambient particulate sulphate monitor. The measurements from aerosol instruments were used to analyze the spatial and temporal distribution of aerosol loading while measurements from meteorological instruments were used to compile pollution roses and pollution episodes of pollutants.

CHAPTER THREE

TEMPORAL VARIATIONS

Seasonal and diurnal variations of atmospheric aerosols over the South African Highveld will be explored and discussed in this chapter. Average monthly concentrations of pollutants and meteorological data are analyzed to determine the factors responsible for seasonal and twenty-four hourly variations in concentrations of particulate matter. The effects of meteorology on changes in concentration are also investigated.

3.1 Monthly concentrations of data captured at the Elandsfontein site

The mean, minimum, maximum and standard deviation of monthly concentrations of data captured in 2005 is shown in Table 3.1. PM10, black carbon, backscattering coefficient of light, and sulphates show highest annual concentrations during winter (June, July and August) and early spring (September and October). Both nitrate and sulphur dioxide show maximum concentration only in winter. Lowest concentrations occur in summer (December, January and February) for PM10, black carbon, and sulphate, while nitrates and sulphur dioxide show minimum concentrations during summer and spring (September, October and November). Minimum scattering occurs during spring, early summer (December), and late summer (February) for backscattering coefficient of light by the nephelometer. Compared to other pollutants, PM10, backscattering coefficient and sulphates showed a distinct seasonal variation with a significant peak in mean concentrations in January. Meteorological parameters (temperature and humidity) show similarity in their maximum and minimum. Temperature is highest during spring and summer and there is minimum temperature during autumn and winter. There is occurrence of higher humidity in spring, summer and early autumn (March and April). Lowest humidity occurs in late autumn (May), winter and early spring (September).

Table 3.1: Monthly concentrations of data captured at the Elandsfontein site in 2005.

Season	Parameter		PM10(µg/m3)	BC(µg/m3)	HAZ(m-1)	NO_3^-(µg/m3)	SO_4^{2-} (µg/m3)	SO^{2-}(ppb)	TMP(°C)	HUM(%)
Summer	January	Mean	36.82	0.52	0.45	0	5.2	8.63	19.16	65.03
		Minimum	0	0	0	0	0.31	0	12.7	1.2
		Maximum	970	7.5	1.91	0	19.7	92.5	30.8	86.3
		Std deviation	58.5	0.65	0.4	0	3.2	12.82	4.28	19.54
	February	Mean	30.18	0.66	0	0	4.14	9.58	19.15	61.57
		Minimum	1	0.1	0	0	0.22	0	9.3	0
		Maximum	284	5.8	0	0	13.7	206	33.7	92.5
		Std deviation	30.14	0.67	0	0	3.06	20.83	5.25	28.97
Autumn	March	Mean	20.88	0.65	0.36	0.35	3.03	10.14	16.94	62.41
		Minimum	0	0.2	0	0	0.09	0.16	8.9	0
		Maximum	241	2.5	2.13	4	19	177	29.1	93.5
		Std deviation	19.1	0.38	0.32	0.46	2.85	17.78	4.73	28.89
	April	Mean	25.84	0.98	0.46	0.7	2.35	8.88	14.91	62.35
		Minimum	1	0.2	0	0	0.28	0.25	3.9	0
		Maximum	250	6.5	3.44	10	11.1	202	25.8	97.7
		Std deviation	22.28	0.71	0.41	0.96	1.73	15.79	4.5	27.92
	May	Mean	45.88	1.53	0.63	1.55	4.21	13.53	13.65	45.87
		Minimum	2	0.2	0	0	0.14	0.08	3.7	0
		Maximum	435	8	3.21	10	64.7	167	27	99
		Std deviation	45.08	1.03	0.47	1.57	4.05	20.32	4.79	31.8
Winter	June	Mean	51.35	2.28	0.73	2.09	5.77	14.76	12.28	34.05
		Minimum	2	0.4	0.03	0	0.13	0.31	2.1	0
		Maximum	422	7.6	2.68	11	57.7	356	23.5	100
		Std deviation	42.8	1.34	0.46	1.7	5.59	22	4.71	33.77
	July	Mean	48.61	1.9	0.58	6.82	5.76	10.78	11.27	35.05
		Minimum	1	0.3	0.01	0	0.35	0.42	1.3	0
		Maximum	346	10.5	4.56	26	36.9	111	25.2	100
		Std deviation	38.41	1.5	0.52	4.81	5.19	14.26	5.65	34.64
	August	Mean	63.08	2.9	0.83	5.77	4.99	13.3	14.18	43.51
		Minimum	1	0.3	0.03	0	0.46	0.08	4.5	0
		Maximum	599	9.8	5.45	36	24.1	205	26.5	99.9
		Std deviation	39.99	1.34	0.45	4.6	3.82	22.09	5.21	36.05
Spring	September	Mean	61.43	2.58	0.73	1.44	5.4	9.32	17.73	25.84
		Minimum	2	0.4	0	0	0.96	0.05	1.3	0
		Maximum	360	9	4.23	8	18.7	100	31.9	99.9
		Std deviation	40.54	1.37	0.4	0.99	2.88	13.44	6.62	29.58
	October	Mean	45.36	1.31	0.38	1.35	4.14	9.28	17.98	47.88
		Minimum	1	0.2	0	0	0.61	0	7.8	0
		Maximum	370	6.3	1.57	6	23.2	138	31.4	100
		Std deviation	38.91	0.8	0.24	1.16	2.87	13.84	5.86	35.66
	November	Mean	39.73	1.03	0.25	0.35	3.15	8.94	17.99	52.71
		Minimum	0	0.2	0	0	0.44	0.05	6.3	0
		Maximum	878	4.3	1.38	4	18.5	158	33.1	100
		Std deviation	58.41	0.69	0.21	0.49	2.3	15.23	5.42	34.09
Summer	December	Mean	32.18	0.73	0.21	0.77	3.39	8.01	18.36	56.41
		Minimum	0	0.2	0	0	0.78	0	8.8	0
		Maximum	216	3.7	1.35	3	9.67	91.6	30.8	98.6
		Std deviation	29.64	0.51	0.17	0.46	1.96	11.74	4.9	28.29

3.2 Seasonal pattern between PM10, black carbon, sulphate and nitrate

In this section seasonal pattern between PM10, black carbon, NO_3, and SO_4 are analyzed among the species at all time frames. PM10, black carbon, NO_3, and SO_4 concentrations have considerable seasonal variation with low values during summer and high values during winter and early spring (Figure 3.1). It is important to note that meteorological conditions such as temperature, precipitation, humidity and wind direction influenced the minimum and maximum concentration of pollutants during summer and winter. According to Yang (2002), high PM10 concentration in winter is due to increase in suspended dust coupled with lower temperature and less precipitation. Increase in burning of coal and biomass fuels for space heating, shallow boundary layer and low wind speed explain the high pollutant levels in winter for black carbon (Safai *et al*., 2007; Saha and Despiau, 2009).

When nitrate is high in winter, it is due to its formation from its precursor NO_x. Emissions of NO_x released from coal combustion during winter are marginally higher and in turn cause higher concentration of nitrate and sulphate. The formation of sulphate and nitrate is chemically linked to the abundance of oxidants (OH and H_2O_2) and therefore to the emissions of NO_x. Nitrogen oxides released into the atmosphere undergo series of photochemical transformations involving volatile organic compounds which form a variety of oxidants like hydroxyl radical (OH) and hydrogen peroxide (H_2O_2). These oxidants react with SO_2 and NO_2 and consequently lead to the formation of SO_4^{2-} and NO_3^- respectively (Stein and Lamb, 2003).

However, Stein and Lamb (2003) compare the high and low NO_x regime and explain that in the high NO_x regime which is typical of winter, the oxidizing capacity of the atmosphere is reduced because the NO_2 rapidly combines with and thereby depletes hydroxyl radicals, producing nitric acid while the concentrations of OH and H_2O_2 are reduced and thus enhancing the formation of nitrate. On the other hand, the low NO_x condition which is typical of summer enhances the formation of excess radicals, OH and H_2O_2 whereby nitrogen dioxide is readily consumed during nitric acid formation creating a highly oxidizing state unfavorable to nitrate formation. This suggests that both theories are feasible for nitrate formation.

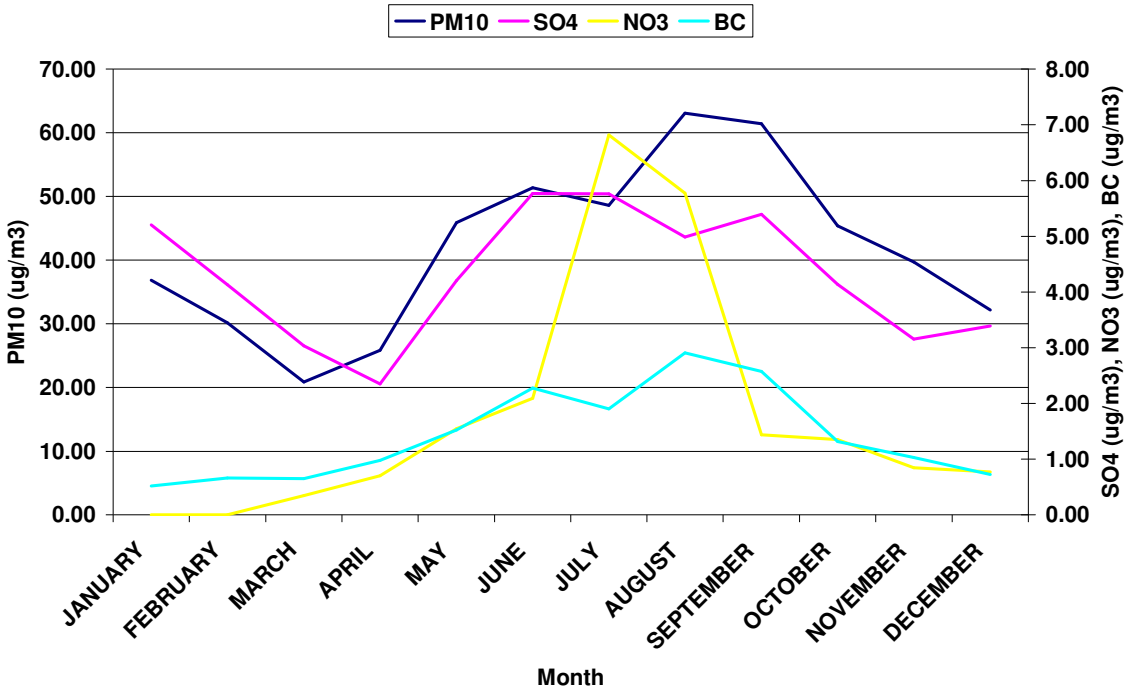

Figure 3.1. Monthly variation of pollutant showing similarity in PM10, sulphates, nitrates and black carbon concentrations.

Monthly variation in sulphate concentration may be attributed to meteorological conditions, prevailing winds and to different oxidation rates experienced during summer and winter. High winter concentration of sulphate is due to oxidation of sulphur dioxide to sulphate aerosol through the gas phase process. Sulphur dioxide is emitted into the atmosphere from coal combustion and power stations.

Although PM10, black carbon, NO_3, and SO_4 show higher concentration in winter, it is important to note that PM10 and black carbon emissions come from different sources while nitrate and sulphate precursors are emitted from the same source. Higher concentration of nitrate and sulphate precursors comes from coal combustion which is a solid fossil fuel. Low PM10 concentration during summer is largely associated with rainfall that washes away particulate matter accumulated over time in the atmosphere. Black carbon is lower in summer due to less biomass burning, decrease in domestic energy demand and less coal burning for space heating. NO_x emissions from coal combustion during summer are relatively lower and this accounts for the lower concentration of nitrate in summer.

Scheifinger and Held (1997) observed that the seasonal cycle of subsidence inversions represents the dominant physical feature of the atmosphere on the Highveld, which determines the seasonal cycle of the dispersion conditions. They also observed that the stronger elevated inversions occur more frequently during winter. The elevated inversion are found between 760 and 700 hPa and can be related to the dominant subtropical anticyclonic belt generating significant subsidence during the winter months (Garstang *et al*., 1996b). The winter maximum of the gases and aerosols in the atmosphere including nitrates can be seen as a result of the frequent occurrence of elevated inversions over the area during winter which restricts the height of the mixing layer (Tosen and Turner, 1990). The physical conditions for atmospheric reactivity is likely to be at a maximum during summer compared to winter, given that summer has more solar radiation available, higher temperatures and a higher level of vapor pressure. Hence, It was suggested that the seasonal variation of nitrates, sulphur dioxide and sulphates is enhanced by an interaction of meteorological conditions and, additionally, by different oxidation rates of nitrates and sulphates (Scheifinger and Held, 1997).

3.3 Seasonal variations in atmospheric aerosol concentrations

PM10 concentrations are at a maximum during winter and early spring (September and October) and peak in August and September (Figure 3.2). Minimum concentrations occur in summer (December, January and February). The seasonal variation of PM10 mass concentration can be explained by meteorological conditions such as wind direction, precipitation days and temperature. The minimum concentration during summer is largely associated with rainfall. Rainfall washes away particulate matter that has accumulated over time in the atmosphere especially during summer period. Therefore, more precipitation days and higher temperature lower the concentration of PM10. There is a significant reduction in rainfall during late autumn (May) and at the same time a gradual increase in suspended dust, hence gradual increase in PM10 concentrations. This gradual increase in suspended dust leads to consistently higher concentrations throughout the months of May to November. Wind direction also influences the phenomenon of high PM10 concentration found during winter. In Elandsfontein downwind of Middleburg and Witbank, the prevailing wind pattern from north-westerly direction transports pollutant from industries in Middleburg and Witbank. In addition, industrial activities highly distributed around Elandsfontein such as in Standerton and Secunda may result in the largest

concentration of PM10. Temperature can act as a surrogate for many processes and temperature pattern at Elandsfontein is higher in summer and early autumn and lower during winter and spring. Lower temperature and less precipitation during winter explain higher PM10 concentration in winter (Yang, 2002). PM10 has diversified sources which include emissions from vehicle exhausts, road dust, industries and aerosol mass formed by gas-to-particle conversion.

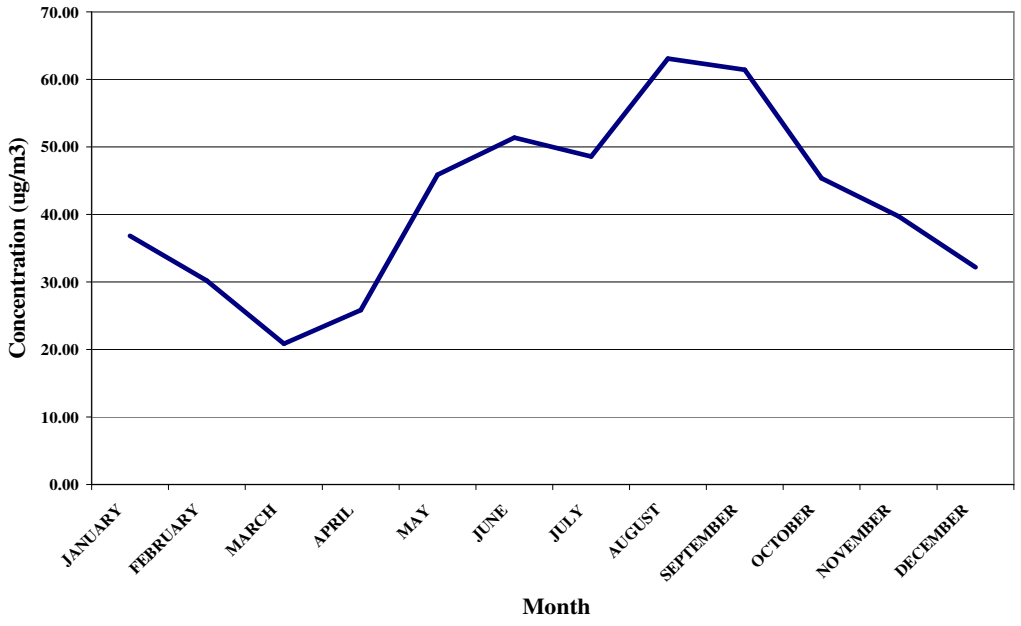

Figure 3.2. Average monthly concentration for Elandsfontein showing variations in PM10.

Black carbon shows a similar monthly mean variation with maximum concentrations in winter and early spring and lowest concentrations during late summer (Figure 3.3). The higher concentration of black carbon during winter months is as a result of increase in biomass burning, and an increase in domestic energy demand and associated coal burning in residential areas. Higher black carbon may also be attributed to the stability in the atmosphere during winter months which invariably prevents pollution dispersion. The dispersion in the atmosphere is as a result of low wind speed and shallow boundary layer; hence the absence or reduction of

dispersion causes an enhancement in the black carbon concentrations during winter. Incomplete combustion of fossil fuel and biofuel, industrial pollution, traffic, and outdoor fires are the dominant sources influencing the concentrations of black carbon. Higher black carbon concentration during winter and the cause effect of boundary layer and coal burning for space heating has been reported previously (Safai *et al*., 2007). Saha and Despiau (2009) observed, as in this study, a prominent secondary peak in black carbon concentrations during winter season. Several factors responsible for the peak are shallow boundary layer, low wind speed and usage of space heating.

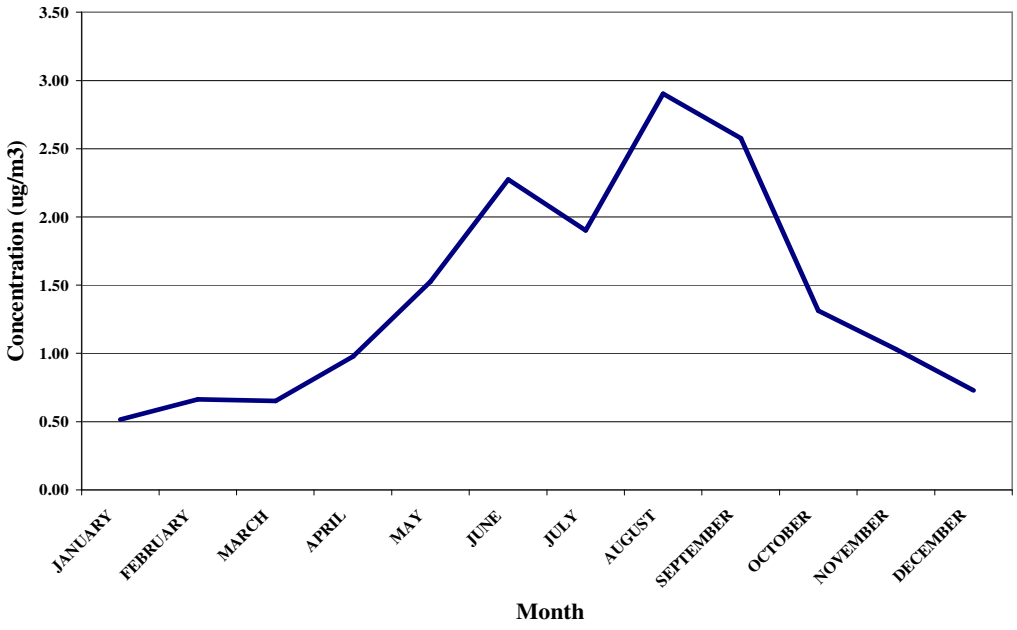

Figure 3.3. Average monthly concentration of monthly variations in black carbon at Elandsfontein.

Monthly average backscattering measured using the nephelometer shows a distinct seasonal variation which is quite similar to monthly average PM10 concentrations (Figure 3.4). There is maximum scattering during the cold winter months and early spring as a result of biomass burning and accumulation. The drop in concentration during late spring is highly dependent on

precipitation. There is a gradual increase in particle mass concentration in autumn (March, April and May) which marks a period of reduced rainfall and increase in particle mass concentration.

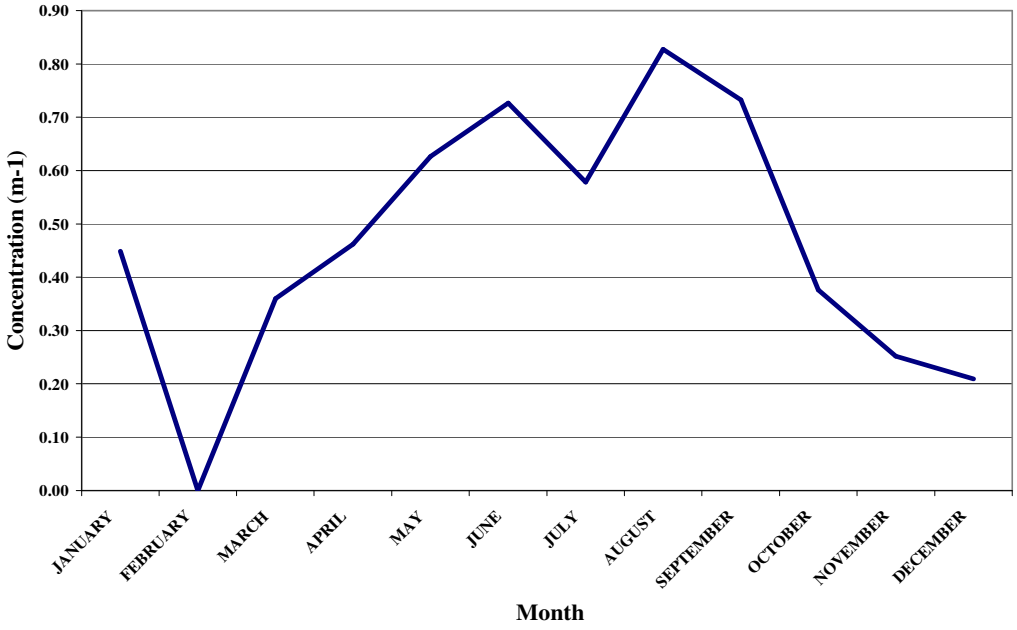

Figure 3.4. Average monthly concentration of monthly variations in backscattering coefficient at Elandsfontein.

Nitrate concentrations show a very distinct seasonal variation with significant peak concentration in July (Figure 3.5). There is a build up of nitrate from around March until August with a decline over four months between September and December. However, data recovery for nitrate was 18% in summer, 77% in autumn, 84% in winter and 37% in spring. The low nitrate values in summer and spring may be attributed to low data availability, hence, it influences the conclusions for these seasons. The peak in nitrate concentration does not correspond with the peak in black carbon concentration due to their emissions from different sources. This is because the peak in black carbon concentration results from domestic burning and pronounced biomass burning between June and October while the peak concentration of nitrate is due to the formation of nitrate from its precursor NO_x. During winter, emissions of NO_x released from coal combustion are marginally higher and this accounts for higher concentration. Additionally, lower

concentration is experienced in summer due to low emissions of NO_x.

The seasonal variation in nitrate concentration may be attributed to the high and low NO_x conditions in the atmosphere. It has been demonstrated that changes in NO_x emission strengths or variations in the radical sources establish a seasonal cycle in photochemical species concentrations (Stein and Lamb, 2003). For instance, when the NO_x emission rates are higher than the sources of radicals, the formation of HNO_3 via reaction 1.6 constitutes the main radical sink. The NO_x can also participate in various reactions which include reactions in equations 1.2 and 1.8; it could be dry deposited and could be transported outside the region. However, these alternative removal pathways are slow compared to the NO_x radical reactions, leading to the accumulation of NO_x in the gas phase (Kleinman, 1991).

In this high NO_x regime, the concentration of OH and H_2O_2 is reduced, further increasing the possibility of NO_3 formation in reaction 1.6. On the other hand, when the radical sources OH and H_2O_2 exceed the NO_x emissions strength, NO_2 is easily removed by the formation of nitric acid, leaving an excess of radicals. These low NO_x conditions enhance the formation of OH and H_2O_2, creating a low oxidizing state to nitrate formation (Stein and Lamb, 2003).

Peak nitrate concentration during winter may also be as a result of stability in the atmosphere which leads to less atmospheric mixing and which prevents the dispersion of pollution. High concentration of nitrate in winter could also be due to recirculation of air from the industrialised areas surrounding Elandsfontein air quality monitoring site.

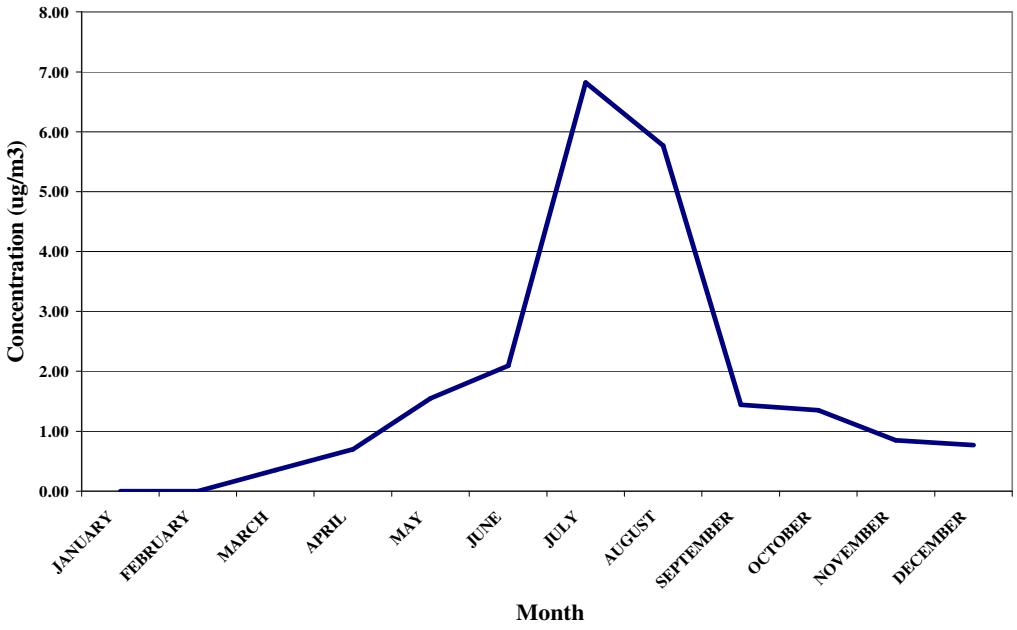

Figure 3.5. Average monthly concentrations of nitrate concentrations at Elandsfontein.

Concentrations of sulphate are highest in winter (June to August) and lowest in late autumn (March and April; Figure 3.6). Mean concentrations have a peak in January but gradually decline to a minimum during the summer period. Monthly variation in sulphate concentration is most likely due to changes in prevailing winds, and to differences in oxidation rates which is largely influenced by the meteorological condition surrounding Elandsfontein (Igbafe *et al.*, 2007). Higher sulphate concentrations occur when sulphur dioxide concentrations are higher (Lin *et al*., 2008).

Oxidation rate is accelerated during summer. The increased oxidation rate influenced by meteorological conditions such as high temperature observed during summer in Figure 3.7, cause sulphur dioxide to be oxidised to sulphate aerosol. This explains its increase in summer and the peak in January. Conversely, sulphur dioxide oxidation rates are lower due to lower levels of atmospheric moisture during winter. Oxidation rates are lower in winter, which does not explain higher sulphate concentrations in winter. These concentrations show a distinct monthly variation.

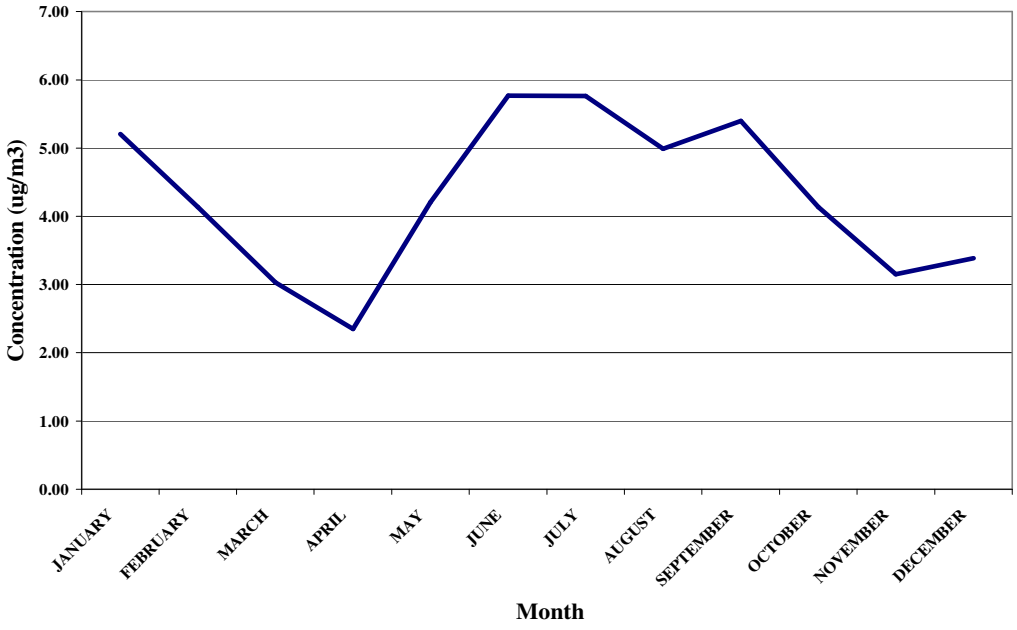

Figure 3.6. Average monthly concentrations showing monthly variations in sulphate concentrations at Elandsfontein.

On the other hand, higher winter sulphate concentration may be explained by the presence of sulphur dioxide the primary precursor of sulphate which is oxidized to form sulphur acid via gas and liquid phase reactions under the influence of meteorological conditions (low relative humidity and low temperature). Sulphur dioxide emissions originate from coal-fired power plants. The meteorological conditions influenced the oxidation of sulphur dioxide to sulphate aerosol during winter, formed principally through gas-phase reactions. Gas-to-particle conversion processes controlling the secondary particulate emissions are very dependent on the meteorological conditions (insolation, temperature and humidity) and important seasonal variations in the levels of secondary particulate pollutants must be expected (Querol et al., 1998). Particulate sulphate monthly variation in concentrations may also be accredited to variations in dry and wet deposition rates. Dry deposition is the process whereby particles and gases through a number of atmospheric processes in the absence of precipitation are transported to the ground. Wet deposition on the other hand occurs when particles and gases are removed from the atmosphere and brought to ground level via precipitation mechanisms (rain, snow etc.). Dry deposition is high in winter and low in summer while wet deposition is high in summer and low

in winter. There is high removal rate of particulate sulphate due to wet deposition.

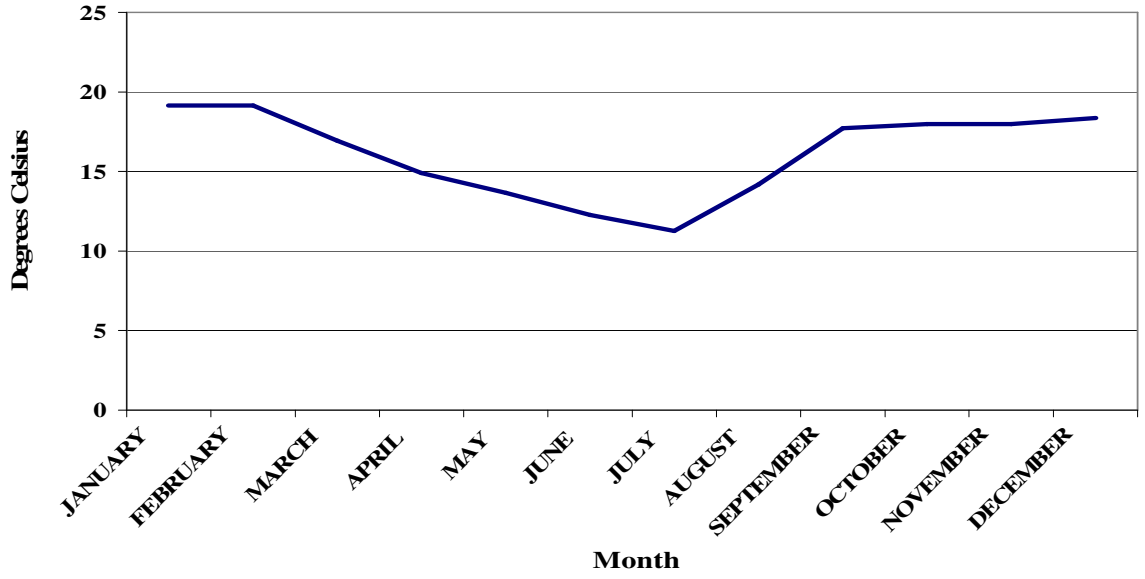

Figure 3.7. Average monthly concentration for Elandsfontein showing monthly variation in temperature.

A higher concentration of sulphur dioxide occurs in winter (May to August) and lowest concentrations in spring (September to November) and summer (December to February; Figure 3.8). This highest concentration during winter is as a result of substantially lower mixing heights encountered during the winter months and also due to increase of north-westerly winds during winter months (Held *et al.*, 1996). The increase of north-westerly winds is as a result of large sources of sulphur dioxide advected towards the north-west direction of the study area. An example is the presence of power plants adjacent to Elandsfontein monitoring station.

Sulphur dioxide's highest concentration during winter may be due to large quantities released into the atmosphere from many industrial and domestic processes as a result of burning of fossil fuels in coal combustion. The influence of the emissions from power stations largely account for higher concentration of sulphur dioxide during winter. Sulphur dioxide largely derived from fossil fuel combustion has a high concentration during winter months due to a marginal increase in the demand for electricity and associated increased emissions from power stations (Igbafe, *et*

al., 2007). However, this condition may vary through the year.

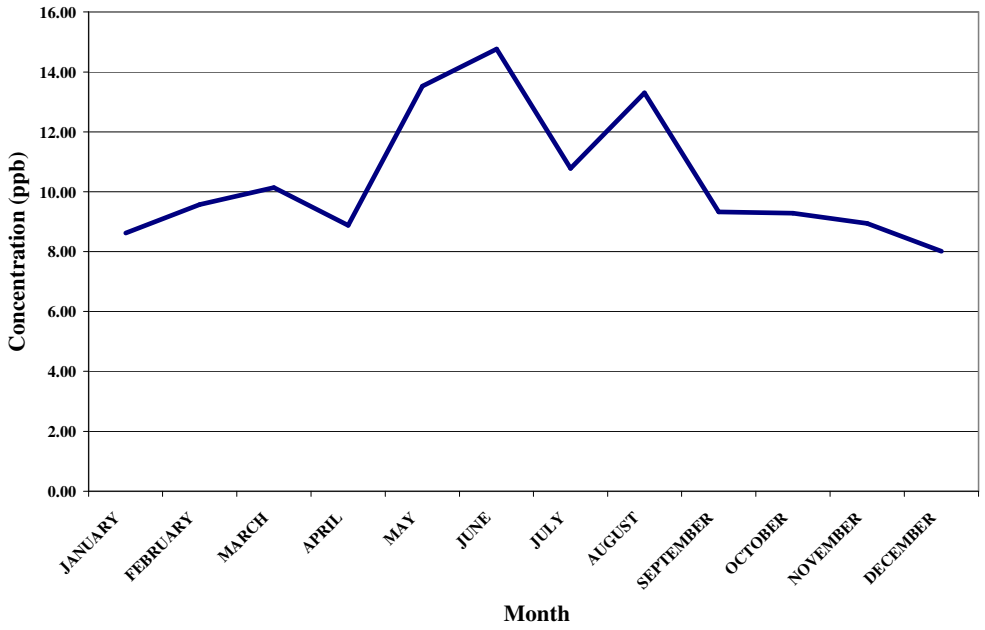

Figure 3.8. Average monthly concentration for Elandsfontein showing variations in sulphur dioxide.

3.4 Diurnal variations in atmospheric aerosol concentrations

Hourly variations in atmospheric aerosol concentrations indicate that pollution concentration levels fluctuate from day to day and at different times of the day to the changing state of atmospheric stability and the source strength.

Diurnal variation in PM10 concentration is observed over the four seasons. Concentrations are at a maximum in the evenings, peaking between 18:00 and 21:00, after which they gradually decrease through the night (Figure 3.9). Mean diurnal concentrations of PM10 are higher during spring and this shows a significant variation. Concentrations of PM10 increase slightly in the mornings but remain low until late afternoon. In addition, there is a morning peak in all the four seasons which may be as a result of domestic burning.

Maximum concentrations of particulate matter in the early morning and at night indicate the effects of stable conditions and surface inversions, and suggest that most particulate matter is derived from sources at the surface. The nocturnal surface inversion that builds at night does not allow pollution released into stable inversion air to rise through but to disperse very slowly. Consequently, particulate matter emissions at night are trapped near the surface. Spontaneous coal combustion, domestic coal combustion or residential wood burning are potential sources that dominate the variations of the concentrations of particulate matter.

Lower levels of particulate concentrations during the day indicate unstable atmospheric conditions. Particulates detected during the day might be as a result of particulate emissions from tall stacks brought down to the surface by turbulence. The daytime decrease of particulate concentrations clearly shows a distinctive pattern. Also, daytime particulate could be due to particulates released at the surface. However, the unstable daytime mixing, horizontal transport and advection dilute the concentrations and slowly disperse some of the particulate accumulated emissions from the previous night.

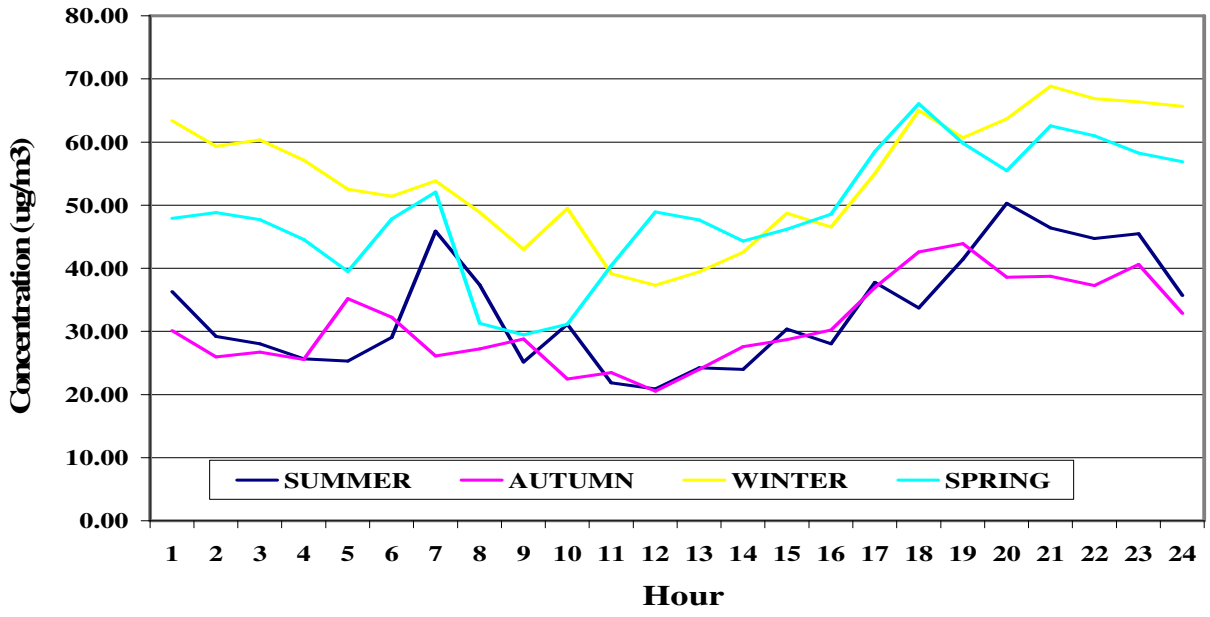

Figure 3.9. Diurnal variation of PM10 concentration at Elandsfontein for the period 1 January to 31 December 2005.

Black carbon displays a distinctive diurnal pattern in all seasons with minimum concentrations between 10:00 and 19:00 (Figure 3.10). A common phenomenon during all four seasons is the peak in black carbon concentrations in the late evenings. From 19:00 onwards black carbon concentrations begin to rise, until around 23:00, thereafter they gradually decrease through the night. There is a notable similarity between PM10 concentration and black carbon. They both showed maximum and minimum concentrations at the same time of the day. There is peak concentration for both PM10 and black carbon in the mornings and late evenings and this is mainly related to domestic activities. The comparison between PM10 and black carbon indicates sources like domestic heating and coal combustion for space heating as the primary influence on their maximum and minimum concentration. However, there is marked seasonal dependence on the diurnal variations of black carbon.

This is because black carbon concentrations during winter season show stronger diurnal variations with higher concentrations compared to the other seasons. This may be as a result of seasonal changes in the boundary layer dynamics, biomass burning during winter months, more domestic fires from townships, and more stable atmospheric conditions. Saha and Despiau (2009) have also observed pronounced diurnal variations in the black carbon mass concentrations, with very high concentrations in the morning and night, and reduced concentrations in the afternoon. They attributed the diurnal variations mainly to the emission rate of black carbon and the mixing of black carbon upwards by the development of the convective boundary layer during the day.

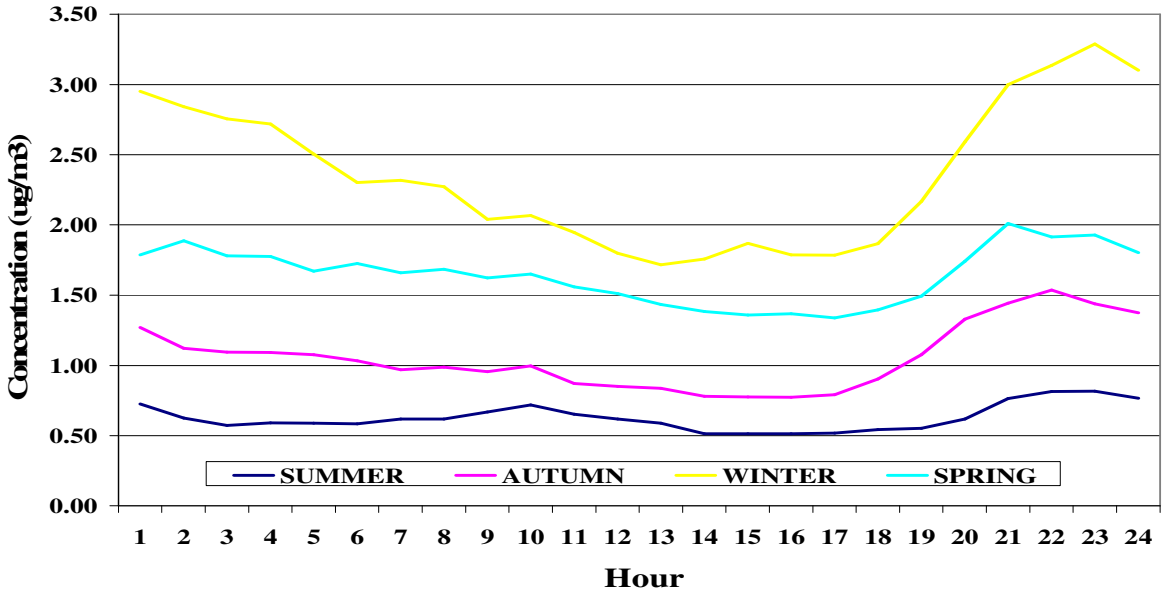

Figure 3.10. Diurnal variation of pollutant concentration at Elandsfontein for the period 1 January to 31 December 2005 for black carbon.

Nitrate concentrations show a small diurnal variation during summer, autumn and spring but exhibit a significant diurnal variation during winter (Figure 3.11). However, data recovery for nitrate was 18% in summer, 77% in autumn, 84% in winter and 37% in spring. This data recovery provides interrupted diurnal profiles in nitrate concentrations. In every season there is high concentration of nitrate in the morning and night with lower concentration in the afternoon. This is more pronounced in winter compared to summer, autumn and spring. The average hourly nitrate concentrations during winter were characterized by maximum in the early morning between 01:00-07:00, a decrease during the day between 08:00-21:00 and an increase during nighttime. This is explained by the daytime and nighttime diurnal profile of nitrate. During daytime, most of the nitric acid production is generated by the reaction in equation 1.6 and it is limited by the OH radical concentration. Reaction in equation 1.2 only occurs during nighttime because the gaseous NO_3 radical is rapidly photolyzed during the day. N_2O_5 formation through reactions in equation 1.2 and 1.7 is followed by reaction in equation 1.8 to generate nitric acid. This takes place in hydrated aerosols rather than in the gas phase. The radical NO_3 also reacts rapidly with NO in equation 1.4 in such a way that both NO_3 and NO cannot coexist at NO

concentrations above a few parts per trillion. As a consequence, it is only possible to find the radical NO_3 during nighttime and not at ground level in urban scenarios (Brown *et al*., 2003).

The maximum and minimum concentrations of nitrate were clearly influenced by the meteorological conditions such as temperature and humidity. Monthly variation in temperature is illustrated in Figure 3.7. During summer the temperature was high shifting the equilibrium towards the gas-phase, while during winter the temperature was low and the particulate phase was predominant. Also, there were nocturnal increases as a result of higher humidity at night. The early morning formation and nighttime increase in nitrate concentration is attributed to some mechanisms which produced the accumulation. The NO_2 hydrolysis in equation 1.6 is noted as the most probable mechanism while another possible mechanism could be nitric acid absorbed and dissolved in water droplets generated by the high humidity condition.

Furthermore, the decrease showed in the afternoon during winter may be due to dry deposition of HNO_3 and the increase in early morning probably due to heterogeneous formation of nitrate (Fisseha *et al*., 2005).

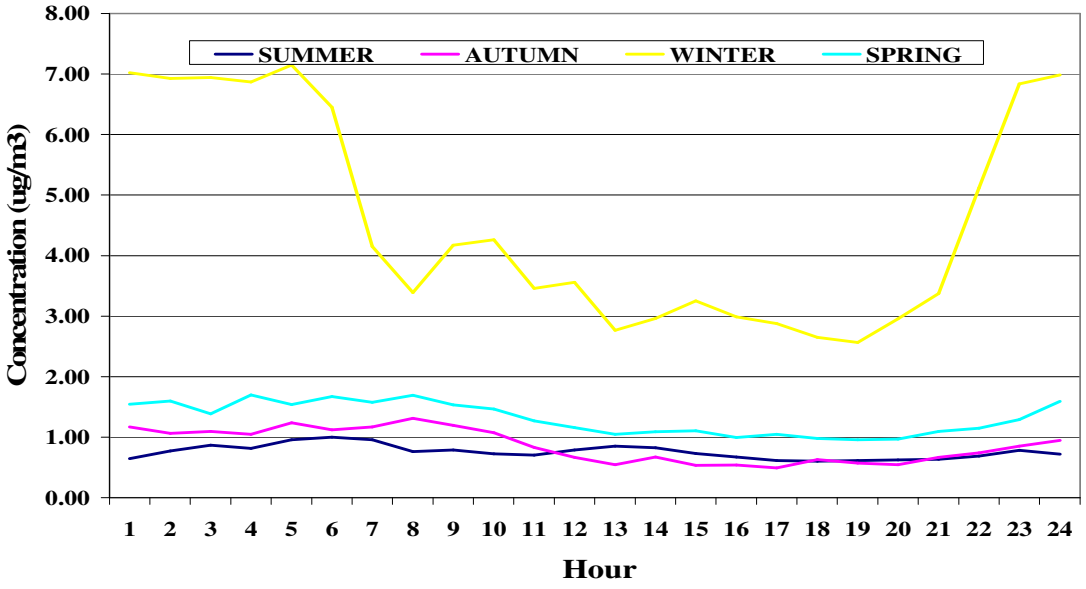

Figure 3.11. Diurnal variation at Elandsfontein for the period 1 January to 31 December 2005 showing variation in nitrates concentration.

Concentrations of particulate sulphate have a very different pattern to those of the other aerosol types, since SO_2 is derived from tall stack sources although not exclusively. In spring, summer and autumn, particulate sulphate concentrations are higher in the afternoons and lower in the evenings but a significant difference occurs in winter where sulphate concentrations are higher in the morning and gradually increase into the night (Figure 3.12). Particulate sulphate, while fairly constant in the mornings in all seasons, exhibits a maximum concentration during the day and stays constantly low at night. Sulphur dioxide is oxidised to form sulphate aerosol therefore the higher concentration of particulate sulphate in the day is related to the influence of tall stack emissions from where the SO_2 is derived. In addition, sulphur dioxide is largely derived from fossil fuel burning in coal combustion, industrial processes and coal-fired power stations.

There is distinct difference between the diurnal pattern of sulphate in the afternoon during summer and winter. Higher concentration during summer is due to high oxidation rate while lower concentration in winter is due to low oxidation rate and therefore no formation of sulphate. The moist, unstable conditions and rainfall are almost exclusively confined to the summer period when the anticyclonic belt is located further south. These conditions in addition to increased ambient temperature and solar radiation are favorable for the formation of secondary pollutants. Hence, there are several occasional episodes with notably high aerosol concentrations of sulphates in summer. The dry, highly stable winter period is obviously of great importance in association with the accumulation of atmospheric pollutants.

Also, in winter, the mixing layer height reduces significantly with reduction in the surface inversion, resulting in higher concentrations of surface pollutants (Annegarn *et al*, 1996). Hence higher particulate sulphate in the morning during winter compared to the summer period has been shown to result from meteorological condition which is influenced by wind direction. Highest winter concentration is in association with flow from the north-west and this condition suggests that long range air mass transport and oxidation of sulphur dioxide from local sulphur emissions are potential sources of ambient particulate sulphate.

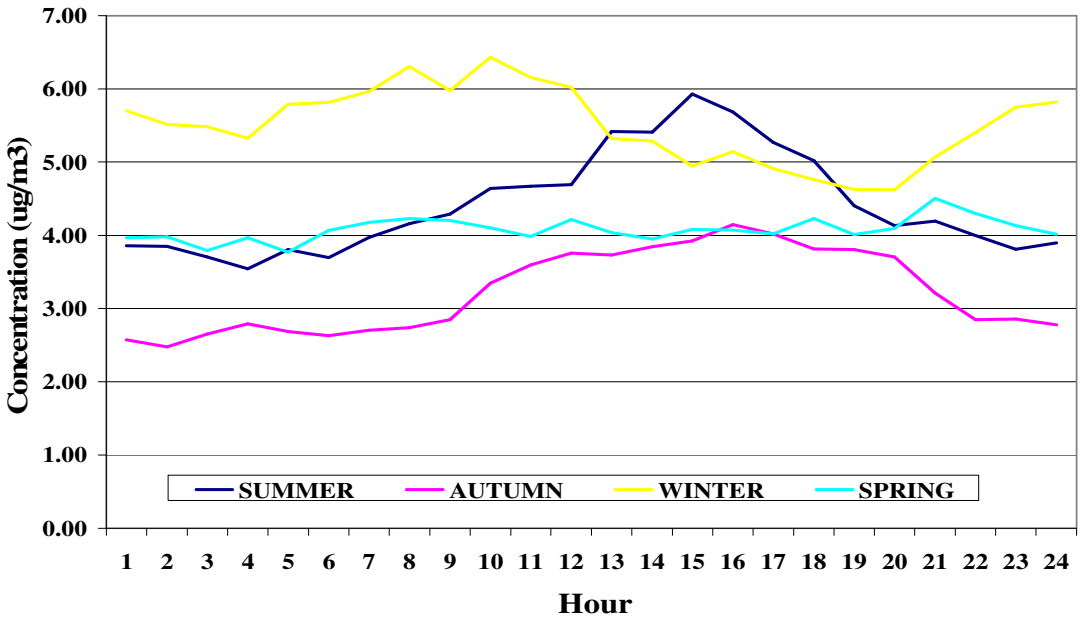

Figure 3.12. Diurnal variation of pollutant concentration in sulphate at Elandsfontein for the period 1 January to 31 December 2005.

The sulphate concentrations are clearly related to sulphur dioxide concentrations over the Highveld, which show a distinctive diurnal pattern in all seasons with a maximum between 11:00 and 13:00. Hourly average sulphur dioxide concentrations increase sharply after sunrise from 07:00 and peak at 12:00. Concentrations gradually decrease until 20:00 and level off during the course of the night (Figure 3.13).

Mean concentrations and diurnal variations are similar in autumn, summer and spring but concentrations of sulphur dioxide are higher in the night during winter. Higher night-time winter concentrations are probably due to the pronounced atmospheric stability in winter associated with fossil fuel burning from coal combustion. In spring, peak concentration close to elevated sources occurs about two hours earlier coinciding with the period of greatest insolation and turbulence when sulphur dioxide emitted becomes mixed throughout the boundary layer. Peak concentrations occur at midday for the other seasons.

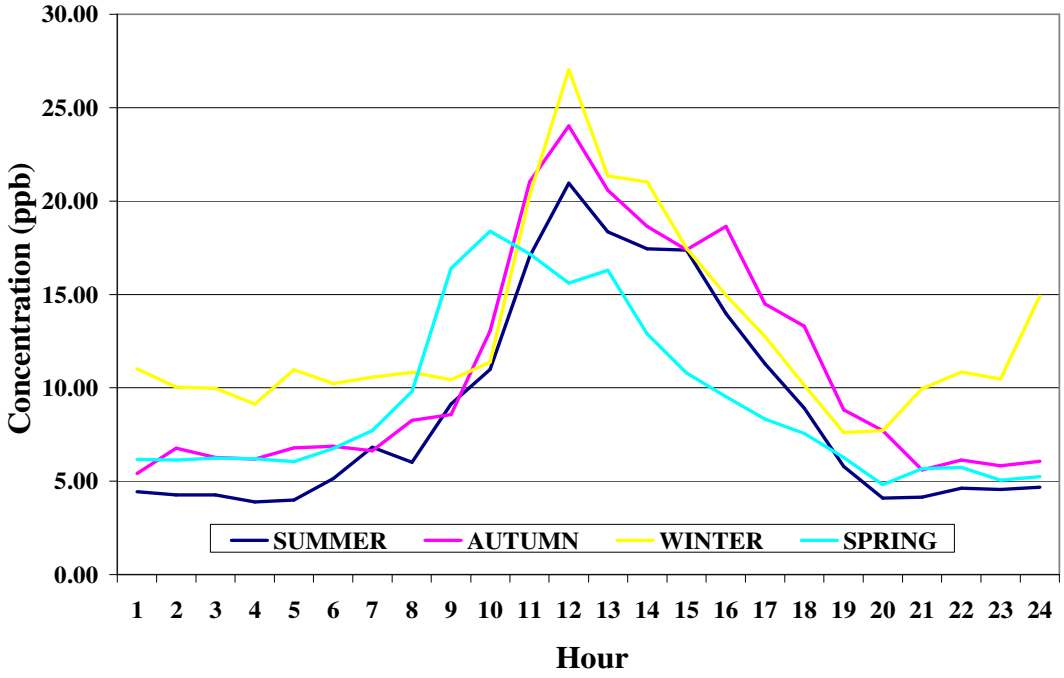

Figure 3.13. Diurnal variation of sulphur dioxide concentration at Elandsfontein for the period 1 January to 31 December 2005.

****

Average concentrations of atmospheric aerosols on the industrialized Highveld are highest during late evenings and at night and lowest during the afternoon. The opposite is true for sulphate aerosols and sulphur dioxide as concentrations peak during the day. The maximum concentrations during the night are enhanced by stable atmospheric conditions while minimum concentrations during the day are due to atmospheric instability and mixing. Sulphur dioxide is derived from tall stack emissions which are brought to the surface during the day. Monthly mean aerosol concentrations are highest in winter and early spring, and lowest in summer and autumn. Lower concentrations of aerosols in summer and autumn are attributed to rainfall which cleans out aerosols from the air.

CHAPTER FOUR

AEROSOL SOURCES AND CHEMICAL COMPOSITION

Pollution and wind roses are created to investigate the sources of aerosols and seasonal effects on the concentration of aerosols. The chemical composition of particulate matter and time series of particulates, gases and meteorological parameters during a pollution episode are also analyzed.

4.1 Overview of meteorology

4.1.1 Wind roses

At Elandsfontein, wind speed is predominantly between 3 and 9 ms^{-1}, with wind speed of less than 3 and greater than 9 ms^{-1} occurring less than 10% of the time throughout the period. Easterly winds are more prevalent in summer and autumn while north-north-westerly winds are more prevalent in winter and spring (Figure 4.1). The 4 spokes around the northwest direction (N, NNW, NW and WNW) in winter and spring comprise 65% of all hourly wind directions. This also shows that the wind rarely blows from the south, south east and northeast directions during winter and spring. Also in summer and autumn, the 3 spokes around the east direction (E, ENE and ESE) comprise 50% of all hourly wind directions. This is also an indication that wind rarely blows from the north, west and south directions in summer and autumn. The changes in the prevailing wind directions are due to changes in the synoptic circulation systems affecting the area. Anticyclonic conditions are associated with north-westerly flow whereas easterly waves are associated with easterly flow.

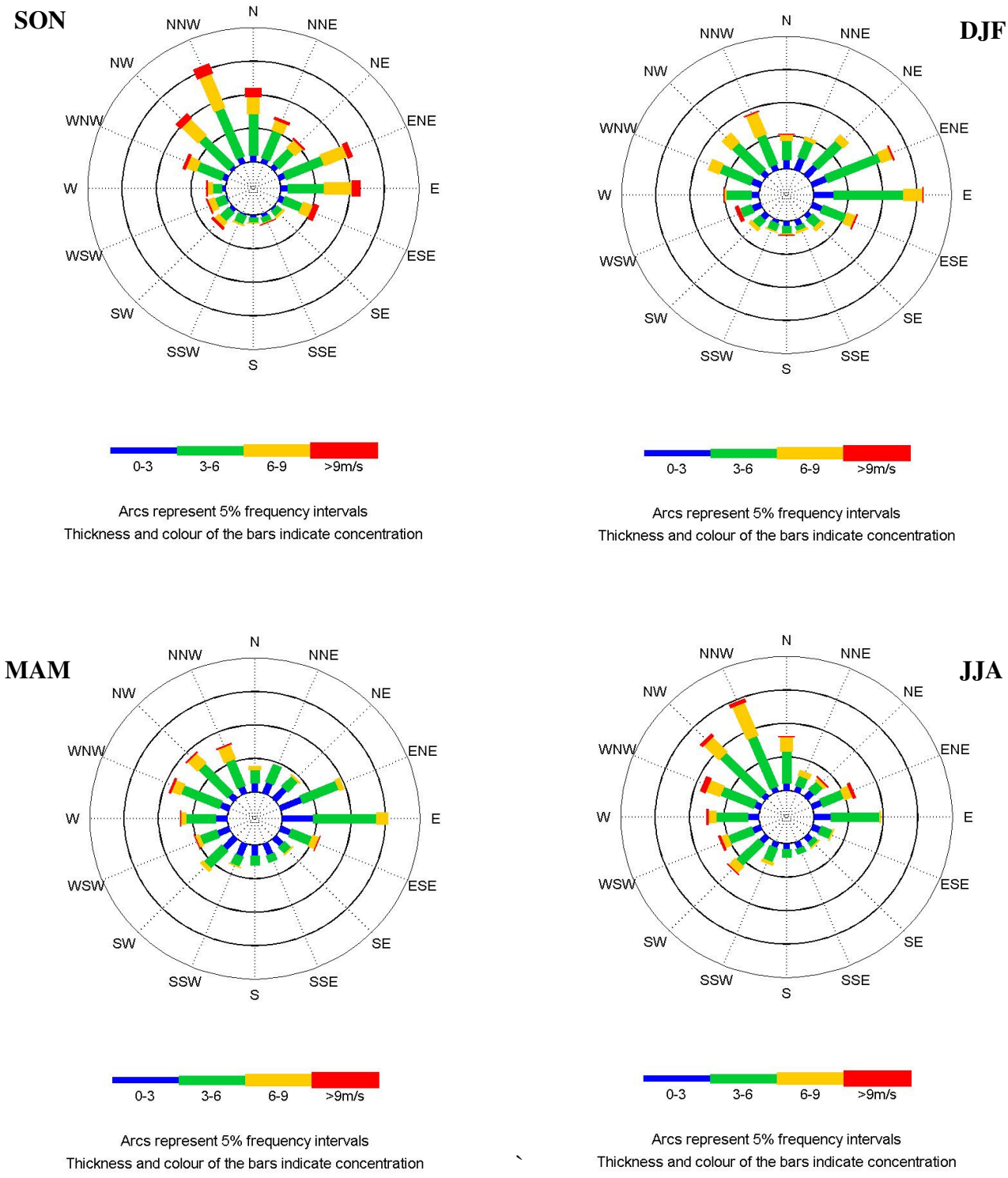

Figure 4.1. Seasonal wind roses at Elandsfontein for spring (September/October/November), summer (December/January/February), autumn (March/April/May) and winter (June/July/August) for the period 1 January to 31 December 2005.

4.2 Pollution roses

Major industries and power plants which influence the concentration of pollution are located around Elandsfontein monitoring site. Located at the north in Middleburg and Witbank and at the south in Secunda and Standerton are major industries. Also located at the north, north-east, west and north-west are major power plants such as Duvha, Arnot, Hendrina, Komati, Kriel, Matla and Kendal power stations. Agricultural and grassland areas are found to the east. Therefore there is highest concentration of pollution in association with north-westerly wind and lowest concentration is associated with easterly wind. Pollution is mainly derived from the major industries and power plants while other potential sources of pollution include biomass burning, domestic fires, incomplete combustion of fossil fuel and bio fuel, forest fires, motor vehicles, coal burning, metallurgical smelters, precursor species like ammonia, nitric acid, SO_2, NO_x and windblown dust.

Black carbon, PM10, nitrate and sulphate highest concentration is most frequent in winter and spring with wind blowing from all sides but most frequently from the northwest much of the time (Figure 4.2 - 4.5). The 4 spokes around the northwest direction (N, NNW, NW and WNW) for black carbon, PM10 and sulphate comprise 65% each of all hourly concentration of pollutants. This also shows that the wind rarely brings pollutants from the south east and south-south-east directions during winter and spring. Although nitrate also has the highest concentration in winter and spring in association with north-westerly wind, it comprises 55% in winter and 60% in spring of all hourly pollutants concentrations (Figure 4.4).

Black carbon, PM10, sulphate and nitrate have lowest concentration during summer and autumn in association with easterly wind. In summer and autumn, black carbon concentration is less than 2 $\mu g/m^3$, PM10 concentration is less than 90 $\mu g/m^3$, sulphate concentration is less than 9 $\mu g/m^3$ and nitrate concentration is less than 2 $\mu g/m^3$.

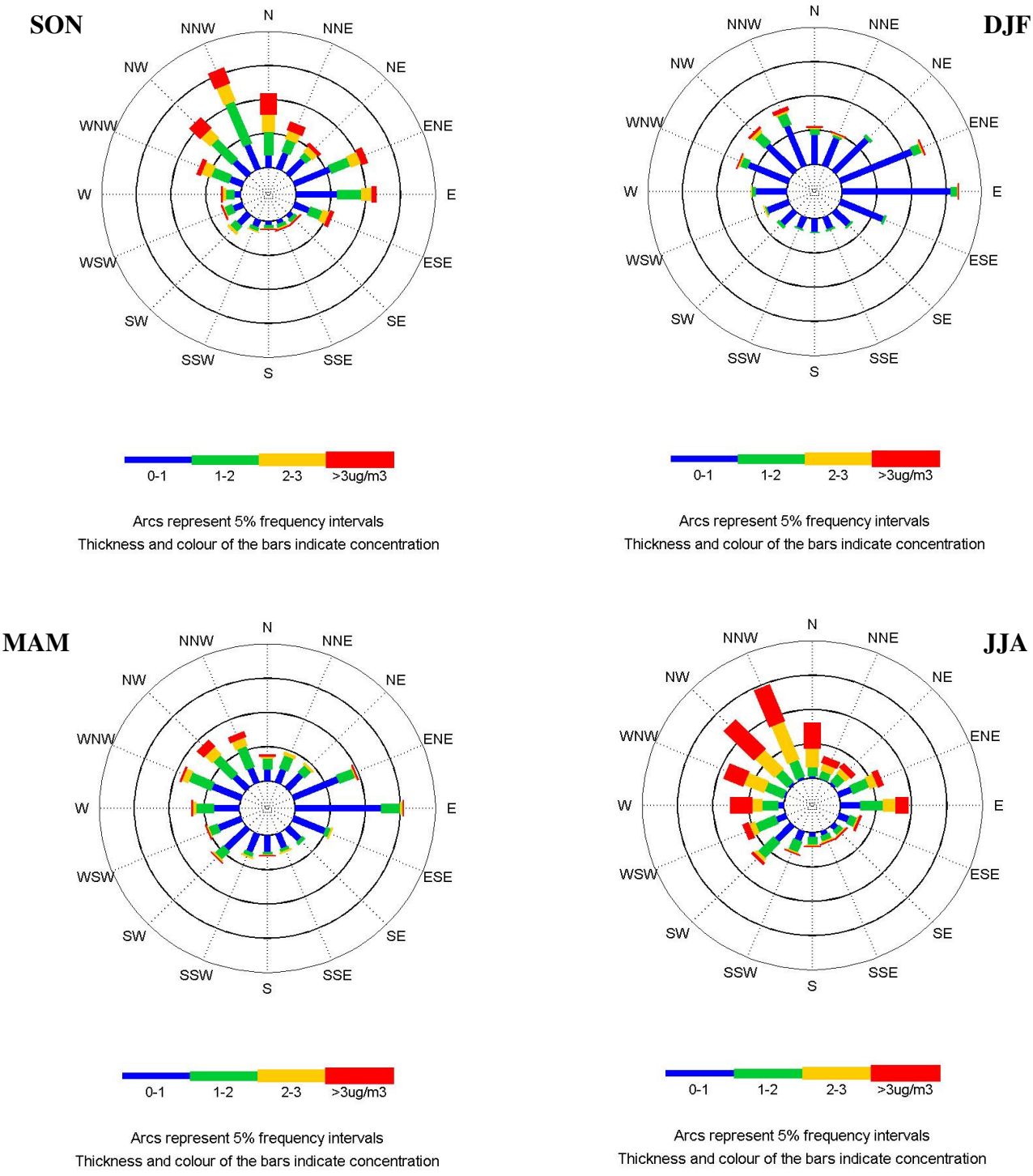

Figure 4.2. Pollution roses for black carbon concentrations recorded at Elandsfontein for spring (September/October/November), summer (December/January/February), (March/April/May) and winter (June/July/August) for the period 1 January to 31 December 2005.

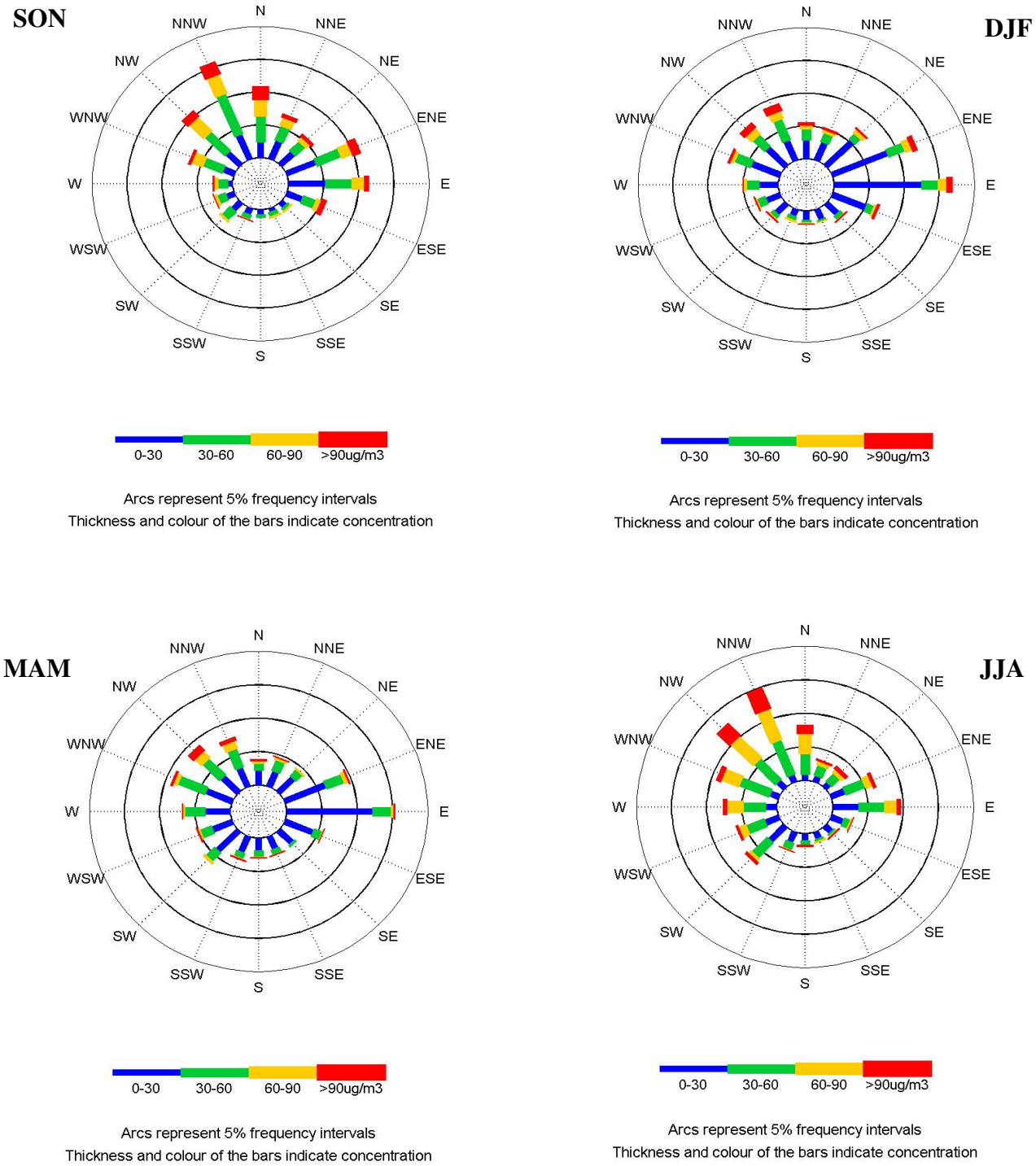

Figure 4.3. Pollution roses for PM10 concentrations recorded at Elandsfontein for spring (September/October/November), summer (December/January/February), autumn (March/April/May) and winter (June/July/August) for the period 1 January to 31 December 2005.

Although black carbon, PM10, nitrate and sulphate have their highest concentration in association with wind blowing from the northwest direction, all the pollutants do not come from the same source (Figure 4.2 – 4.5). For instance, PM10 and black carbon come from the same sector, northwest direction but not from the same source. However, both PM10 and black carbon concentrations show a notable similarity of minimum and maximum at the same time of the day. This pattern indicates that they are both derived from sources at the surface. Outdoor fire, forest fires, domestic heating and coal combustion are potential sources that may result in black carbon and PM10 occurring at the same time of the day.

Secondly, sulphur dioxide oxidized to sulphate, NO_x oxidized to nitrate and black carbon emissions come from the same source. Sulphur dioxide, NO_x and black carbon are released from industrial and domestic processes as a result of the burning of fossil fuels. Sulphate, nitrate and black carbon also have highest concentration in association with north-westerly wind. Furthermore, black carbon, PM10 and NO_x (nitrate precursor) also have the same source in association with wind blowing from the northwest direction. Industrial processes from various industries located at Middleburg and Witbank are the sources of the pollutants.

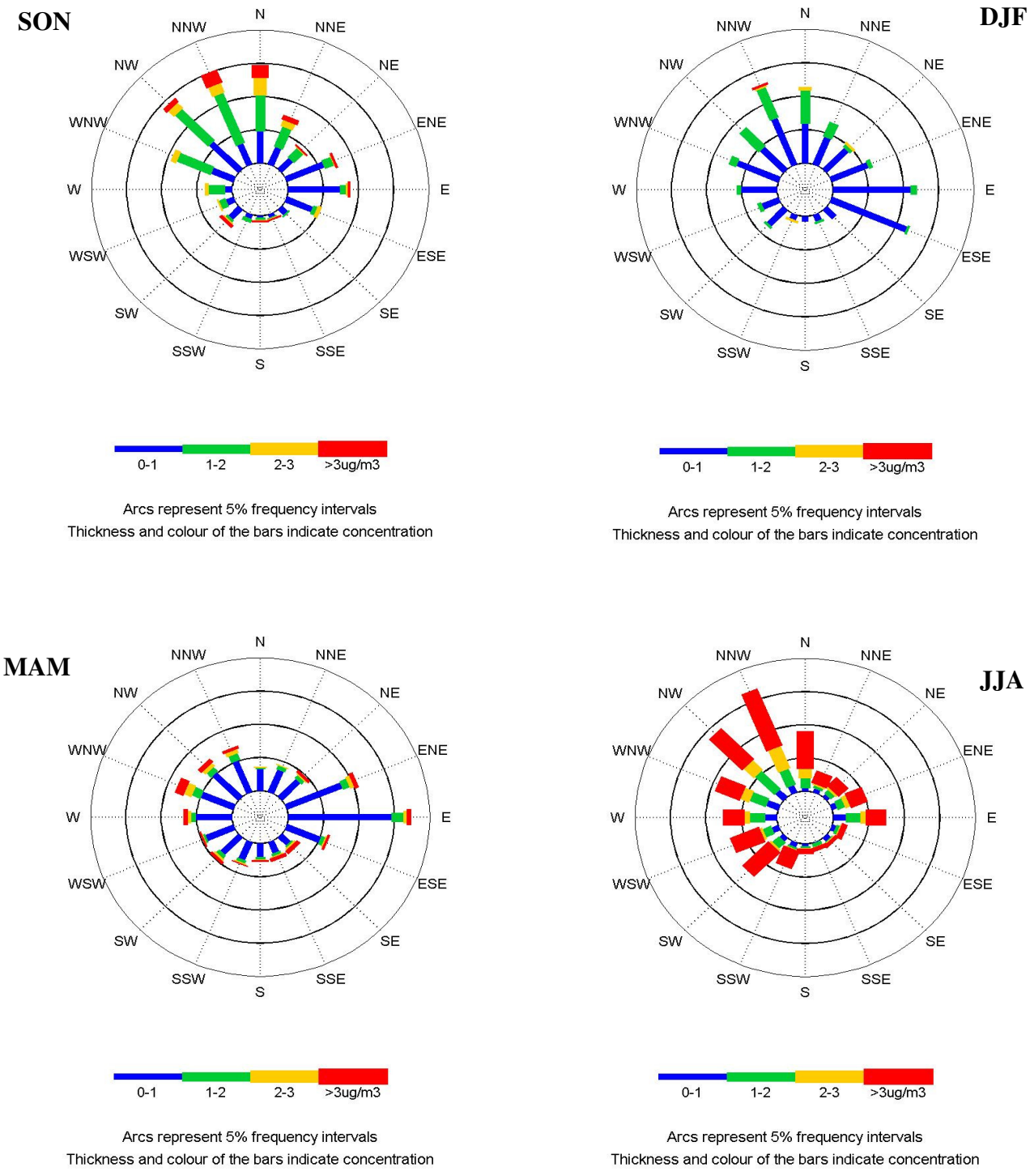

Figure 4.4. Pollution roses for nitrate concentrations recorded at Elandsfontein for spring (September/October/November), summer (December/January/February), autumn (March/April/May) and winter (June/July/August) for the period 1 January to 31 December 2005.

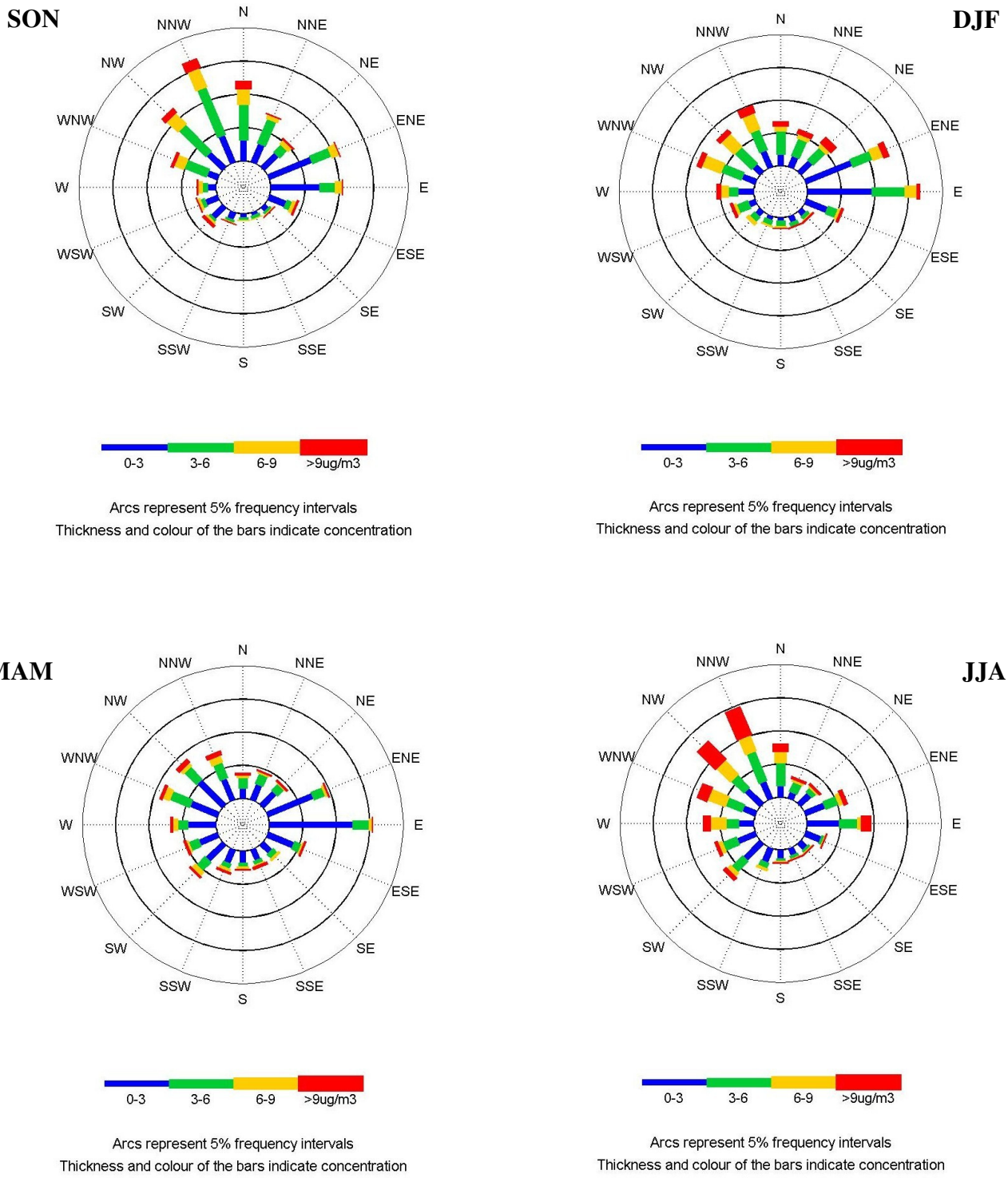

Figure 4.5. Pollution roses for sulphate concentrations recorded at Elandsfontein for spring (September/October/November), summer (December/January/February), autumn (March/April/May) and winter (June/July/August) for the period 1 January to 31 December 2005.

4.3 Chemical composition

Black carbon accounted for 5% of the PM10 mass in summer. Its contribution increased a little to 6% in autumn, remained at 6% in winter but significantly increased to 15% in spring (Figure 4.6). The significant increase in black carbon in spring is probably due to biomass burning which occurs frequently during spring.

Nitrates accounted for only 1% of the PM10 mass in summer. Their contribution increased to 4% in autumn, further increasing to 11% in winter (Figure 4.6). The contribution from nitrates dropped to 3% in spring. Sources of nitrates include precursor species of ammonia (NH_3) and nitric acid (HNO_3), and precursors from industries surrounding Elandsfontein. Nitrate aerosol also forms by oxidation from its gaseous precursor NO_x which is emitted from coal combustion.

Sulphate aerosol contributed 25% of the PM10 mass in summer and 22% in autumn (Figure 4.6). Sulphates accounted for only 15% of PM10 mass in winter, but sulphate constitutes the major percentage of total PM10 in spring – 49%. Sulphates are formed downwind when sulphur dioxide from coal combustion in coal-fired power plants oxidizes. The increase of sulphate in spring is attributed to the substantially lower mixing heights during this season which are dependent on temperature. However, industrial processes largely influenced by meteorological condition may be accountable for the concentration build up of sulphate in spring.

The unknown contribution to PM10 mass constitutes the largest percentage in three seasons (Figure 4.6). It was found to be the largest contributor in summer (69%), autumn (68%), and winter (68%) but accounted for only 33% of the aerosol mass in spring. The black carbon, nitrate and sulphate aerosols do not account for all the PM10 mass. However, many other sources accounting for the total PM10 mass originate from the unknown contribution. Aerosol species contributing to the unknown may include ammonium, crustal elements (soil dust and windblown material), trace metals, organic carbon, sodium and chloride.

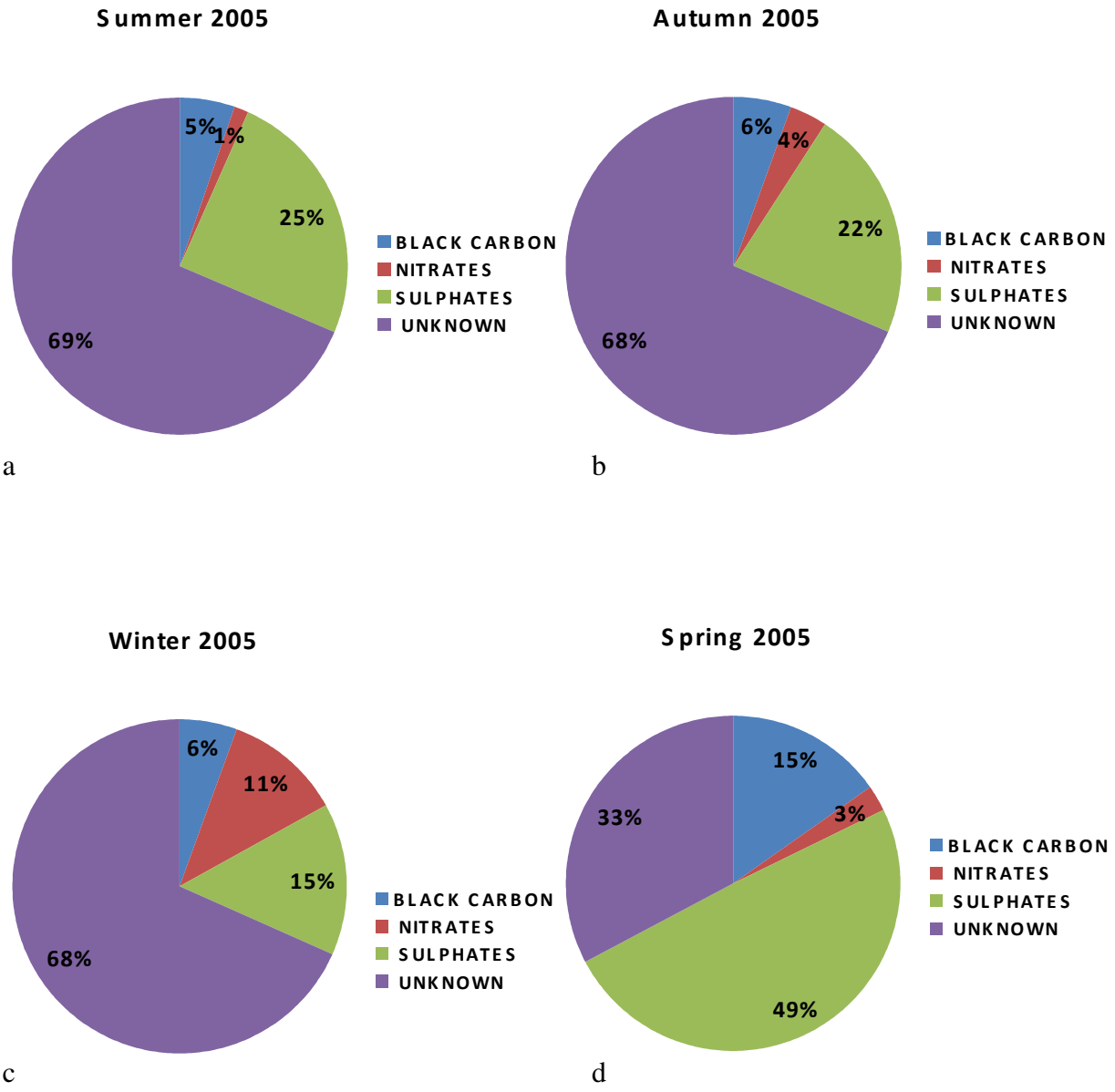

Figure 4.6. Pie chart showing sulphates, nitrates and black carbon as percentage of total PM10 in a. summer (December/January/February); b. autumn (March/April/May); c. winter (June/July/August); and d. spring (September/October/November).

4.4 Causes of high aerosol concentrations

Time series of a pollution episode from 21-23 January 2005 and 29-31 August 2005 has been analyzed to identify some of the causes of high particulate concentrations recorded at the Elandsfontein monitoring site.

Between 21 and 23 January 2005, the concentration of PM10 is highest in the morning on 22 January 2005 between 09:00 and 12:00, reaching a peak at 11:00 (Figure 4.7a). This may be as a result of nocturnal accumulation of particulates in elevated stable layers, which are mixed towards the ground surface by morning convective eddies. Although the concentrations of black carbon, sulphur dioxide and sulphates are slightly elevated during the high PM10 incident, sulphates only account for a small fraction of the total PM10 and most of the PM10 is likely to be from dust. The high levels of PM10 may be as a result of soil dust, road dust, coal combustion, and domestic fires. Sulphur dioxide concentrations peak in the afternoon at around 14:00. This suggests that the high PM10 episode is not due to direct emissions from a source which also emits significant quantities of sulphur dioxide (Figure 4.7b).

Humidity remained high at around 80% in the mornings but there is a sudden decrease in humidity at 11:00. It stays low all through the afternoon and starts to climb high again in the evening from 18:00 (Figure 4.7c). Wind speed is moderate, ranging from calm to around 8 ms^{-1}. Peak concentrations of PM10 and black carbon are typically associated with north-westerly wind which is due to the numerous sources of particulates found to the north-west of Elandsfontein. However, peak concentrations of sulphur dioxide and sulphates are associated with westerly wind and originate from Kriel and Matla power stations. The sources (domestic heating and coal combustion) controlling variation of PM10 and black carbon concentrations are largely influenced by low or high wind speed. High temperature and high humidity favor aqueous-phase reactions of sulphur dioxide oxidation to sulphate aerosol. Moreover, higher humidity causes aerosols to have higher mass. Consequently, sulphate aerosol remains dry with increasing humidity until their deliquescent point is attained at which time a sudden uptake of water occurs with a corresponding increase in particle size.

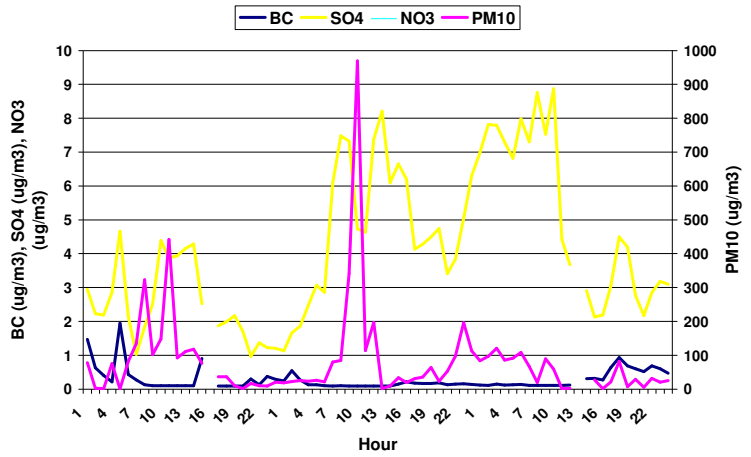

a.

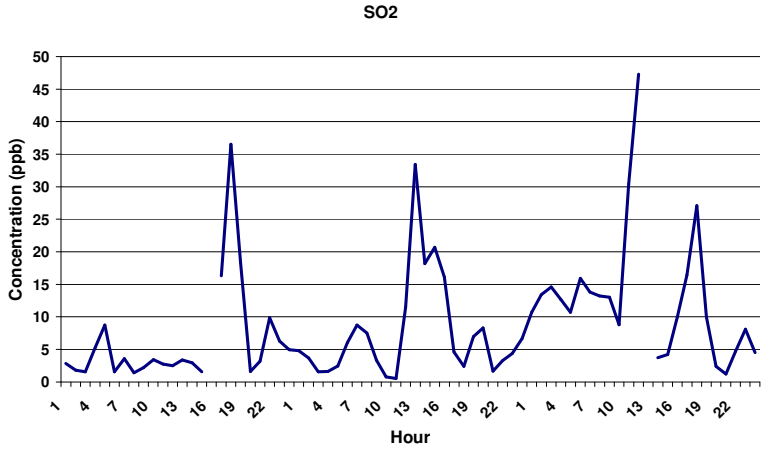

b.

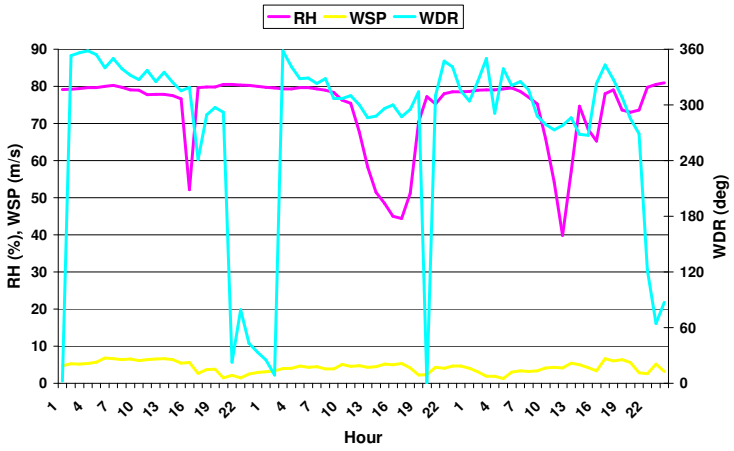

c.

Figure 4.7. Time series during the pollution episode of 21-23 January 2005. a. Black carbon, sulphate, nitrate and PM10 concentrations; b. sulphur dioxide concentrations; and c. humidity, wind speed and wind direction.

The peak in PM10 concentrations on 30 August 2005 coincides with peaks in sulphate and black carbon concentrations. PM10 concentrations were at a maximum between 13:00 and 16:00 with peak concentration at 15:00 (Figure 4.8a). The higher concentration of particulates is probably due to a combination of particulate emissions from tall stacks brought down to the surface by turbulence and due to particulates released at the surface. Sulphur dioxide concentration from 29 to 31 August is at a maximum between 13:00 and 16:00, at the same time as peak concentrations of PM10, sulphate and black carbon (Figure 4.8b). Tall stack and industrial emissions contribute to the high sulphur dioxide concentrations. Perhaps the situation is exacerbated by the accumulation of pollutants and more stable conditions that occur during the winter months.

However, the peak concentrations of PM10, black carbon, sulphate and sulphur dioxide may represent a power station stack impact. Apparently, there is a black carbon start-up even though black carbon is not normally emitted from power stations. On the other hand, coal is not burnt in this situation but there is burning of fuel oil which may lead to black carbon start-up. Although particulate controls in power stations have high efficiency rates of nearly 99.9% for electrostatic precipitators, considerable amounts of primary and secondary particulate pollutants are emitted into the environment due to the high coal combustion without electrostatic precipitators (Querol et al., 1998). Therefore, the black carbon start up may also be a result of electrostatic precipitators which are yet to be switched on but are likely to be off at this time.

The peak concentration of PM10, black carbon, sulphur dioxide and sulphate, is associated with north-westerly wind originating from Kendal power station (Figure 4.8c). Nitrate peak concentration is associated with northerly wind originating from Duvha power station and from open-cast coal mines. Prevailing wind direction and particulate formations which occur at different time periods account for these concentration changes over time. For example, nitrate is constantly higher at night due to its formation mainly at night and both black carbon and PM10 are formed from domestic heating and coal combustion for space heating.

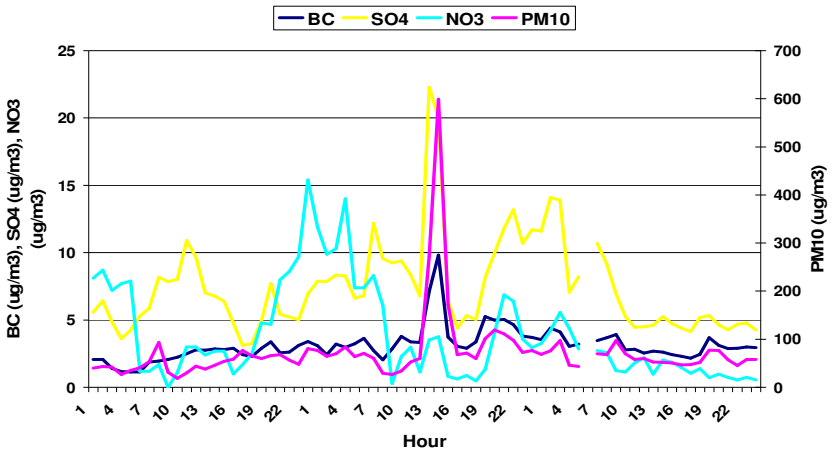

a.

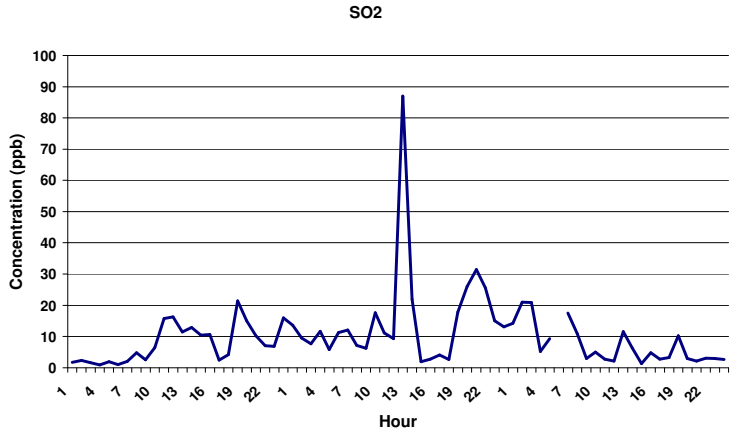

b.

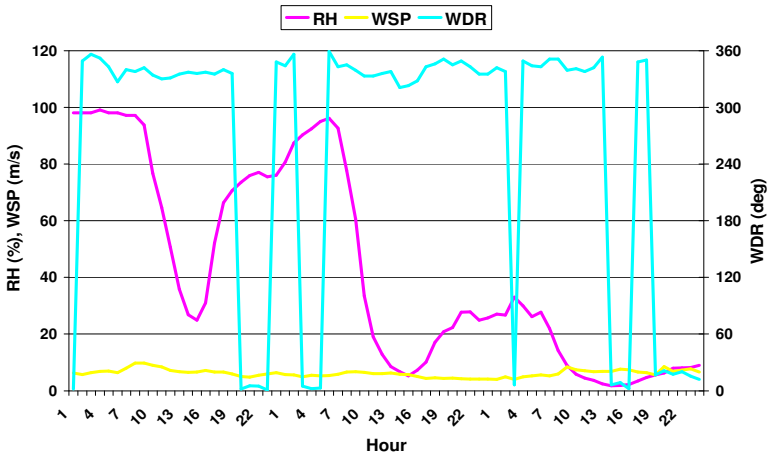

c.

Figure 4.8. Time series of the pollution episode from 29-31 August 2005. a. Black carbon, sulphate, nitrate and PM10 concentrations; b. sulphur dioxide concentrations; and c. humidity, wind speed and wind direction.

****

Particulate matter concentration is highest in association with north-westerly flow and lowest in association with easterly flow. Major industries and power plants are located north and south of Elandsfontein while agricultural and grassland areas are found to the east. Pollution is mainly derived from the major industries and power plants while potential sources of pollution include biomass burning, domestic fires, incomplete combustion of fossil fuel and bio fuel, dusts, coal combustion, and tall stack emissions. The contribution of black carbon and sulphate to PM10 mass is highest in spring. The unknown contribution of aerosol species not mentioned includes sodium, chloride, ammonium, water, mineral dust, and trace metals.

CHAPTER FIVE

SUMMARY AND CONCLUSIONS

Aerosols significantly influence the radiative budget of the Earth's atmosphere both directly by scattering and absorbing radiation and indirectly by affecting cloud properties. In southern Africa, urban and industrial areas are important sources of aerosols, and the accumulation of aerosols in the atmosphere is controlled by consistent atmospheric stability and recirculation associated with the mean anticyclonic circulation of the atmosphere over the southern Africa region.

The aim of this study is to investigate the characteristics of particulate matter over the industrialised Highveld of South Africa. Continuous measurements of PM10, black carbon, nitrates, sulphur dioxide, particulate sulphate, light scattering properties of aerosol by nephelometer, and meteorological parameters were collected at Eskom's Elandsfontein air quality monitoring site from January to December 2005.

The important findings from the research work are summarised as they relate to the temporal behaviour of aerosols on diurnal and seasonal time scales. The effects of meteorological parameters such as temperature, humidity, wind direction and wind speed on the concentration and properties of the aerosols were identified. The fraction of PM10 composed of sulphate, nitrate, and black carbon was determined as well as the identification of major sources of pollutants at Elandsfontein.

Diurnal variations in atmospheric aerosol concentration

Hourly variations in atmospheric aerosol concentration showing daily and fluctuating pollution levels at different times of the day in response to the changing state of atmospheric stability and instability are discussed.

1. Average concentrations of atmospheric aerosols on the industrialized Highveld are highest during late evenings and at night (18:00-22:00) and lowest during the afternoon (12:00-17:00).
2. Maximum concentrations of aerosols in the early morning and at night indicate the trapping effects of stable atmospheric conditions and surface inversions, suggesting that most particulate matter is derived from sources at the surface. Higher humidity in the morning may also enhance particulate matter mass concentration. Changes in wind speed further explain lower aerosol concentrations during the day and higher concentrations at night. Concentrations are at a minimum during the day due to atmospheric instability and mixing.
3. Particulate matter measured during the day may be emitted from tall stacks and brought down to the surface by turbulence, or released at the surface.
4. There is a notable similarity between variations in PM10 and black carbon concentrations. They both show maximum and minimum concentrations at the same time which indicates that they are both derived from sources at the surface.
5. Diurnal variation is much more pronounced in winter than in autumn, spring and summer for PM10 and black carbon concentrations and scattering coefficient.
6. Sulphate aerosol and sulphur dioxide concentrations peak during the day and are lower at night. Higher concentrations during the day are related to the influence of tall stack emissions from where the sulphur dioxide is derived.
7. Particulate sulphate concentrations are higher in well-aged air masses and are controlled by the local meteorology and by the recirculation pattern of atmospheric aerosol over southern Africa.

Seasonal variations in atmospheric aerosol concentrations

1. Monthly mean aerosol concentrations are highest in winter and early spring, and lowest in summer and autumn. Lower concentrations of aerosols in summer and autumn are attributed to rainfall which cleans out aerosol from the air. Aerosol concentration is elevated by emissions from biomass burning, more domestic fires from townships, and increase in domestic energy demand during the winter and spring.

2. The higher concentration of aerosols during winter months may be aggravated by the accumulation of pollutants and may also be due to stability in the atmosphere which invariably prevents pollution dispersion.
3. High concentrations of aerosols could also be attributed to recirculation of air from the industrialised areas surrounding Elandsfontein air quality monitoring site as well as various industries within the vicinity.
4. Particulate sulphate seasonal variation depends predominantly on meteorology, and on variations in dry and wet deposition rates, which contributes to episodes of high concentration.

Pollution and wind roses

The sources of aerosols are identified and the seasonal effects on the concentration of aerosols are investigated using pollution and wind roses.

1. North-westerly and easterly winds prevail at Elandsfontein.
2. Particulate concentrations are highest in association with north-westerly winds and lowest in association with easterly winds, since major industries and power plants are located north and south of Elandsfontein while agricultural and grassland areas are found to the east.
3. Particulate sulphates sources include oxidation of sulphur dioxide from coal combustion in coal-fired power plants and other industries, and long range air mass transport of sulphate aerosols.

Chemical composition and causes of high aerosol concentrations

The chemical composition of particulate matter and causes of particularly high particulate concentrations are discussed.

1. The contribution of black carbon and sulphate to PM10 mass is highest in spring. The increase in black carbon concentrations in spring may be due to biomass burning which occurs frequently in spring while sulphate increase in spring is due to the influence of local meteorology.
2. The nitrate contribution to PM10 mass is highest in winter. This is as a result of the formation of nitrate from its gaseous precursor NO_x which is emitted from coal combustion. High winter NO_x concentration could be a result of recirculated air from the industrialized areas to the north of the monitoring site.
3. During a pollution episode on 30 August 2005, the peak in PM10 concentration coincided with peaks in sulphate, black carbon and sulphur dioxide concentrations but during the episode of 22 January 2005 only the concentration of sulphate was slightly elevated. Episode on 30 August 2005 which shows high particulate matter concentration appear to be related to particulate emissions from tall stacks, industrial emissions and fossil fuel combustion. Other episodes of 22 January 2005 are not related to industrial emissions but are mainly due to dust. It is indicated that the causes of high aerosol concentrations is reflected in the two episodes considered.
4. The peak concentration of PM10, black carbon, sulphur dioxide and sulphate, is associated with north-westerly wind originating from Kendal power station while nitrate peak concentration is associated with northerly wind originating from Duvha power station and from open-cast coal mines.

References

Alfarra, M.R., 2004: Insights into atmospheric organic aerosols using an aerosol mass spectrometer, PhD Thesis, University of Manchester, Manchester, UK.

"Air quality and health" <http://www.who.int/mediacentre/factsheets/fs313/en/index.html> (05 June 2010).

Annegarn, H.J., Turner, C.R., Helas, G., Tosen, G.R. and Rorich, R.P., 1996: Gaseous pollutants. In: Air pollution and its impacts on the South African Highveld (Eds: 228 Held, G., Gore, B.J., Surridge, A.D., Tosen, G.R., Turner, C.R. and Walmsley, R.D.), *Environmental Scientific Association*, Cleveland, South Africa, pp. 25 - 33.

Anderson, B., Grant, W., Gregory, G., Browell, E., Jnr, J.C., Sachse, G., Bagwell, D., Hudgins, C., Blake, D. and Blake, N., 1996: Aerosols from biomass burning over the tropical south atlantic region: Distributions and impacts, *Journal of Geophysical Research*, 101 (D19), 24117–24137.

Anderson, T.L., Covert, D.S., Marshalll, S.F., Laucks, M.L, Charlson, R.J., Waggoner, A.P., Ogren, J.A., Caldow, R., Holm, R.L., Quant, F.R., Sem, G.J., Wiedensohler, A., Ahlquist, N.A., and Bates, T.S., 1996: Performance characteristics of a high-sensitivity three-wavelength total scatter/backscatter nephelometer, *Journal of Atmospheric and Oceanic Technology*, 13, 967-986.

Anderson, T.L., and Ogren, J.A., 1998: Determining aerosol radiative properties using the TSI 3563 Integrating Nephelometer, *Aerosol Science and Technology*, 29, 57-69.

Anderson, T.L., Covert, D.S., Wheeler, J.D., Harris, J.M., Perry, K.D., Trost, B.E., Jaffe, D. J., and Ogren, J.A., 1999: Aerosol backscatter fraction and single scattering albedo: Measured values and uncertainties at a coastal station in the Pacific Northwest, *Journal of Geophysical Research*, 104, 26793-26807.

Andreae, M.O., 2001: The dark side of aerosols, *Nature*, 409, 671-672.

Andreae, M.O., and Rosenfeld, D., 2008: Aerosol-cloud-precipitation interactions. Part 1. The nature and sources of cloud-active aerosols, *Earth-Science Reviews*, 89, 13-41.

Andrienko, N., and Andrienko, G., 2006: *Exploratory Analysis of spatial and temporal data: A systematic approach*, Springer Berlin, Heidelberg, New York.

Ballach, J., Hitzenberger, R., Schultz, E., and Jaeschke, W., 2001: Development of an improved optical transmission technique for black carbon (BC) analysis, *Atmospheric Environment,* 35, 2089–2100.

Bauer, S.E., Koch, D., Unger, N., Metzger, S.M., Shindell, D.T., and Streets, D.G., 2007: Nitrate aerosols today and in 2030: A global simulation including aerosols and tropospheric ozone, *Atmospheric Chemistry and Physics*, 7 (19), 5043-5059.

Beirle, S., Platt, U., Wenig, M., and Wagner, T., 2004: Highly resolved global distribution of tropospheric NO_2 using GOME narrow swath mode data, *Atmospheric Chemistry and Physics*, 4, 1913–1924.

Bond, T.C., Anderson, T.L. and Campbell, D., 1999: Calibration and inter-comparison of filter based measurements of visible light absorption by aerosols, *Aerosol Science and Technology,* 30, 582-600.

Brasseur, G.P., Prinn, R.G. and Pszenny, A.A.P. (Eds.), 2003: *Atmospheric Chemistry in a Changing World: An Integration and Synthesis of a Decade of Tropospheric Chemistry Research*, Springer-Verlag Berlin, Heidelberg, New York.

Brown, S.S., Stark, H., Ryerson, T.B., Williams, E.J., Nicks, D.K., Trainer, M., Fehsenfeld, F.C., and Ravishankara, A.R., 2003: Nitrogen oxides in the nocturnal boundary layer: simultaneous in situ measurements of NO_3, N_2O_5, NO_2, NO and O_3, *Journal of Geophysical Research*, 108, D9.

Carr, S.B., and Burridge, M.A., 2004: *The operation of a three wavelength nephelometer and some measurement made at Jabiru during 2002*, DSTO-TN-0594, Department of Defence, Science and Technology Organisation, Australian Government.

CEPA, 1998: *National ambient air quality objectives for particulate matter*, A report by the CEPA/FPAC working group on air quality objectives and guidelines, ISBN 0-662-63486 1, Minister, public works and Government services, Ontario.

Charlson, R.J., Langner, J., Rodhe, H., Leovy, C.B. and Warren, S.G., 1991: Perturbation of the northern hemisphere radiative balance by backscattering from anthropogenic sulfate aerosols, *Tellus,* 43AB (4), 152-163.

Charlson, R.J., Schwartz, S.E., Hales, J.M., Cess, R.D., Coakley Jr., J.A., Hansen, J.E. and Hoffman, D.J., 1992: Climate forcing by anthropogenic aerosols, *Science,* 255, 423-430.

Cheng, Y., Ho, K.F., Lee, S.C., and Law, S.W., 2006: Seasonal and diurnal variations of PM1.0, PM2.5 and PM10 in the roadside environment of Hong Kong, *China Particuology*, 4(6), 312-315.

Chueinta, W. and Hopke, P.K. 2001: Beta gauge for aerosol mass measurement, *Aerosol Science and Technology,* 35(4), 840-843.

Chylek, P., Videen, G., Ngo, D., Pinnick, R.G., and Klett, J.D., 1995: Effects of black carbon on the optical properties and climate forcing of sulphate aerosols, *Journal of Geophysical Research,* 100 (D8), 1635-16332.

Cohan, D.S., Xu, J., Greenwald, R., Bergin, M.H., and Chameides, W.L., 2002: Impact of atmospheric aerosol light scattering and absorption on terrestrial net primary, productivity, *Global Biogeochemical Cycles,* 16 (4), 1090.

Cosijn, C. and Tyson, P.T. 1996: Stable discontinuities in the atmosphere over South Africa, *South African Journal of Science*, 92, 381-386.

Courtney, W.J., Shaw, R.W., and Dzubay, T.G., 1982: Precision and accuracy of a beta gauge for aerosol mass determinations, *Environmental Science Technology,* 16, 236–239.

D'Abreton, P.C., Zunckel, M. and Gondwe, P.M., 1998: Estimating mixing heights over southern Africa using surface based measurements, *South African Journal of Science*, 94, 375 - 380.

Dentener, F., Kinne, S., Bond, T., Boucher, O., Cofala, J., Generoso, S., Ginoux, P., and Wilson, J., 2006: Emissions of primary aerosol and precursor gases in the years 2000 and 1750 prescribed data-sets for AeroCom, *Atmospheric Chemistry and Physics*, 6(12), 4321-4344.

Derwent, R.G., Collins, W.J., Jenkin, M.E., Johnson, C.E., and Stevenson, D.S., 2003: The global distribution of secondary particulate matter in a 3-D Lagrangian chemistry transport model, *Journal of Atmospheric Chemistry*, 44 (1), 57-95.

Dockery, D.W., Schwartz, J., and Spengler, J.D., 1992: Air pollution and daily mortality: association with particulates and acid aerosols, *Environmental Research,* 59, 326-373.

Dresia, H. and Spohr, F., 1971: Experience with the radiometric dust measuring unit beta staubmeter, *Staub,* 31, 12–27.

Drewnick, F., Schwab, J.J., Hogrefe, O., Peters, S., Husain, L., Diamond, D., Weber, R. and Demerjian, K.L., 2003: Intercomparison and Evaluation of Four Semi-Continuous PM 2.5 Sulphate Instruments, *Atmospheric Environment*, 37, 3335 - 3350.

EPA, 1997: *National ambient air quality standard for particulate matter*, Vol. 62, No.138. <http://www.epa.gov/fedrgstr/epa-air/1997/july/day-181> (1 September 2007).

Eskom intranet, 2006: *Map of all monitoring stations*, http://acgdev/envirmetadatabase/Metadatabse/Metadatabase_INDEX.asp Website accesses: 10 August 2006.

Etyemezian, V., Nikolich, G., Ahonen, S., Pitchford, M., Sweeney, M., Purcell, R., Gillies, J., and Kuhns, H., 2007: The portable in situ wind erosion laboratory (PI-SWERL): A new method to measure PM10 windblown dust properties and potential for emissions, *Atmospheric Environment* 41, 3789–3796.

Fisseha, R., Dommen, J., Gutzwiller, L., Weingartner, E., Gysel, M., Emmenegger, C., Kalberer, M., and Baltensperger, U., 2005: Seasonal and diurnal characteristics of water soluble inorganic compounds in the gas and aerosol phase in the Zurich area, *Atmospheric Chemistry and Physics Discussions*, 5, 5809–5839.

Freiman, M.T. and Piketh S.J., 2003: Air transport into and out of the industrialized Highveld region of South Africa, *Journal of Applied Meteorology,* 42, 994-1002.

Garstang, M., Tyson, P.D., Swap, R., Edwards, M., Kallberg, P. and Lindesay, J.A., 1996b: Horizontal and vertical transport of air over southern Africa, *Journal of Geophysical Research,* 101 (D13), 721-736.

Garstang, M. and Tyson, P.D., 1997: Atmospheric circulation, vertical structure and transport, in Van Wilgen, B., Andreae, M.O., Goldammer, J., and Lindesay, J.A. (Eds.), *Fire and the Southern African Savannahs: Ecological and Atmospheric Perspectives*, Witwatersrand University Press, Johannesburg.

Glassman, I., 1996: *Combustion*; Academic Press, San Diego, CA.

Gomez-Moreno, F.J., Nunez, L., Plaza, J., Alonso, D., Pujadas, M., and Artinano, B., 2007: Annual evolution and generation mechanisms of particulate nitrate in Madrid, *Atmospheric Environment*, 41, 394-406.

Gotoh, T., 1992: Application of digital image-processing to a beta gauge for determining mass concentration of suspending particulate matter in atmosphere, *Applied Radiation and Isotopes,* 43:659–662.

Gourdon, F., 1983: New advances in beta gauge dust measurements: An automatic chain of

samplers and association, *Proceedings of the 76th Annual Meeting of the Air Pollution Control Association*, June 19–24, Atlanta, GA, 83–17.2.

Hanel, G., 1987: Radiation budget of the boundary layer: Part II, Simultaneous measurement of mean solar volume absorption and extinction coefficients of particles, *Beiträge zur Physik der Atmosphäre,* 60, 241–247.

Harrison, M.S.J., 1993: Elevated inversion over southern Africa: Climatological properties and relationships with rainfall, *South African Geographical Journal*, 75, 1-8.

Harrison, D., Park, S.S., Ondov, J., Buckley, T., Kim, S.R., and Jayanty, R.K.M., 2004: Highly time resolved fine particle nitrate measurements at the Baltimore Supersite, *Atmospheric Environment*, 38, 5321-5332.

Heintzenberg, J., and Charlson, R.J., 1996: Design and applications of the integrating nephelometer: A review, *Journal of Atmospheric and Oceanic Technology*, 13, 987-1000.

Heintzenberg, J., and Erfurt, G., 2000: Modification of a commercial integrating nephelometer for outdoor measurements, *Journal of Atmospheric and Oceanic Technology*, 17(12), 1645-1650.

Held, G., Snyman, G.M., and Scheifinger, H., 1993: Seasonal variation and trends of atmospheric particulates on the South African Highveld, *The Clean Air Journal*, 8 (8), 4-11.

Held, G., Gore, B.J., Surridge, A.D., Tosen, G.R., Turner, C.R., and Walmsley, R.D. (Eds.), 1996: *Air pollution and its impacts on the South African Highveld,* Environmental Scientific Association, Cleveland, 144pp.

Husar, R.B., 1974: Atmospheric particulate mass monitoring with a β radiation detector, *Atmospheric Environmen*t, 8, 183–188.

Igbafe, A.I., 2007: Resolving the atmospheric sulphur budget over the Elandsfontein area of the Mpumalanga Highveld, PhD Thesis, University of the Witwatersrand, Johannesburg, South Africa.

Igbafe, A.I., Ross, K.E., Jewell, L., Snow, N.H., and Piketh, S.J., 2007: *Preliminary sulphate budget findings at Elandsfontein air quality monitoring station*, Research Report RES/RR/05/26693, Eskom Holdings Ltd, Johannesburg.

IPCC, 2007: *Climate Change 2007: The Physical Science Basis: Contribution of WorkingGroup I to the Fourth Assessment Report of the Intergovernmental Panel on Climate Change* [Solomon, S., D. Qin, M. Manning, Z. Chen, M. Marquis, K.B. Averyt, M. Tignor and H.L. Miller (eds.)]. Cambridge University Press, Cambridge, United Kingdom and New York, NY, USA.

Jaklevic, J.M., Madden, N.W., and Weigand, C.E., 1983: A precision beta gauge using a plastic scintillator and photomultiplier detector, *Nuclear Instrumental Methods,* 214, 517–518.

Jenkin, M.E., and Clemitshaw, K.C., 2000: Ozone and other secondary photochemical pollutants: chemical processes governing their formation in the planetary boundary layer, *Atmospheric Environment*, 34 (16), 2499-2527.

Kleeman, M.J., Hughes, L.S., Allen, J.O., and Cass, G.R., 1999: Source contributions to the size and composition distribution of atmospheric particles: Southern California in September 1996, *Environmental Science and Technology*, 33 (23), 4331-4341.

Kleinman, L.I., 1991: Seasonal dependence of boundary layer peroxide concentration: the low and high NO_x regimes, *Journal of Geophysical Research*, 96, 20721–20733.

Laskin, A., Cowin, J.P., and Iedema, M.J., 2006: Analysis of individual environmental particles using modern methods of electron microscopy and X-ray microanalysis, *Journal of Electron Spectroscopy and Related Phenomena*, 150 (2-3), 260-274.

Lighty, J.S., Veranth, J.M., Sarofim, A.F., 2000: Combustion aerosols: factors governing their size and composition and implications to human health, *Journal of the Air and Waste Management Associations* 50(9), 1565-1618.

Lilienfeld, P. and Dulchinos, J., 1972: Portable instantaneous mass monitor for coal mines dust, *American Industrial Hygiene Asso*ciation *Journal,* 33, 136–143.

Limbeck, A., Rendl, J., Heimburger, G., Kranabetter, A., Puxbaum, H., 2004: Seasonal variation of palladium, elemental carbon and aerosol mass concentrations in airborne particulate matter, *Atmospheric Environment,* 38, 1979–1987.

Lin, C.H., Wu, Y.L., Lai, C.H., Watson, J.G., Chow, J.C., 2008: Air quality measurements from the southern particulate matter supersite in Taiwan, *Aerosol and Air Quality Research,* 8(3), 233-264.

Lindberg, J.D., Douglass, R.E. and Garvey, D.M., 1993: Carbon and the optical properties of atmospheric dust, *Applied Optics* 32, 6077–6081.

Lindberg, J.D., Douglass, R.E., and Garvey, D.M., 1999: Atmospheric particulate absorption and black carbon measurement, *Applied Optics*, 38, 2369-2376.

Lippmann, M. and Schlesinger, R.B., 1979: *Chemical Contamination in the Human Environment,* 1st Ed., Oxford University Press, New York, 217-231.

Long, R.W. and McClenny, W.A., 2006: Laboratory and field evaluation of instrumentation for the semicontinuous determination of particulate nitrate (and other water-soluble particulate components), *Journal of Air and Waste Management Association*, 56, 294 305.

Maenhaut, W., Salma, I., Cafmeyer, J., Annegarn, H.J., and Andreae, M.O., 1996: Regional atmospheric aerosol composition and sources in the eastern Transvaal, South Africa, and impact of biomass burning, *Journal of Geophysical Research,* 101 (D19) 631-650.

McGonigle, A.J.S., Thomson, C.L, Tsanev, V.I., and Oppenheimer, C., 2004: A simple technique for measuring power station SO2 and NO2 emissions, *Atmospheric Environment*, 38, 21-25.

Meagher, J.F., Bailey, E.M., and Luria, M., 1983: The seasonal variation of the atmospheric SO_2 to SO_4 conversion rate, *Journal of Geophysical Research,* 88, 1525-1527.

Menon, S., Hansen, J., Nazarenko, L. and Luo, Y., 2002: Climate effects of black carbon aerosols in China and India, *Science*, 297, 2250-2253.

Metzger, S., Dentener, F., Pandis, S., and Lelieveld, J., 2002b: Gas/aerosol partitioning: 1. A computationally efficient model, *Journal of Geophysical Research* D: Atmospheres, 107 (16), 4312.

Moosmuller, H., Chakrabarty, R.K., and Arnott, W.P., 2009: Aerosol light absorption and its measurement: A review, *Journal of Quantitative Spectroscopy and Radiative Transfer*, 110, 844-878.

"National ambient air quality standards"
< http://www.epa.gov/air/criteria.html> (20 February 2008).

Novakov, T., Ramanathan, V., Hansen, J.E., Kirchstetter, T.W., Sato, M., Sinton, J.E., and Sathaye, J.A., 2003: Large historical changes of fossil-fuel black carbon aerosols, *Geophysical Research Letters*, 30 (6), 1324, doi:10.1029/2002GL016345.

Novakov, T., Menon, S., Kirchstetter, T.W., Koch, D., and Hansen, J.E., 2005: Aerosol organic carbon to black carbon ratios: Analysis of published data and implications for climate forcing, *Journal of Geophysical Research*, 110, D21205, doi:10.1029/2005JD005977.

Pakkanen, T.A., 1996: Study of formation of coarse particle nitrate aerosol, *Atmospheric Environment*, 30 (14), 2475-2482.

"Particle pollution standard"

<http://www.epa.gov/air/particlepollution/standard.html> (20 February 2008)

Penner, J.E., Charlson, R.J., Hales, J.M., Laulainen, N.S., Leifer, R., Novakov, T., Ogren, J., Radke, L.F., Schwartz, S.E., and Travis, L., 1994: Quantifying and minimizing uncertainty of climate forcing by anthropogenic aerosols, *Bulletin of the American Meteorological Society,* 75 (3), 375-400.

Penner, J.E., Chuang, C.C., and Grant, K., 1998: Climate forcing by carbonaceous and sulfate aerosols, *Climate Dynamics*, 14, 839-851.

Penner, J.E., Andreae, M., Annergan, H., Barrie, L., Feichter, J., Hegg, D., Jayaraman, A., Leaitch, R., Murphy, D., Nganga, J., and Pitari, G., 2001: Aerosols, their direct and indirect effects. In: *Climate Change 2001*: *The Scientific Basis*. *Contribution of Working Group I to the Third Assessment Report of the Intergovernmental Panel on Climate Change* [Houghton, J.T., Y. Ding, D.J. Griggs, M. Noguer, P.J. van der Linden, X. Dai, K. Maskell, and C.A. Johnson (eds.)]. Cambridge University Press, Cambridge, UK and USA.

Petzold, A., Kopp, C., and Niessner, R., 1997: The dependence of the specific attenuation cross section on black carbon mass fraction and particle size, *Atmospheric Environment*, 31, 661-672.

Petzold, A., Kramer, H., and Schonlinner, M., 2002: Continuous measurement of atmospheric black carbon using a Multi-Angle Absorption Photometer, *Environmental Science and Pollution Research*, 4, 78-82.

Petzold, A. and Schonlinner, M., 2004: Multi-Angle Absorption Photometry- A new method for the measurement of aerosol light absorption and atmospheric black carbon, *Journal of Aerosol Science,* 35, 421-441.

Petzold, A., Schloesser, H., Sheridan, P.J., Arnott, W.P., Ogren, J.A., and Virkkula, A., 2005: Evaluation of multi-angle absorption photometry for measuring aerosol light absorption, *Aerosol Science and Technology,* 39 (1), 40-51.

Piketh, S.J., Annegern, H.J., and Tyson, P.D., 1999: Lower tropospheric aerosol loading over South Africa: The relative contribution of Aeolian dust, industrial emission and biomass burning, *Journal of Geophysical Research,* 104 (D1), 1587-1607.

Piketh, S.J., 2000: Transport of aerosols and trace gases over southern Africa, PhD Thesis, University of the Witwatersrand, Johannesburg, South Africa.

Preston-Whyte, R.A., and Tyson, P.D., 1993: *The Atmosphere and Weather of Southern Africa*, Oxford University Press, Cape Town.

Querol, X., Alastuey, A., Puicercus, J.A., Mantilla, E., Miro, J.V., Lopez-Soler, A., Plana, F., and Artinano, B., 1998: Seasonal evolution of suspended particles around a large coal fired power station: particulate levels and sources, *Atmospheric Environment*, 12 (11), 1963-1978.

Reiner, T. and Arnold, F., 1993: Laboratory Flow Reactor Measurements of the Reaction SO3 + H2O + M → H2SO4 + M: Implications for Gaseous H2SO4 and Aerosol Formation in the Plume of a Jet Aircraft, *Geophysical Research Letters*, 20, 2659 - 2662.

Ross, K.E., 2003: Aerosol-cloud interactions over southern Africa, PhD Thesis, University of the Witwatersrand, Johannesburg, South Africa.

Ross, K., Piketh, S., Bruintjes, R., Burger, R., Swap, R., and Annegarn, H., 2003: Spatial and seasonal variations in CCN distribution and the aerosol CCN relationship over Southern Africa, *Journal of Geophysical Research,* 108 (D13), 8481.

Rupprecht and Patashnick., 2001: Series 8400S Ambient Particulate Sulphate Monitor Operations Manual, Revision A, R&P Part Number 42-007039, Rupprecht and Patashnick Co., Inc. Albany, New York.

Russell, P.B., Hobbs, P.V., and Stowe, L.L., 1999: Aerosol properties and radiative effects in

the United States East coast haze plume: An overview of the tropospheric aerosol radioactive forcing observational experiment (TARFOX), *Journal of Geophysical Research,* 104 (D2), 2213-2222.

Safai, P.D., Kewat, S., Praveen, P.S., Rao, P.S.P., Momin, G.A., Ali, K., and Devara, P.C.S., 2007: Seasonal variation of black carbon aerosols over a tropical urban city of Pune, India, *Atmospheric Environment*, 41, 2699-2709.

Saha, A., and Despiau, S., 2009: Seasonal and diurnal variations of black carbon aerosols over a Mediterranean coastal zone, *Atmospheric Research*, 92, 27–41.

Salkowski, M., 1964: *Prototype Fly Ash Monitor for Incineration Stacks*, Final report, IIT Research Inst., Chicago, IL.

Scheifinger, H. and Held, G., 1997: Aerosol behaviour on the South African Highveld, *Atmospheric Environment,* 31 (21), 3497-3509.

Scorgie, Y., 1999: Development of a methodological framework and supporting data base for air pollution impact scoping in South Africa industrial planning, Dissertation, University of the Witwatersrand, Johannesburg, South Africa.

Seinfeld, J.H. and Pandis, S.N., 1998: *Atmospheric Chemistry and Physics*: *From Air Pollution to Climate Change*, John Wiley and Sons, Inc., New York.

Seinfeld, J.H. and Pandis, S.N., 2006: *Atmospheric Chemistry and Physics*: *From Air Pollution to Climate Change*, John Wiley and Sons, Inc., Hoboken, New Jersey.

Seinfeld, J.H., 2008: Atmospheric science: black carbon and brown clouds, *Nature Geoscience,* 1, 15-16.

Sivertsen, B., Matale, C., and Pereiira, L.M.R., 1995: *Sulphur Emissions and Transfrontier, Air Pollution in Southern Africa*, Report No: 35, SADC Environment and land management sector coordination unit, Maseru.

Stein, A.F., Lamb, D., 2003: Empirical evidence for the low- and high-NOx photochemical regimes of sulfate and nitrate formation, *Atmospheric Environment*, 37, 3615–3625.

Stevens, R.K., Dzubay, T.G., Shaw, R.W., McClenny, W.A., Lewis, C.W., and Wilson, W.E., 1980: Characterization of the aerosol in the great smoky mountains, *Environmental Science Technology,* 14, 1491–1498.

Stier, P., Feichter, J., Kinne, S., Kloster, S., Vignati, E., Wilson, J., Ganzeveld, L., and Petzold, A., 2005: The aerosol-climate model ECHAM5-HAM, *Atmospheric Chemistry and Physics*, 5 (4), 1125-1156.

Stier, P., Seinfeld, J.H., Kinne, S. and Boucher, O., 2007: Aerosol absorption and radiative forcing, *Atmospheric Chemistry and Physics*, 7 (19), 5237-5261.

Stolzenburg, M.R. and Hering, S.V., 2000: A new method for the automated measurement of atmospheric fine particles nitrate, *Environmental Science and Technology,* 34, 907-914.

Streets, D.G., Gupta, S., Waldhoff, S.T., Wang, M.Q., Bond, T.C., and Yiyun, B., 2001: Black carbon emissions in China, *Atmospheric Environment*, 35, 4281-4296.

Tegen, I. and Fung, I., 1995: Contribution to the atmospheric mineral aerosol load from land surface modification, *Journal of Geophysical Research,* 100 (D9), 18707-18726.

"The AQA implementation: Ambient air quality standards" <http://deat.ecostat.co.za/proposed ambient air quality standards.pdf> (05 June 2010).

Tosen, G.R. and Jury, M.R., 1986: The winter nocturnal wind jet over the eastern Transvaal Highveld, *South African Journal of Science*, 84, 247 - 253.

Tosen, G.R., and Turner, C.R., 1990: Effect of stack height on ground-level concentrations of sulphur dioxide on the eastern Transvaal Highveld, *South African Journal of Science*, 86, 82-86.

Touloumi, G., Pocock, S.J., Katsouyami, K., and Trichopoulos, D., 1994: Short term effects of air pollution on daily mortality in Athens: A time series analysis, *International Journal of Epidemiology,* 23, 959-967.

Tyson, P.D., Garstang, M., and Swap, R., 1996a: Large-scale recirculation of air over southern Africa, *Journal of Applied Meteorology,* 35, 2218-2236.

Tyson, P.D., Garstang, M., Swap, R., Kallberg, P. and Edwards, M., 1996b: Air transport climatology for subtropical southern Africa, *International Journal of Climatology*, 16, 265-291.

Tyson, P.D., 1997: Atmospheric transport of aerosols and trace gases over southern Africa, *Progress in Physical Geography,* 21, 79-101.

Tyson, P.D. and Preston-Whyte, R.A., 2000: *The Weather and Climate of Southern Africa*; Oxford University Press, Cape Town.

Wall, S.M., John, W., and Ondo, J.L., 1988: Measurement of aerosol size distributions for nitrates and major ionic species, *Atmospheric Environment*, 22, 1649-1656.

Wang, W.C., Chen, K.S., Wang, S.K., Lee, H.C., and Tsai, M.Y., 2009: Modeling atmospheric PM10 concentrations during severe pollution events in southern Taiwan, *Atmospheric Research* 92, 159–171.

Warneck, P., 1988: *Chemistry of the natural atmosphere*, Academic press, London.

Weingartner, E., Saathoff, H., Schnaiter, M., Streit, N., Bitnar, B., and Baltensperger, U., 2003: Absorption of light by soot particles: Determination of the absorption coefficient by means of aethalometers, *Journal of Aerosol Science*, *34*, 1445–1463.

Wilson, W.E., Jr., 1981: Sulphate formation in point source plumes: a review of recent field studies, *Atmospheric Environment*, 15, 2573-2581.

www.esrl.noaa.gov/gmd/aero/instrumentation/neph_desc.html (21 April 2007)

www.instrumentcompaniet.no/files/THERMO_Datablad/FH621R-english.pdf (20 August 2009)

Yang, K.L, 2002: Spatial and seasonal variation of PM10 mass concentrations in Taiwan, *Atmospheric Environment*, 36, 3403-3411.

Yang, Hsi-Hsien., Hsieh, Lien-Te., and Cheng, Shih-Kai., 2005: Determination of atmospheric nitrate particulate size distribution and dry deposition velocity for three distinct areas, *Chemosphere*, 60, 1447-1453.

Yeatman, S.G., Spokes, L.J., and Jickells, T.D., 2001: Comparisons of coarse-mode aerosol nitrate and ammonium at two polluted coastal sites, *Atmospheric Environment*, 35, 1321 1335.

Zhang, D., Zang, J., Shi, G., Iwasaka, Y., Matsuki, A., and Trochkine, D., 2003: Mixture state of individual Asian dust particles at a coastal site of Qingdao, China, *Atmospheric Environment*, 37 (28), 3895-3901.

Zhuang, H., Chan, C.K., Fang, M., and Wexler, A.S., 1999: Formation of nitrate and non-sea salt sulfate on coarse particles, *Atmospheric Environment*, 33 (26), 4223-4233.

Zunckel, M., Koosailee, A., Yarwood, G., Maure, G., Venjonoka, K., Tienhoven, A.M.van. and Otter, L., 2006: Modelled surface ozone over southern Africa during the cross border air pollution impact assessment project, *Environmental Modelling and Software*, 21 (7), 911 924.